Arctic Gakkel Vents Expedition

July 1 – August 11, 2007

IB Oden

Cruise Report

Woods Hole Oceanographic Institution
University of Texas
Swedish Polar Secretariat
Alfred Wegener Institute
Goteburg University
National Institute of Advanced Industrial Science and Technology
University o f Tokyo

AGAVE

Table of Contents

1. Introduction and Cruise Objectives

The Arctic GAkkel Vents Expedition (AGAVE) took place on the IB Oden from July 1 – August 10, 2007. Major funding for the cruise came from the United States through the National Science Foundation (NSF), the National Aeronautics and Space Administration (NASA), and the Woods Hole Oceanographic Institution (WHOI). The expedition represented an international collaboration between scientists in the United States, Sweden, Japan, and Germany, and was part of an International Polar Year (IPY) project entitled, '*Biogeography and Geological Diversity of Hydrothermal Venting on the Ultra-Slow Spreading Arctic Mid-Ocean Ridge.*' The participant list for the expedition can be found in Appendix A.

The AGAVE expedition incorporated two sets of complementary, but nevertheless separate, objectives – scientific goals pertaining to hydrothermal venting and engineering goals pertaining to the development of robotic vehicles for deep-sea research under ice. To first-order the scientific goals are associated with the NSF-funded portion of the research and the engineering goals are associated with the NASA-funded portion, but this categorization is not strict. Some of the NSF research was focused on vehicle development, and some of the NASA research was focused on astrobiological science. The complete set of cruise objectives is described below.

1.1 Scientific objectives

The overarching scientific objective of the AGAVE expedition is to study the geological, chemical, and biological characteristics of hydrothermal venting on the Gakkel Ridge.

The Gakkel Ridge in the Eastern Arctic Basin is the ultra-slow spreading end-member in the global mid-ocean ridge (MOR) system. The North American and Eurasian plates diverge at rates of 3-7 mm/yr along the Gakkel Ridge (Figure 1), nearly two orders of magnitude slower than the fast spreading end-member (southern East Pacific Rise). This ultra-slow divergence completely changes the geologic nature of the ridge, and the results of recent work make it clear that many geologic processes have a completely different character in these environments. We are only just beginning to understand how basic ridge processes such as deformation and extension, crustal accretion, and hydrothermal flow play out at such slow spreading rates [Michael et al., 2003; Jokat et al., 2003; Dick et al., 2003; Edmonds et al., 2003].

The unique geology of the Gakkel Ridge affects all of the first-order parameters that control hydrothermal circulation. The thermal structure, permeability, and chemistry of the host rock on the Gakkel Ridge are all directly impacted by the extremely slow spreading rate. Intuitively, hydrothermal systems might be expected to be rare on the magmatically starved Gakkel Ridge, but thermal and particulate signatures indicative of hydrothermal fluids were found in nearly 80% of the CTD casts from the 2001 Arctic Mid-Ocean Ridge Expedition (AMORE) expedition to the ridge (Edmonds et al., 2003; Michael et al., 2003). How do these water column anomalies relate to hydrothermal discharge on the seafloor and fluid circulation within the crust? Are there massive hydrothermal systems that generate pervasive, large-scale anomalies in the water column? Are hydrothermal systems densely distributed along the ridge? Or perhaps are the currents along the ridge and within the axial valley limited such that hydrothermal fluids linger exceptionally long periods of time in the water column? The AGAVE expedition seeks to answer these first order questions so that we can begin to understand the geological and chemical aspects of hydrothermal processes on the Gakkel Ridge.

Along with being an end-member geological environment, the Gakkel Ridge is also a unique MOR in that it is hydrographically isolated within the Arctic Basin. Communication with the rest of the world's oceans is limited to exchange across shallow sills, and this has important implications for the evolution and ecology of resident chemosynthetic vent fauna. Vent-endemic fauna have been characterized in all of the major ocean basins except for the Arctic, and therefore we do not know how vent fauna on the Gakkel Ridge relate to species found in the nearby Atlantic and Pacific basins. Nor do we know how Arctic vent fauna may have evolved in an end-member, hydrographically isolated Arctic ridge system. Characterizing vent fauna on the Gakkel Ridge is the last major piece of the global biogeographic puzzle.

1.2 Engineering objectives

The overarching engineering objective of the AGAVE expedition is to develop new technologies to enable deep-sea research in ice covered oceans.

In order to develop an understanding of hydrothermal processes on the Gakkel Ridge it is necessary to conduct detailed investigations of the deep seafloor in regions that are permanently covered in ice. The ice cover inhibits or precludes many of the standard oceanographic and deep-sea technologies employed to find and study hydrothermal systems in the open ocean. In particular, remotely operated vehicle (ROV) operations are not presently feasible in ice-covered bodies of water, and submersible operations are considered too risky owing to the difficulties of recovery through the ice. Even relatively straightforward operations, such as CTD casts, are hindered owing to the fact that the tending icebreaker cannot make way in the ice with a wire over the side, but rather must drift in the ice pack. These considerations motivate the development of new techniques that decouple the deep-sea surveying process from the drifting ice.

The motivation to develop novel under-ice survey capabilities is not limited to missions on Earth. The search for life on other planets includes the possibility of volcanically hosted vent fields beneath the ice-covered ocean of Europa, a moon of Jupiter. The search for vent fields under the Arctic ice cap on Earth thus presents a technical analogy for similar missions on Europa. In both cases the most efficient technical solution appears to be the development of robotic vehicles that are capable of being deployed and recovered from within the ice, and that are capable of carrying sensors for the detection and localization of chemosynthetic biological communities hosted by vent fields on the deep seafloor. To this end a major objective of the AGAVE expedition is the development of autonomous underwater vehicle (AUV) technology for under-ice missions. AUVs are presently being used at an ever-increasing rate to conduct science missions in the open ocean, but their operation under-ice has been limited to deployments from the ice edge, with limited success to this point. AUVs have never been deployed and recovered from an icebreaker within the ice pack, and all of the previous AUV missions under-ice have operated at shallow depths less than a few hundred meters. A major objective of the AGAVE expedition is to develop and demonstrate AUV technology for deep-sea missions within the permanent pack ice.

Ultimately the AUVs must also be capable of acquiring biological samples, particularly for astrobiology missions to Europa. The development of computer vision and dexterous manipulation systems for an AUV is an active area of research in collaboration between WHOI and the University of Maryland's Space Systems Lab, but these systems were not sufficiently advanced to allow for their utilization on the AGAVE expedition. Therefore it was also

necessary to develop a separate wireline platform for imaging and sampling, and the development and demonstration of such a system was a second major engineering objective. In all three new vehicles were developed for the AGAVE expedition. The PUMA AUV was designed to map hydrothermal plumes in the water column. The JAGUAR AUV was designed to conduct high-resolution bathymetric, magnetic, and photographic surveys on the seafloor. The CAMPER wireline vehicle was designed to conduct high-resolution digital imaging surveys and to acquire geological and biological samples from the deep seafloor. The development and demonstration of these three vehicles and the support systems for their operation under-ice constitute the major engineering activities for the AGAVE expedition.

1.3 Field sites

Ultra-slow spreading ridges are characterized by a heterogeneous crustal structure. The generation and delivery of magma is restricted by a relatively cold thermal structure, and tends to be focused to discrete regions along-strike. As a result, some ridge segments have a reasonably well-developed igneous layer, while others are magma starved and consist primarily of peridotite terrains exhumed by tectonic extension. Hydrothermal circulation in these disparate environments is expected to be fundamentally different in nature owing to the differences in thermal structure, host rock substrate, and permeability structure between basaltic (magmatically robust) and peridotitic (magmatically starved) geologic settings.

Intriguingly, evidence of hydrothermal venting in the form of water column plume anomalies was ubiquitous in wireline sensor data from dredges along essentially all portions of the Gakkel ridge during the AMORE expedition in 2001, including tectonic regions with predominantly peridotite exposures on the seafloor. As a result, one of the objectives of the AGAVE expedition was to conduct a direct comparison between venting in basaltic vs. peridotitic settings. To this end two field areas were chosen for plume mapping and seafloor surveys – the 7°E segment, which is a peridotite environment, and the 85°E segment, which is a basalt environment that is believed to have experienced a large magmatic event in 1999. Given the ports of call for the expedition (Longyearbyen to Tromso) it made sense to begin by working at the 7°E site, and then to finish at the 85°E site (Figure 1).

1.4 Cruise report organization

The body of the cruise report text is organized by site, starting with the 7°E site and finishing with the 85°E site. The salient scientific and engineering results are summarized for each site. Four primary assets were employed for our research – a CTD/rosette, the PUMA AUV, the JAGUAR AUV, and the CAMPER wireline system. The technical details of these vehicles, and a comprehensive description of the data and samples that they acquired, are provided in the Appendix. In addition to the oceanographic research, seismometers were deployed on ice floes at each study site by Vera Schlindwein of the Alfred Wegner Institute with the objective of detecting microearthquakes associated with mid-ocean ridge processes. A basic description of the seismic networks is also provided in this report. The Appendix also includes information regarding the multi-beam system used to generate high-resolution bathymetry, the ice drift observed during the experiment and the prediction thereof, and a discussion by the ship's officers regarding the operational strategies employed to enable our vehicle operations.

2. The 7°E Peridotite Site

2.1 Site Background

The 7°E site is located within the 3° - 29°E "Sparsely Magmatic Zone" (Michael et al., 2003), with extensive exposures of mantle peridotite and very little evidence for volcanic activity. The strongest plume signals in this region observed during the 2001 AMORE cruise were found on Healy Dredge 33 (Figure 2), near the top of an elongated ridge along the northern wall of the rift valley (Figure 3). A weaker manifestation of the same plume at ~2800 m was seen on Dredge 32, but not in neighboring profiles at Dredge 34 or at Polarstern station 239. All of these stations recovered peridotite and/or serpentinite mud. Two Polarstern stations on the southern rift valley wall (without associated MAPR profiles) recovered basalt in addition to peridotite.

Multi-beam bathymetric data from the 7°E site was acquired during the AGAVE expedition, but the coverage was only a fraction of the AMORE maps, and no significant differences were observed in regions covered by both expeditions. As a result, the AMORE grids are used as basemaps for this site, unless otherwise noted.

2.2 CTD operations

Locations for the CTD casts described in this section are shown in Figure 4 and tabulated in Appendix B (Table B2.1).

Scientific operations at 7° E began with an intensive CTD program (~48 hours, CTDs 01 – 09) designed to relocate and map the hydrothermal plume observed in three MAPR profiles on the 2001 AMORE cruise. Our efforts focused on an elongated ridge, consisting mostly if not entirely of peridotite, on the northern side of the rift valley. The strongest plume signal on the AMORE cruise was observed at about 2800 m on Dredge #33, ca. 85°01.10'N, 7°26.83'E, with a weaker signal at the same depth approximately 15 km southeast at Dredge site 32.

CTD01 was intended to be a full-depth (~5000 m) cast in the center of the rift valley in order to provide an accurate sound velocity profile for the Kongsberg multi-beam system. In response to ice conditions, however, the cast was conducted on the northern rift valley wall in approximately 4000 m water depth, a few km southwest of all subsequent work at this site.

CTD02 - CTD05 were conducted in a line across the wall of the ridge from about 3200 m to 4000 m water depth, with the stations approximately 2 km apart. CTD02 was occupied very close to the site of HEALY Dredge 33 and showed a small plume (as seen with the temperature and light transmission sensors) between 2850 to 2950 m. Very weak signals appeared in CTD04 and CTD05 as well.

CTD06 was a yo-yo "section" across the slope from about 3620 to 3820 m, west of the line defined by CTDs 02-05. This cast encountered a sharp plume in temperature and light transmission, with temperature anomalies comparable to that observed in 2001, between 2800 and 2900 m. The ship's drift speed decreased to near zero while the CTD was in the heart of this plume, so the cast was ended and the ship was positioned for **CTD07** approximately 0.5 nm down slope. No plume was encountered at CTD07. **CTD08** was an ESE drift approximately 1 nautical mile in length, to the east and mostly down-slope of CTD06, with no plume signal observed.

CTD09 drifted down-slope approximately 0.25 nm, 0.5 nm to the west of and nearly parallel to CTD06. We observed the 2800 m plume, strengthening as we drifted down-slope, but weaker than at any point of CTD06. Again the drift stopped while the CTD was in the plume.

CTD10 - CTD12 were occupied east of CTD06 and west of CTD08. **CTD10** was aborted at 2000 m due to a communications problem with the underwater unit. **CTD11** started down slope of all of the previous plume observations and did not encounter the plume. **CTD12** encountered the plume between 2775 and 2950 m. The overall plume thickness was greater than at CTD06, with more "layering" indicative of proximity to the source observed as well.

CTD13, west of CTD06, was a near-easterly drift of a little more than half a mile. Plume signals were weaker (in terms of temperature anomaly) than those to the east but also appeared layered.

CTD14 reoccupied the drift track of CTD06 but began above and finished below it, completely transecting the plume. The plume occupies an area of only several hundred meters in the N-S direction. An example of the plume signals in temperature and light scattering from CTD14 is shown in Figure 5.

CTD15 was a very rapid (>0.5 kt.) drift to the west of CTD14 (and crossing CTD13) that completely missed the plume by, we believe, passing underneath it.

CTD16 was our last science operation at the 7° E site. It was a deep cast to over 5000 m in the axial valley, to collect samples for microbiology studies. The full-depth profiles of potential temperature and salinity at this background station are shown in Figure 6.

Several water samples for hydrothermal tracers (helium isotopes and manganese) were collected for possible shore-based analysis at stations CTD02, CTD04, CTD06, and CTD08. The gas chromatograph for onboard analysis of methane and hydrogen concentrations was broken while we were at the 7° E site, and these data are therefore not available (the instrument was fixed during the transit to 85° E). All water sampling is summarized in Appendix B.

2.3 AUV operations

The location for the AUV dive conducted at the 7°E site is shown in Figure 7, and vehicle description and dive details are summarized in Appendix C.

The primary objective for AUV operations at the 7°E site was to continue/complete engineering trials for the vehicles. Owing to several factors, and most importantly the cancellation of the engineering trials that were to have been conducted on USCGC Healy in October 2006, neither the PUMA nor JAGUAR vehicle had been through a full cycle of engineering dives. The most pressing issue was the demonstration of deep diving capabilities beneath the ice. Prior to this cruise, the maximum depth under-ice for either vehicle was 150 m, which was achieved during a relatively simple "down and up" dive during the test cruise three weeks earlier.

In preparation for a deep dive, two long-baseline acoustic transponders were deployed down-slope of the dive site (Figure 7) and then surveyed using the helicopter (see Appendix C). Although the primary objective was to conduct an engineering dive, a water column plume surveying mission to follow up the CTD plume mapping data was nevertheless programmed for the PUMA vehicle incorporating ~5 km of horizontal track lines at a nominal depth of 2850 m. The vehicle was ballasted for slightly positive buoyancy and then launched (PUMA 0000) on

July 10, 2007. The vehicle aborted the dive when it reached a depth of 1025 m, approximately 1h 42m into the mission. At this point the vehicle computer rebooted, and came up in a state that allowed it to navigate to an open pool of water near the ship for recovery.

At this point the decision was made to shift the field program to the 85°E site, which, among other things, allowed for a full engineering analysis of the aborted dive. The exact cause of the aborted mission could not be determined, but ballasting and software issues were the most probable candidates. The former issue was addressed by re-ballasting the vehicle prior to the first dive at 85°E, and the latter by cleaning up the vehicle code in a few areas and running the software continuously during the transit.

2.4 CAMPER operations

Locations for the CAMPER dives conducted at the 7°E site are shown in Figure 7, and the dive details are summarized in Appendix D.

Camper completed three dives at the 7°E site (Dives 7, 8, and 9). Along all dive tracks, there was an almost continuous cover of pelagic sediment with abundant animal tracks. Organisms observed included brittle stars (Figure 8), anemones, and shrimp. During dives that occurred higher on the feature (e.g., Dive 9), occasional peridotite blocks were observed outcropping from the sediment and at scarps a few meters high that appeared to be faults along the side of the feature (Figure 9). Samples of sediment were collected both using the mini-corer and the grab sampler (see Appendix D). The recovered sediment was muddy, oxygenated, and absent of infauna. No evidence of hydrothermal activity was detected during any of the CAMPER dives at the 7°E site.

2.5 Seismic operations

A total of 12 seismometers were deployed on 3 ice floes at the 7°E site. Each of the ice floes hosted an array of 4 seismic stations arranged in a triangle with a central station (see Appendix E). The entire equipment for one array could be transported in one helicopter flight. We looked for large multi-year ice floes without large cracks or pressure ridges as suitable seismometer platforms. Depending on the size of the ice floe, the array dimensions were around 1 km. The distance between the arrays was about 15 km. Details of the instrumentation, their installation and the recording parameters are described in Appendix E. The central station of each array was equipped with an ARGOS transmitter to track the array as it drifted with the ice. We received between 4 to 10 ARGOS position reports per day via email with a location error less than 350 m. This information, in combination with ice drift buoy data from the ship (see Appendix E), allowed for sufficiently accurate predictions of the array locations to enable recovery with the helicopter, even in conditions with poor visibility. The arrays drifted perpendicular to the strike of the rift valley from the northern to southern flank during 4.3 days of continuous data acquisition (Figure 10).

3. The 85°E volcanic site

3.1 Site Background

Six dredge stations, two rock core stations, and one CTD cast (Figure 11) were conducted by USCGC *Healy* near the volcanic center at 85°E during the 2001 AMORE cruise (Polarstern did not accompany Healy this far east.) At all of these stations, evidence of a large (~1000 m thick) plume was observed in light scattering and temperature centered at ~2500 m (Figure 12). Evidence for deeper (~3200-3800 m) plume(s) was seen most clearly on Dredge 64 and rock cores 15 and 16. The size and chemical characteristics of the 2500 m plume looked very much like the "event plumes" observed in the NE Pacific (Graham et al., in prep.), suggestive of very recent or ongoing volcanic activity during the observation period in 2001. A teleseismically recorded earthquake swarm in 1999 (250 events in 7 months) suggested that this site experienced a volcanic eruption at that time. The large magnitude of the earthquakes and the duration of the swarm are exceptional for mid-ocean ridge volcanic episodes. Evidence for an eruption in 1999 is also provided by high-reflectivity acoustic backscatter returns observed by the SCICEX program over large areas of the axial valley. In 2001, a swarm of 200 explosive sounds from the seafloor was detected by seismic stations on nearby ice floes, which provides additional evidence for active volcanism during the 2001 field season (Schlindwein et al., 2005).

During multi-beam operations on this cruise we discovered a new chain of volcanoes within the axial valley, south of the central volcanic ridge (Figure 13). We named this chain the Asgard Volcanic Chain, as Asgard is the home of the gods in Norse mythology. We named the primary three volcanoes in the Chain – Oden, Thor, and Loke, to honor the crew of Oden, who provided fantastic shipboard support for our science. In addition, we named the two prominent ridges in the center of the axial valley, where much of our work was conducted, in honor of Jessica Hill and Stephen Duque – two crewmen from the Healy during the AMORE expedition who died in a tragic diving accident under the ice in 2006.

3.2 CTD operations

Locations for the CTD casts described in this section are shown in Figure 13 and tabulated in Appendix B (Table B2.2).

Science operations at 85°E began with twelve hours of CTDs (CTD17 - CTD19). We chose to focus the initial surveys on the area of the strongest plume signals observed on the 2001 AMORE cruise. CTD17 – CTD23 were all conducted on and around Jessica's Hill on the central volcanic ridge. **CTD17 – CTD19** encountered small (0.5 – 5 mV) Eh anomalies indicating the presence of relatively fresh hydrothermal fluids, along with anomalies in temperature and light transmission. The largest anomalies were observed at depths of approximately 3500-3550 and 3300-3400 m for CTD17 and CTD18, respectively, with the different depths suggesting the possibility of multiple sources. **CTD20** was an opportunistic short cast north of Jessica's Hill, with no plume anomaly. **CTD21**, near the SW base of Jessica's Hill, exhibited a temperature anomaly centered at 3500-3550 m but exhibited no Eh signals. **CTD22** was a yo-yo drift across the top of the hill, intersecting the start of CTD17 near its end. This cast exhibited temperature anomalies centered both at 3350 (more pronounced at the southern, upslope end of the drift) and at 3500 m, and a very small (<0.5 mV) Eh excursion near 3400 m on the final downcast. A water

sample collected on the ensuing (final) upcast at 3350 m exhibited a methane concentration of 19 nM. **CTD23** began on the southwestern flank of the hill and drifted to the NNW, towards CTD17 and down slope of CTD22. Eh excursions of up to 26 mV, centered at 3400-3500 m, were observed on all portions of the yo-yo, with the strongest anomalies at the beginning (southern) part of the drift. Methane and hydrogen concentrations also decreased from south to north, with maximum concentrations of 125 nM CH_4 and 14 nM H_2 observed on the first upcast of the yo-yo.

After CTD23, a large, multi-year, ice floe moved into the study area and blocked access to the region surrounding Jessica's Hill for several days. As a result, it was necessary to shift the focus of our operations to other parts of the 85°E segment.

CTD24, which contained no plume signals, was conducted southwest of the central volcanic rift. The full depth temperature and salinity profiles at this station are shown for reference in Figure 14.

CTD25 – CTD28 were conducted on and around Duque's Hill, southeast of Jessica's Hill. **CTD25**, along the eastern side of the hill, contained a temperature peak near 3550 m on the first downcast but no Eh anomalies. **CTD26,** a NW drift along the western slope at about 4000 m, encountered the largest Eh excursion of any CTD cast on this cruise (~47 mV) between 3400 and 3800 m, on the first downcast. Methane concentrations on the ensuing upcast, where plume signals were already weaker, reached 44 nM. The hydrogen concentration in the same sample was 6.4 nM. Following PUMA Dive 002, **CTD27** took a westerly drift down the western slope of Duque's Hill, passing to the south of the area of the PUMA dive that had strong Eh signals. Plume signatures were observed in temperature and light scattering below 3500 m but the Eh anomalies observed on this yo-yo were only on the order of 1 mV. **CTD28** began at the top of the hill and drifted WNW, approximately parallel to and upslope of CTD26. Eh anomalies of over 15 mV, at ~3700 m, were seen near the top of the hill, and dissipated along the track of the yoyo. The cast was terminated before encountering the CTD26 plume. **CTD31** was a long traverse of Duque's Hill, crossing it from east to west and extending almost to Oden volcano. The largest Eh anomaly was only about 1 mV, and was encountered near the largest CTD26 signal of ~50 mV. **CTD34** was a short cast (two yoyos) uphill of CTD26 and also encountered weak plume signals.

CTD29 was a long cast with a NW drift taken across the northern axial valley wall. A plume signal at 3800-3900 m depth was detected when this cast crossed into the axial valley, strengthening steadily to the end of the cast, with a maximum Eh excursion on the final downcast of 16-17 mV.

CTD30 and **CTD32** both crossed portions of the small, circular volcanic feature at the SE end of Duque's Hill. **CTD30** began in the center of the feature, encountering a plume in Eh, temperature, and light scattering that began at 3600 m and extended to the bottom (~4000 m). A plot of dEh/dt versus pressure from this cast is included as Figure 15. Hydrogen concentrations in excess of 100 nM were measured at 3800 m, with accompanying methane concentrations of only about 20 nM. The strength of the plume signature decreased as the cast drifted to the western side of and off the feature. Later, **CTD32** crossed this feature to the north of CTD30, and encountered only a weak (<1 mV) Eh excursion, no measurable hydrogen, and ~8 nM methane.

CTD33 and **CTD35** each traversed Oden volcano from east to west. The first downcast of CTD33, on the eastern edge of the feature, revealed a 45 mV excursion in Eh between 3200 and 3700 m. Methane concentrations were in excess of 150 nM and hydrogen at least 40 nM. It is important to note that these samples were collected near the beginning of the cast, more than four

hours before the rosette came on deck, and so the hydrogen concentrations may actually be significantly higher. Near the end of the cast, on the western flank of the volcano, we encountered strong temperature (0.03°C), light scattering, and Eh (70 mV) signatures in the bottom 10 m. This sample had 95 nM methane and no measurable hydrogen. Plots of temperature, Eh, and light scattering for the first and fifth yo-yos of this drift, as well as dEh/dt for the full drift, are shown in Figure 16 and Figure 17, respectively, to illustrate the two types of plume signatures encountered. Plume signals in the eastern part of **CTD35** were clear but generally weaker (e.g., 5 mV Eh) than at CTD33 to the north, but appeared in two distinct layers at about 3300 m and 3700 m, and measured methane in excess of 200 nM but very little hydrogen. These plume signals dissipated to the west. A stronger (~20 mV Eh), deeper (~3800 m) plume appeared about a third of a mile west of Oden volcano.

CTD36 drifted across the northern edge of Loke volcano. A plume similar to those observed on the eastern side of Oden volcano, but with only ~2 mV Eh anomalies, was observed east of Loke between about 3500 m and 3700 m. A near-bottom anomaly (10 mV, ~4000 m) was observed later in the cast.

Water samples collected at several of these stations were analyzed for methane and hydrogen on board, and collected/processed for shore-based determinations of helium, manganese, iron, particle chemistry, microbiology, and protists/protozoans, as detailed in Appendix B.

3.3 AUV operations

The locations of the AUV dives conducted at the 85°E site are shown in Figure 18, and vehicle descriptions and dive details are summarized in Appendix C.

AUV work at the 85°E site began with PUMA dive 001 to map the water column plume observed on Jessica's Hill in the CTD data. Two transponders were deployed on the east side of Jessica's Hill in preparation for the dive, and the transponders were surveyed with the helicopter (see Appendix C for details). The dive was programmed as a zigzag across the hill from south to north with a 'yo-yo' depth profile varying between 3200 to 3550 m (Figure 19). Time-series sensor data for PUMA dive 001 is shown in Figure 20, and spatial data is shown in Figure 21. In general, the vehicle was in a plume whenever the depth was below about 3300 m (down to the bottom of the profile at 3550 m), with a fairly constant potential temperature anomaly of ~0.04°C and an optical backscatter anomaly of ~30 mV. Eh during the dive was nearly constant except for a fairly sharp anomaly of 40 mV on the southwest side of Jessica's Hill (Figure 21).

The results of the CTD casts and PUMA dive 001 suggested the next PUMA dive should be focused on the southwest side of Jessica' Hill, where the Eh anomaly was observed, but a large, multi-year ice floe moved into the study area that prevented field work on and around Jessica's Hill for several days. In response it was decided to temporarily shift operations to the next topographic peak to the south, Duque's Hill. PUMA dive 002 was designed to follow up on CTD26, which detected the largest Eh anomaly of any CTD cast during the cruise (~47 mV) on the southwest side of Duque's Hill (see Figure 13). The dive was programmed as a zigzag mission along the southwest side of Duque's Hill at a constant depth of 3650 m. In order to test the LROBS (Long-Range Optical Backscatter Sensor) two down and up 'pogos' were added to the mission on the 3rd and 6th legs of the zigzag, where the vehicle was programmed to drop down XXX m to search for a buoyant plume stem. Because the vehicle was not controlling X-Y position during the descent, the torque of the vertical propeller would naturally spin the vehicle,

allowing the LROBS sensor to do an azimuth scan for a plume stem. It was necessary to deploy an additional transponder to enable long-baseline navigation for this dive.

The tracklines and depth profile for PUMA dive 002 are shown in Figure 22. The vehicle was not able to complete the mission because the pin connecting the propeller to the vertical thruster shaft sheared off during the dive. This prevented the vehicle from being able to conduct the 'pogo' legs, and ultimately prevented the vehicle from being able to complete the last (6^{th}) leg of the zigzag because it was unable to hold depth. Time-series data from the dive is shown in Figure 23, and the corresponding spatial data is shown in Figure 24. The largest plume anomalies were observed during the 3^{rd} and 4^{th} legs of the mission. Potential temperature anomalies reached 0.04°C with a corresponding optical backscatter anomaly of 10 mV on these legs. An Eh anomaly of ~60 mV was observed on leg 3, which was the largest Eh anomaly observed during AUV dives.

The combined data from CTD26 and PUMA002 appeared to constrain the source of the plume material on the SW side of Duque's Hill to an approximately 1 x 1 km region. PUMA dives 003, 004, and 005 were therefore programmed to better constrain the gradients and source position within this region. It was necessary to attempt this dive three times because the vehicle aborted and returned home during the descent of the first two tries. The cause for the aborted dives was a software problem that was not diagnosable based on the available data, but which had to do with the mission logger. Although the cause was not ultimately determined, it was possible to treat the 'symptoms' by running the sensor drivers and data loggers as separate processes on the CPU. This fix worked, but it did not allow for the LROBS sensor to be used, as it required a direct interaction with the main mission process so that the photomultiplier aperture could be opened and the laser started at the proper depth.

A small aperture zigzag mission with maximum trackline offsets of ~150 m was programmed with a nominal survey depth of 3700 m, which represented a 50 m depth increase compared to PUMA002. The idea was to get data from the bottom of the neutral plume to increase the chance of seeing gradients leading towards a source. A fourth transponder was deployed to allow for operations at this depth, because one of the other transponders would be shadowed by Duque's Hill for the mission. The tracklines and depth profile for PUMA005 are shown in Figure 25. The time-series sensor data and corresponding spatial fields are shown in Figure 26 and Figure 27, respectively. To our surprise, the plume anomalies in the sensor data from PUMA005 are relatively weak, and do not reach the levels observed in PUMA002, in spite of the fact that some of the same areas were surveyed. Maximum potential temperature, optical backscatter, and Eh anomalies during PUMA003 were 0.02°C, 8 mV, and ~5mV, respectively, and were located towards the top of Duque's Hill, rather than on the southwestern flank, as observed in PUMA002. One possible explanation is the difference in depth (3650 vs. 3700), but this is not consistent with the CTD plume anomalies in this region, which extend from 3300 to 3900 m, and also does not explain the spatial difference in the sensor data between PUMA002 and PUMA005. The most likely explanation appears to be time-space variations in the plume signal, itself. The plume anomaly observed on the southwestern side of Duque's Hill appears to have been advected from further southeast within the axial valley. Unfortunately, the cruise timeline called for a shift from plume mapping to seafloor mapping and surveying after the end of PUMA0035, and it was not possible to follow-up on this possibility.

JAGUAR dive 001 was programmed to conduct a microbathymetric and magnetic survey of a small, circular volcanic feature to the southeast of Duque's Hill. Plume anomalies in temperature, backscatter, Eh, and hydrogen were detected over this feature in CTD30, and they

extended essentially all the way to the bottom suggesting that it might be a source region. The AUV also carried a CTD and an Eh sensor to allow for plume detection and mapping during the bathymetric survey. Initially it was desired to also conduct a photographic survey at the end of the dive, but the strobe triggered the emergency acoustic relay transponder that was added to the vehicle when the emergency modem was broken during recovery for JAGUAR 000. This triggering would have compromised long-baseline navigation during the dive, so the photographic portion of the survey had to be deleted. The tracklines and depth profile for JAGUAR001 are shown in Figure 28. The vehicle began the bottom-mapping mission ~200 m east and ~50 m north of the desired starting point, and the individual tracklines are roughly 50% of the desired length owing to a disparity between actual vs. expected speed during the survey. As a result of these issues, the surveyed area was offset and somewhat smaller than the programmed mission. A preliminary microbathymetric map from the survey is shown in Figure 29. As can be seen from the plume mapping sensor time-series and spatial data from the survey (Figure 30 and Figure 31, respectively), no significant plume anomalies were detected. Attitude data and 3-components magnetometer data from the survey are shown in Figure 32 and 33, respectively. The magnetometer data requires further processing before the sub-surface character can be estimated.

JAGUAR dive 002 was programmed to conduct a microbathymetric, magnetic, and photographic survey of the southwest side of Duque's Hill. The issues with the strobe triggering the relay transponder were addressed by disabling the transponder (since it could be acoustically enabled, if necessary in an emergency), so that a photographic survey was again possible. Unfortunately, the vehicle exceeded its maximum depth threshold of 4200 m during the survey, at which point it went into a mode where it held it's altitude at 20 m off the bottom until its batteries ran out some 19 hours later. It appears as though the .config file for the PAROSCI depth sensor was off by ~3% for water density, which amounted to an error of ~120 m at 4000+ m true depth, and that this difference explains the triggering of the depth threshold, because according to the multi-beam maps the survey depth should never have exceeded 4150 m. Attempts to send an 'abort to home' command during this time period with the acoustic modem failed because of the vehicle's proximity to the acoustically reflective bottom. As a result the vehicle eventually floated to the surface without battery power. The relay transponder was enabled such that the vehicle could be tracked, and a helicopter survey revealed its position in a small pool within the pack ice. The vehicle was then recovered and airlifted to the ship using the helicopter. With only two days remaining until the end of station time, it was not possible to recharge the batteries in time for another AUV mission.

3.4 CAMPER operations

Locations for the CAMPER dives conducted at the 85°E site are shown in Figure 34, and the dive details are summarized in Appendix D.

Camper completed 13 dives (CAMPER Dives 10-22) on several targets in the 85°E area, including Duque's Hill, and the Oden and Loke volcanoes in the newly discovered Asgard volcanic chain. The explored 85°E area is dominated by relatively young volcanic lava, showing morphologies varying from large pillows hosting delicate surface ornamentation to lobates and long tubes, to fresh sheet flows **(**Figure 35**)**. In much of the area, the upper surfaces of the volcanics had a layer (up to a few cm thick) of fresh volcanic glass "sediment" **(**Figure 36**)**

suggestive of explosive volcanic activity in the "recent" past. Samples of both the lava flows and the volcanic glass "sediment" were collected.

Dives within the small box surveyed by PUMA002 and PUMA005 revealed areas localized between 4000-4020 m where 1 to 3-feet long hexactinellid sponges were abundant, not only anchored to the top surfaces of rocks, but also on lower parts of the rocks and protruding into the interstices between the large pillows. Other organisms in this area included benthic amphipods, shrimp, and anemones **(**Figure 37**)**. Rocks in this area appeared older than those along the Asgard volcanic chain to the southeast.

On both the Oden and Loke volcanoes to the southeast, microbial material and the (perhaps inorganic) areas around them were designated as fields or pockets of: 1) yellow "fluffy" material that appeared to be very thick (>10 cm) in places, and 2) yellow "pebbly" material that may represent older microbial mat or inorganic material, remnant of past microbial activity **(**Figure 38**)**. Samples were obtained of both types of material. These areas of microbial mats were often associated with weak temperature (e.g., 0.07°C) and Eh anomalies (up to 80mV) in the water immediately above, or sometimes adjacent to, them. The undersides of the rocks adjacent to the microbial mats were stained a vivid orange-brown color, suggesting they had been preferentially altered. This suggests that the microbial mat material may be sustained by weak fluid discharge from cracks in the young volcanic surfaces.

Macrofaunal samples, including sponges and amphipods, were preserved for shore-based studies, including DNA sequencing, phylogenetic analyses, and taxonomic identification in the Shank lab. Water and microbial samples were preserved for genetic and culturing studies in the Helmke lab. Humphris processed all rock samples for lava dating and chemical analyses at WHOI.

3.5 Seismic program

The same survey setup as described for the 7°E survey site was used for the 85°E site (Appendix E). Due to the longer survey duration and to some extent rapidly drifting ice, we had to redeploy the seismic stations twice, resulting in 3 drift paths for each array (Figure 39). The redeployment kept the arrays close to the volcanic complex, and also prevented their drifting out of the 20 nm operational range of the helicopter. In total, we acquired 16 days of data.

4. Education and Outreach Program

During the AGAVE cruise, a communications team – a science writer, a photographer, and a videographer, supported by web and graphics professionals at Woods Hole Oceanographic Institution (WHOI) – reported on the expedition on a daily basis through two websites, each with different objectives and audiences.

Dive and Discover (www.divediscover.whoi.edu) was created in 2000 by Susan Humphris and Dan Fornari (WHOI Geology & Geophysics Dept.) and the Web and Graphics Department to immerse students in the excitement of exploring the oceans. It is targeted mainly at middle-school students (Grades 6-8) and the general public, but is structured to provide multiple layers and levels of information to cover a wide range of educational experience. The backbone of the site is a series of educational modules that address basic science concepts central to marine science and research being conducted at sea. Prior to the AGAVE cruise, a new module was

developed to address Arctic oceanography, the history of Arctic exploration, and the Arctic ecosystem with funding from the NASA Astrobiology Program. During the AGAVE cruise – the eleventh to be featured as a ***Dive and Discover*** cruise, and funded by NASA, NSF Office of Polar Programs, and WHOI's Deep Ocean Exploration Institute – the site provided daily updates on the progress of the cruise with slide shows, videos and animations, explanations about the technology being used, and general information about life at sea and the scientists, engineers, and mariners that make oceanographic research possible. In scientists responded directly to e-mails sent to a "Mail Buoy" on the ***Dive and Discover*** website. During the cruise, there were 148,000 hits on the site with an average visit duration of 11 minutes.

The ***Polar Discovery*** website (www.polardiscovery.whoi.edu) is part of a project called "Live from the Poles" that is designed to heighten public awareness of the Arctic and Antarctic environments during International Polar Year. AGAVE was the second in a series of four expeditions that this project will cover through funding from the NSF-EHR Informal Science Education program and the Richard King Mellon Foundation. During the cruise, ***Polar Discovery*** told the story of the research and engineering activities through daily photo essays, as well as video clips, animations and responses to e-mails from the public. During the cruise, there were 29,290 hits on the site with an average visit duration of 9 minutes. In addition, live satellite phone question-and-answer sessions were conducted with broadcast partners, and with natural history and science museums across the US and in Sweden (Table 1) to audiences that ranged from the general public, to teacher and student summer programs.

Institution	Date	Program time	Audience	Contact person	Speaker
1. NPR SciFriday	7/6	2-2:40pm EST	Radio listeners	Ira Flatow Karin Vergoth	Rob Reves-Sohn, Tim Shank
2. Birch San Diego, CA	7/9	7-8pm PST	General public, mostly adult	Debbie Zmarzly	Hedy Edmonds
3. Field Chicago, IL	7/14	11am-12pm CST	Family	Kulsoom Ghias Brian Droege	Hanu Singh
4. SERC Edgewater, MD	7/17	2:45-3:15pm EST	Teachers, students	Mark Haddon	Susan Humphris
5. 6. Teknikens Hus Sweden	7/17 7/24	12:30pm CEST 12:30pm CEST	Museum visitors	Britt-Marie Forslund	Peter Winsor
7. 8. CMNH Pittsburgh, PA	7/27 7/28	12-1pm EST 1-2pm EST	Teachers & summer camp General public	Kerry Handron	Susan Humphris & Clay Kunz Peter Winsor & Chris Murphy
9. LSC Jersey City, NJ	7/28	2:30-3pm EST	General public	Karen DeSeve	Hedy Edmonds
10. PaSC Seattle, WA	8/2	2:30-3pm PST	Robot summer camp	Mark Latz	Hanu Singh & Frank Weyer
11. Michigan State U/ KBS	8/3	1:30-2:30pm EST	Teacher workshop	Laurel Hartley	Susan Humphris
12. MoS, Boston, MA	8/8	2:30-3pm EST	General public	Greg Murray	Rob Reves-Sohn, Tim Shank

Table 1. Live Museum Talk Schedule During AGAVE

Figures

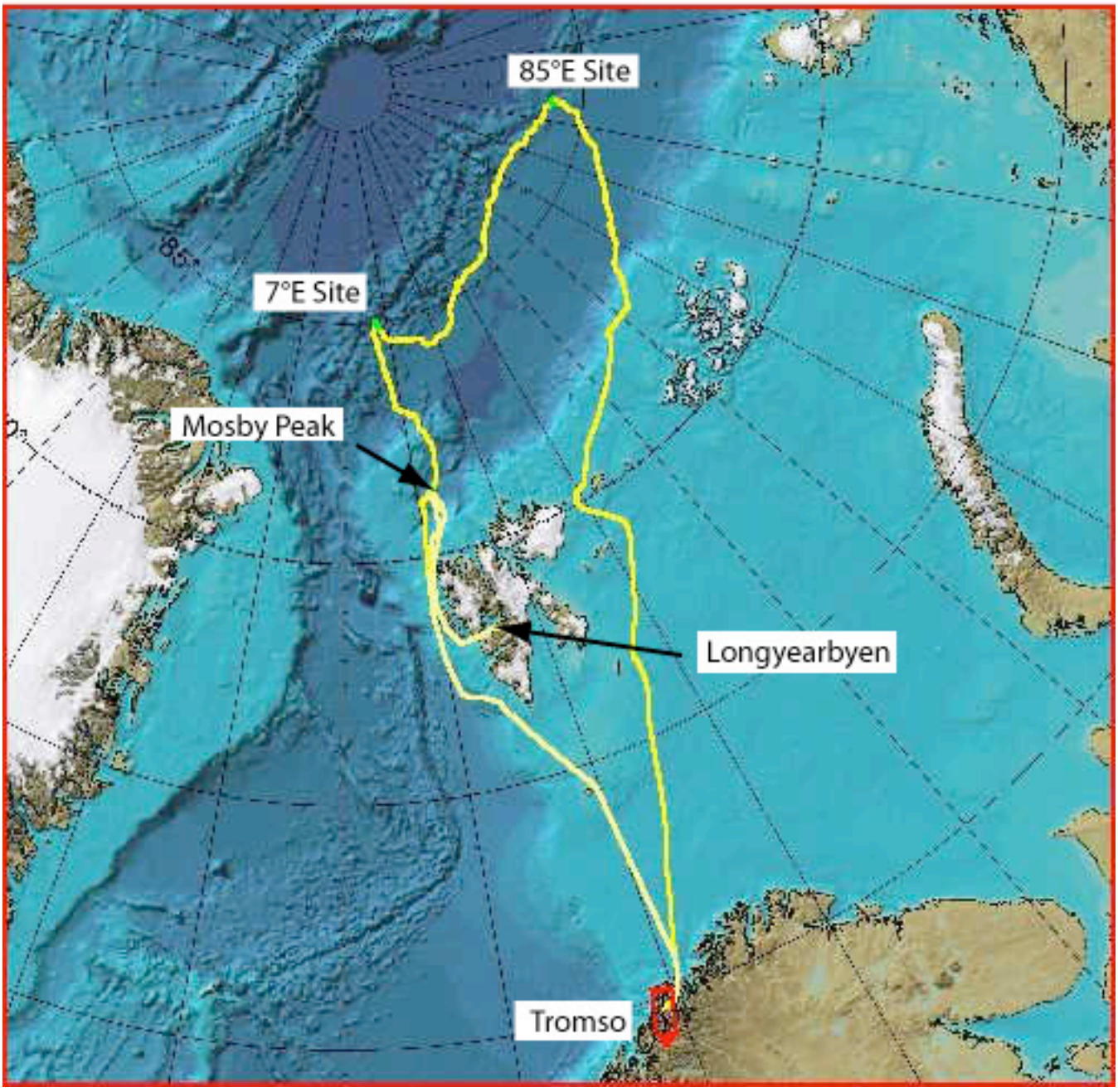

Figure 1. Oden's tracklines during the AGAVE test leg to the Mosby Peak (Tromso to Longyearbyen) and the AGAVE leg to the Gakkel Ridge (Longyearbyen to Tromso).

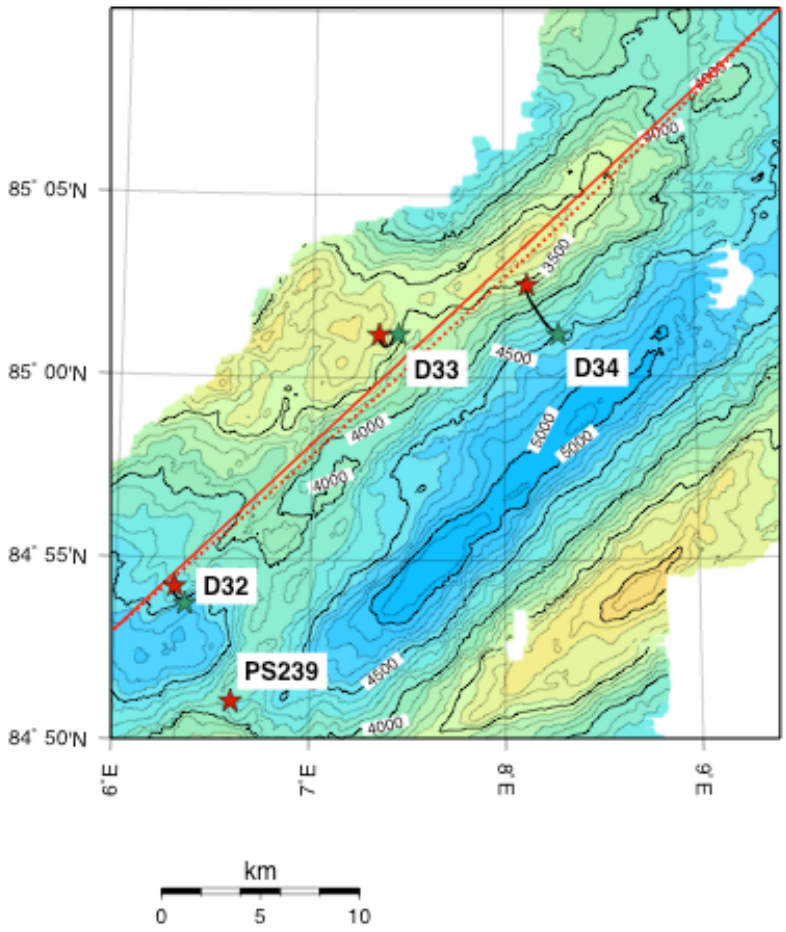

Figure 2. Detail map of the 7.°E study site indicating AMORE station locations (Dxx for Healy dredge sites, PSxxx for Polarstern). Adapted from Baker et al. (2003).

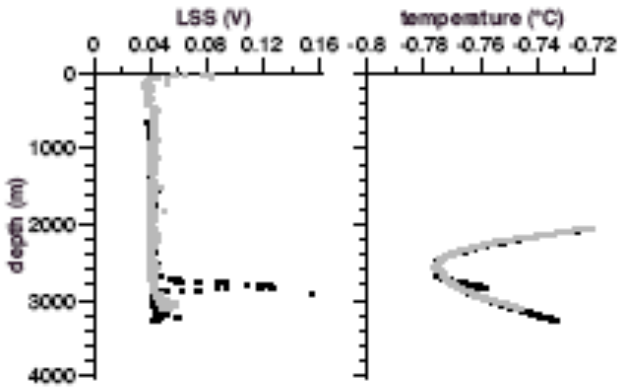

Figure 3. MAPR profiles, at Healy Dredge site 33, of optical backscatter (voltage output from Seapoint Turbidity Meter) and in situ temperature. In each panel, black is used to represent data from the downcast, and grey the up cast, of the dredge. From Edmonds et al. (2003), Supplementary Information.

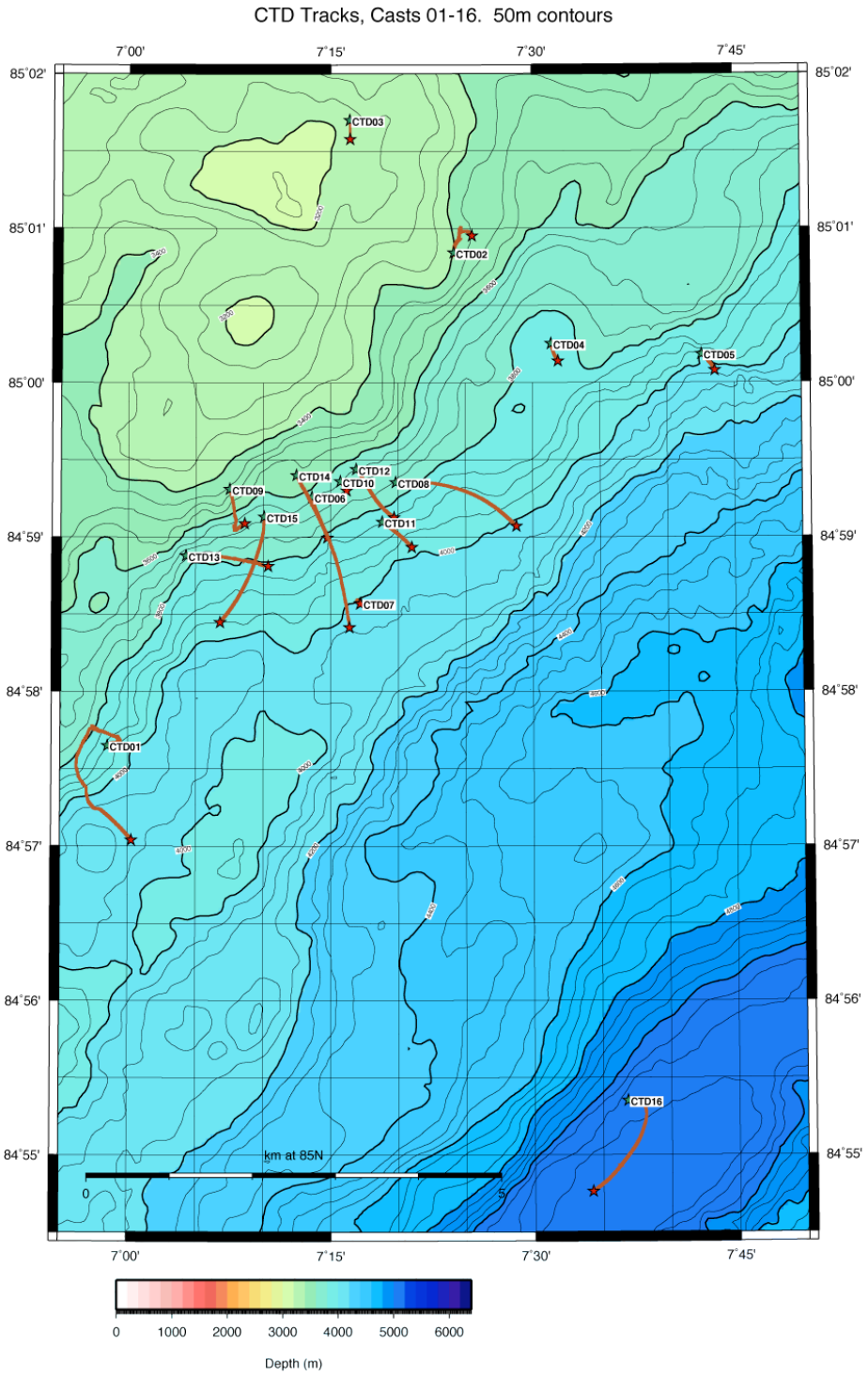

Figure 4. CTD tracklines (of ship position, not CTD position) from 7°E site. Casts start at green stars, and end at red stars. Bathymetry from AMORE cruise.

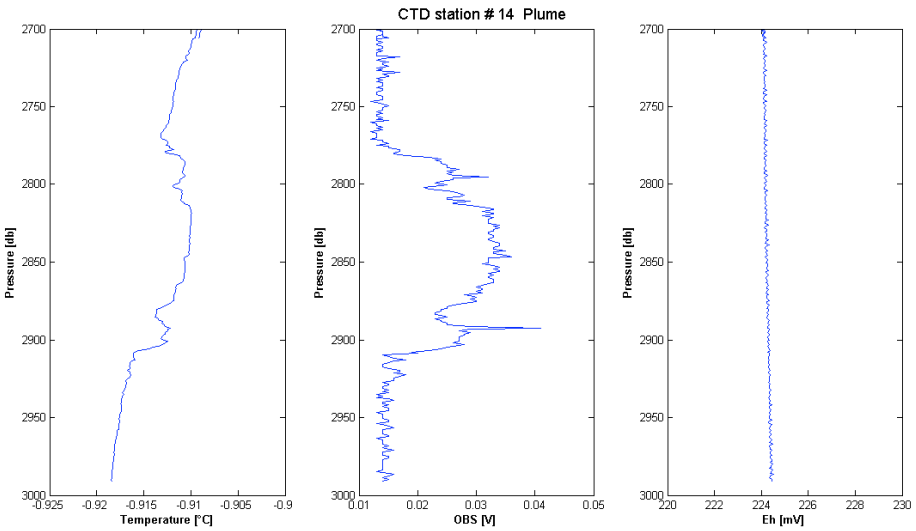

Figure 5. Example of plume signal at 7°E site from CTD14 (note that depth interval extends from 2700 to 3000 m).

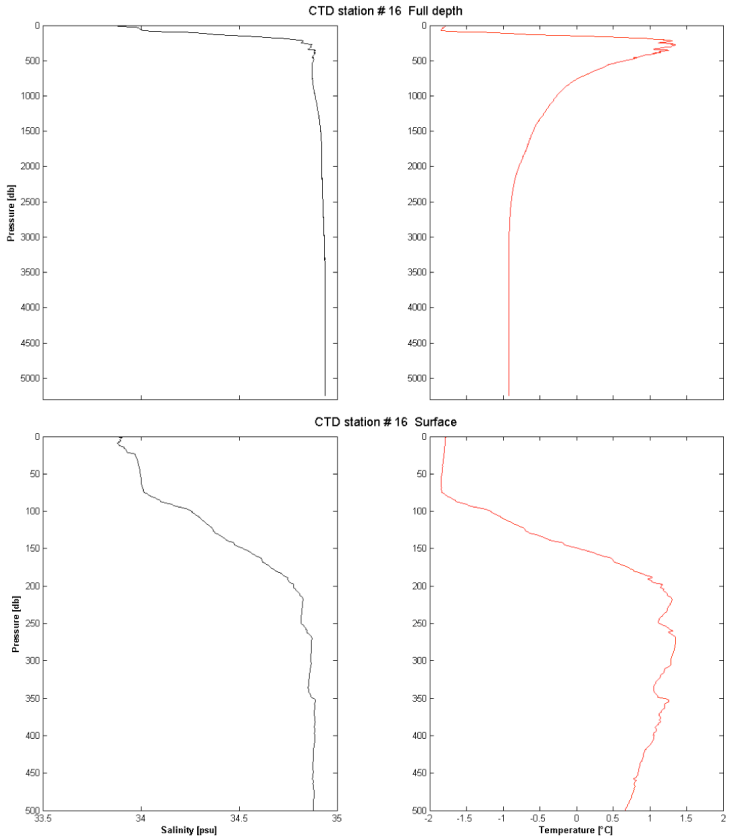

Figure 6. Example of the background temperature and salinity profiles from the 7°E site from CTD16. Top panels are full depth cast, and lower panels zoom in on upper depth interval from 0 - 500 m.

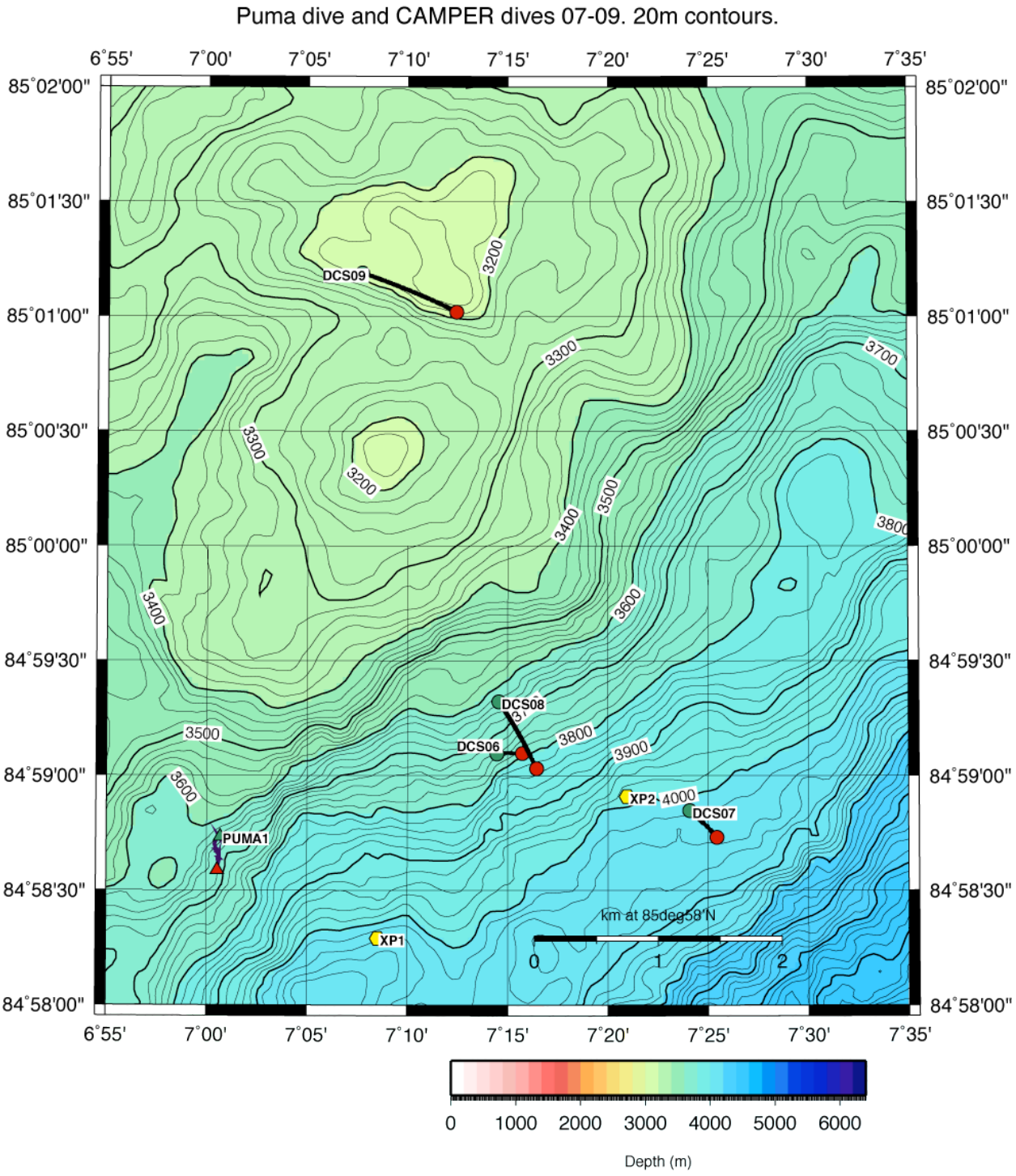

Figure 7. AUV and CAMPER tracklines from the 7°E site. Starting points are green (circles for CAMPER dives, labeled DCSxxx, triangle for AUV dive, and ending points are red). Transponder locations shown as yellow circles. Bathymetry from AMORE maps.

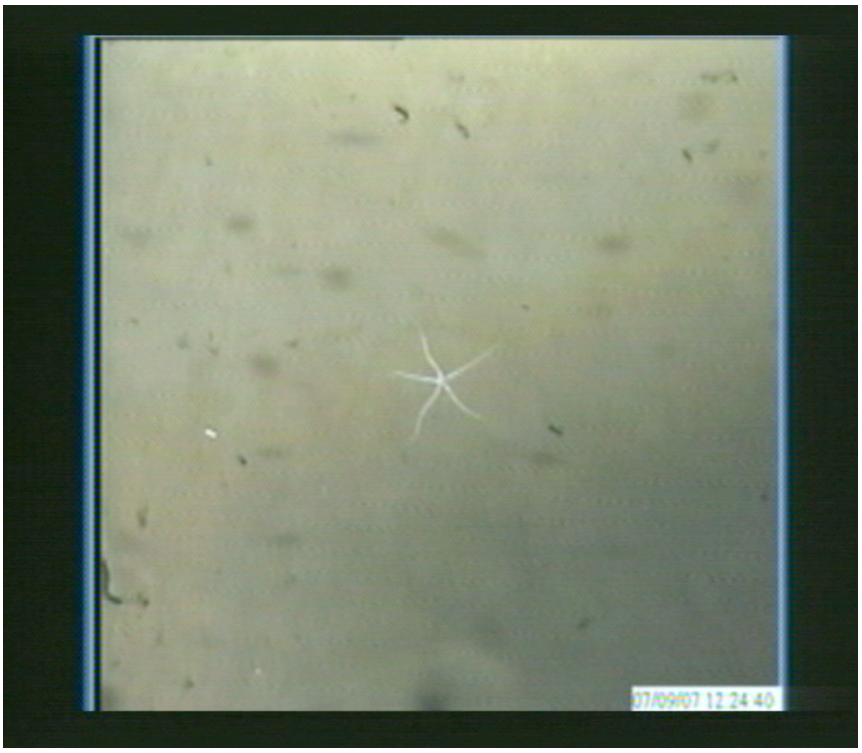

Figure 8. CAMPER frame grab of a brittle star observed at the 7°E site.

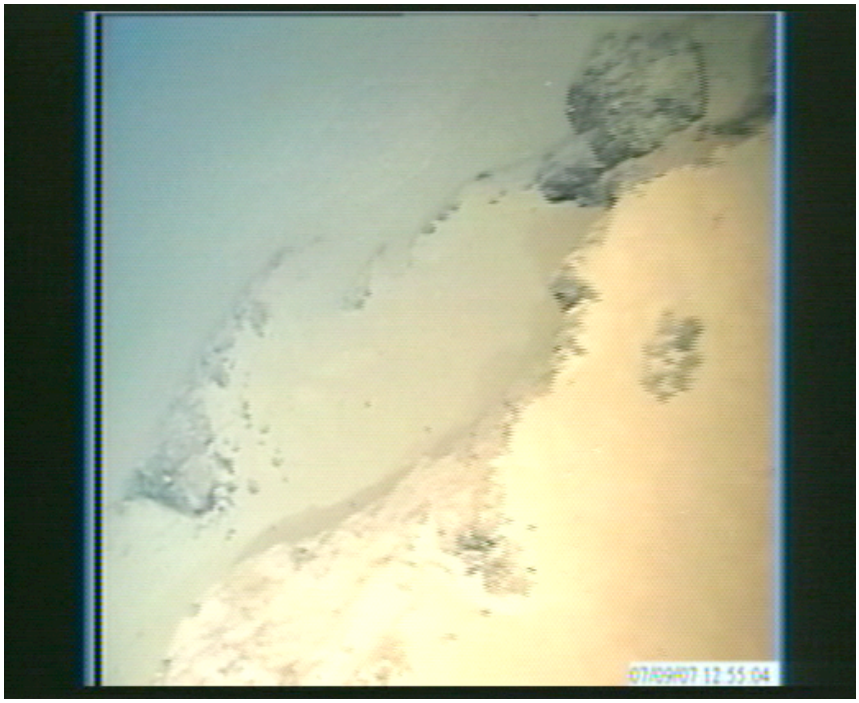

Figure 9. Frame grab of a sediment covered peridotite outcrop from the 7°E site.

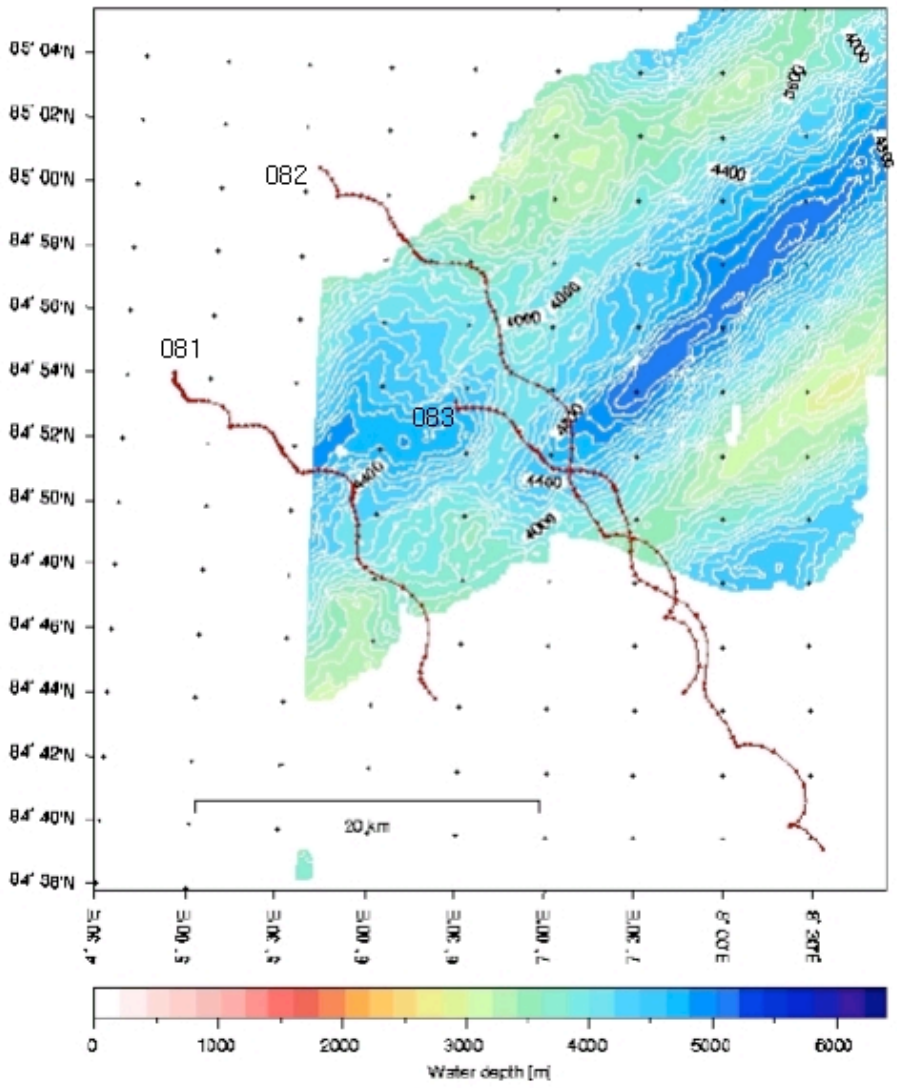

Figure 10. Drift patterns of seismic networks deployed at the 7°E site.

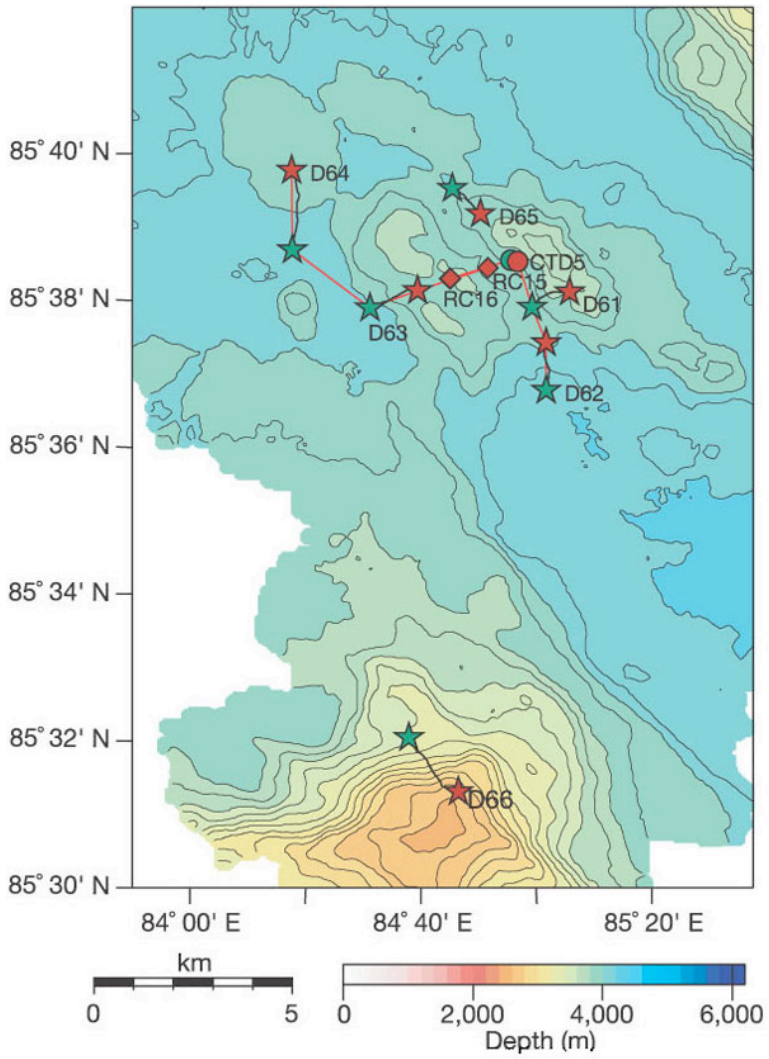

Figure 11. Area map of the 85°E study site indicating Healy0102 station locations (Edmonds et al., 2003).

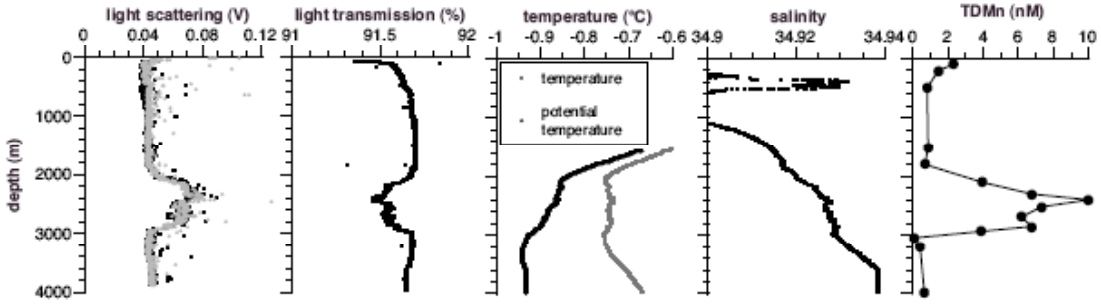

Figure 12. “Sections” of a) light scattering and b) temperature along the line indicated in Figure xx. c) Data from Healy0102 CTD05, at the 85E volcanic site. Edmonds et al. (2003).

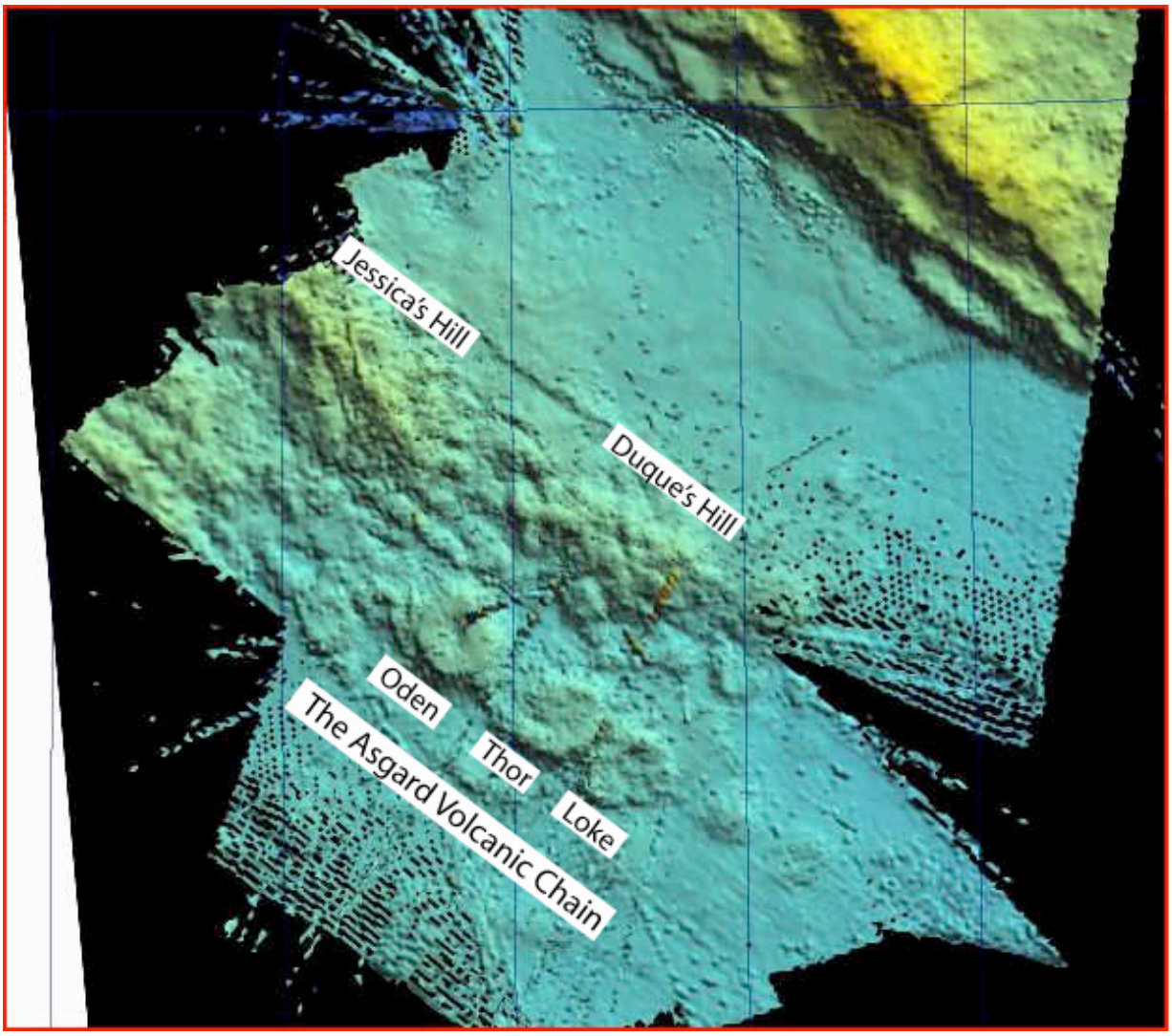

Figure 13. Preliminary bathymetry of 85°E site showing the Asgard Volcanic Chain.

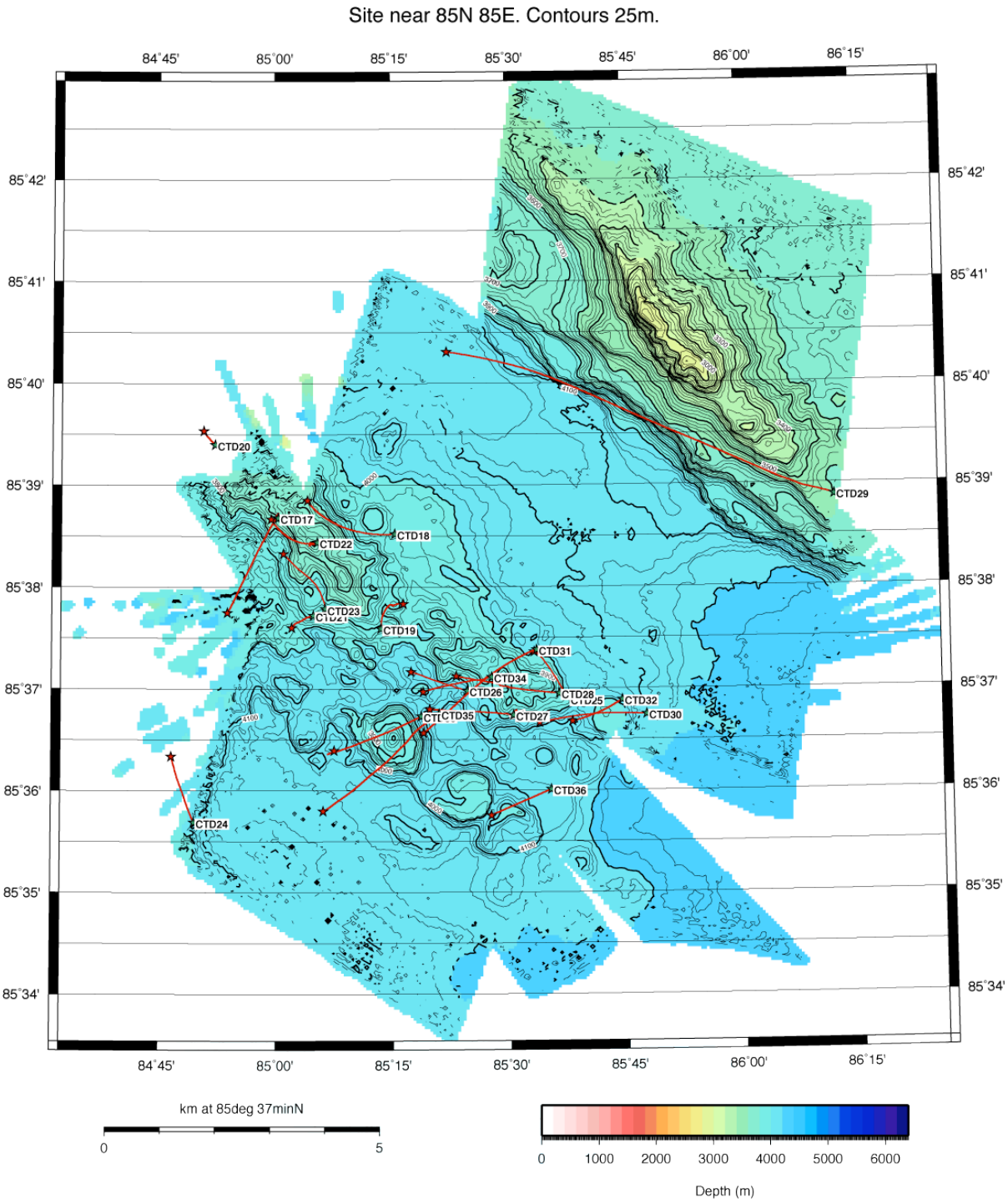

Figure 14. CTD tracklines (of ship position, not CTD position) from 85°E site. Casts start at green stars, and end at red stars. Un-processed bathymetry from AGAVE cruise.

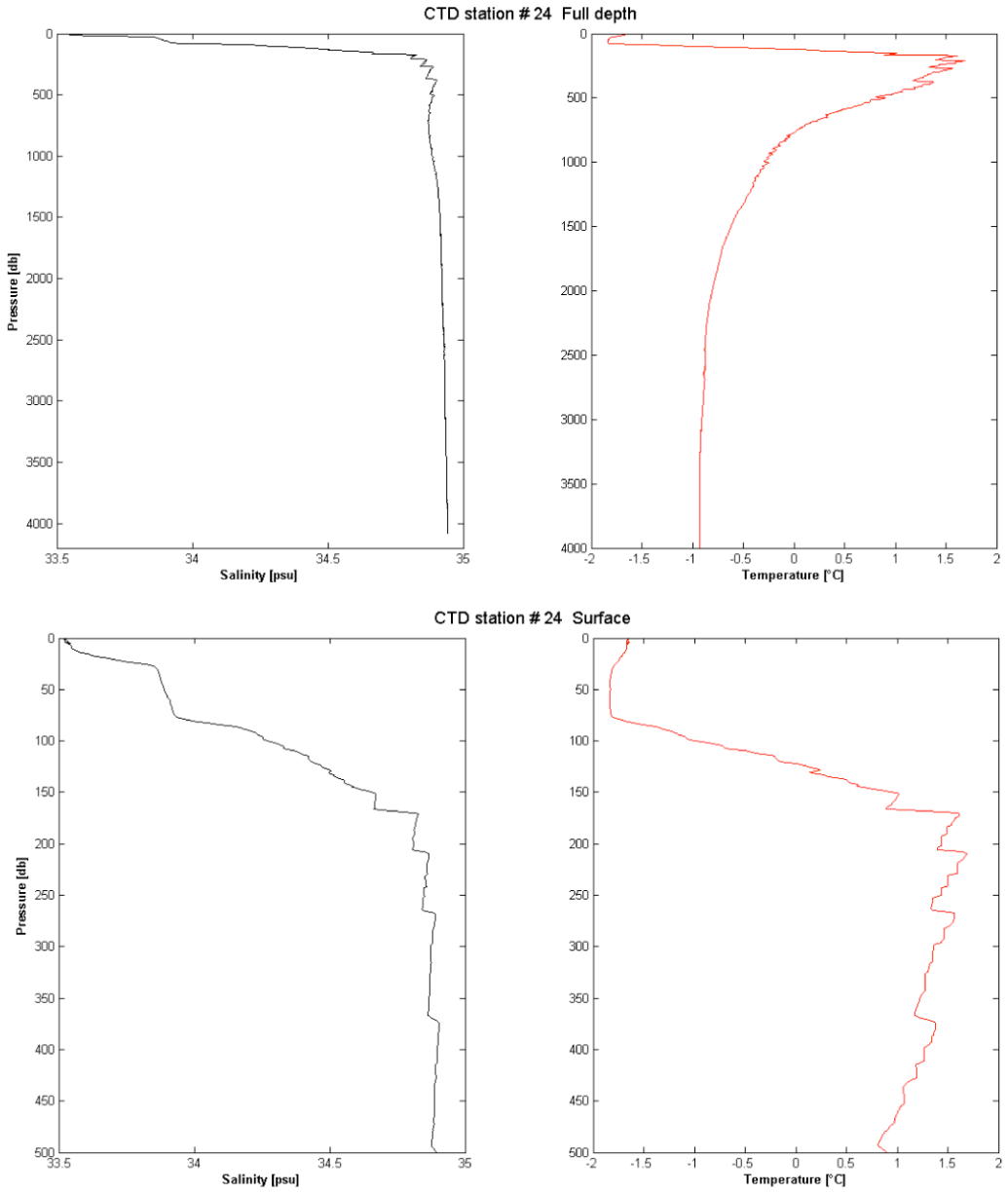

Figure 15. Example of the background temperature and salinity profiles from the 85°E site from CTD24. Top panels are full depth cast, and lower panels zoom in on upper depth interval from 0 - 500 m.

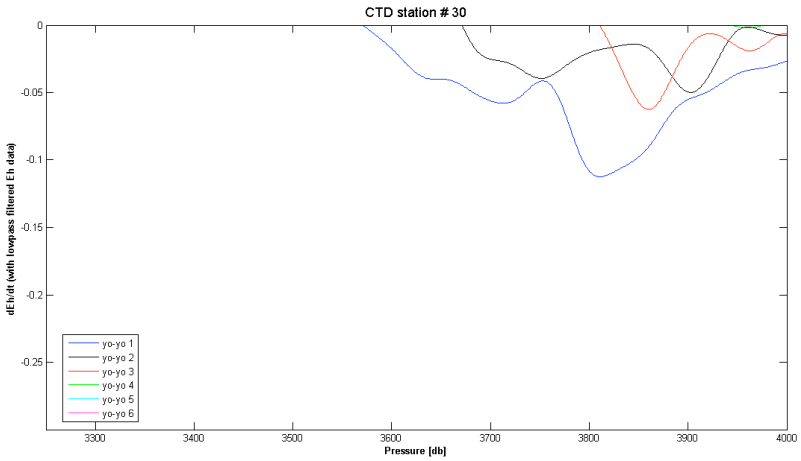

Figure 16. Change in Eh signal with respect to time (dEh/dt) for CTD cast 30, taken on a drift across the small volcanic feature southeast of Duque's Hill (site of JAGUAR 001).

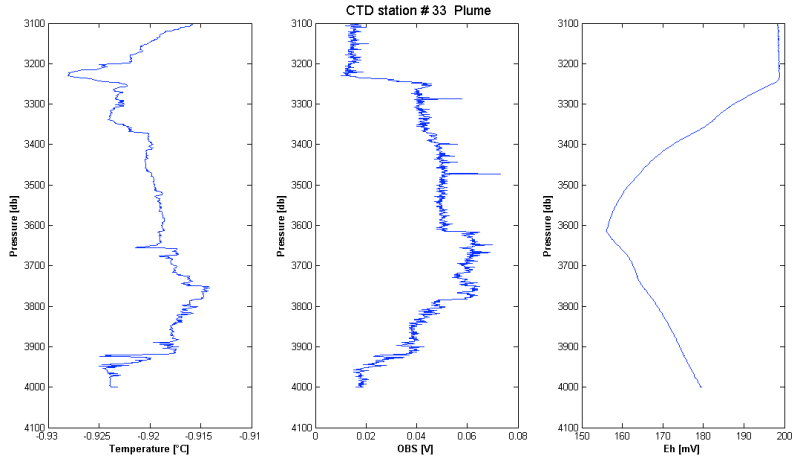

Figure 17. Example of a mid-water column plume from the 85°E site as measured during CTD33 on tow-yo #1.

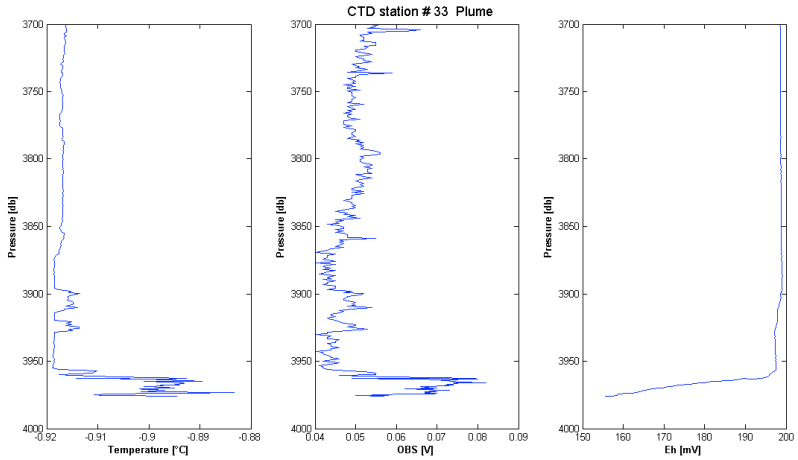

Figure 18. Example of a near-bottom plume from the 85°E site as measured during CTD33 on tow-yo #5.

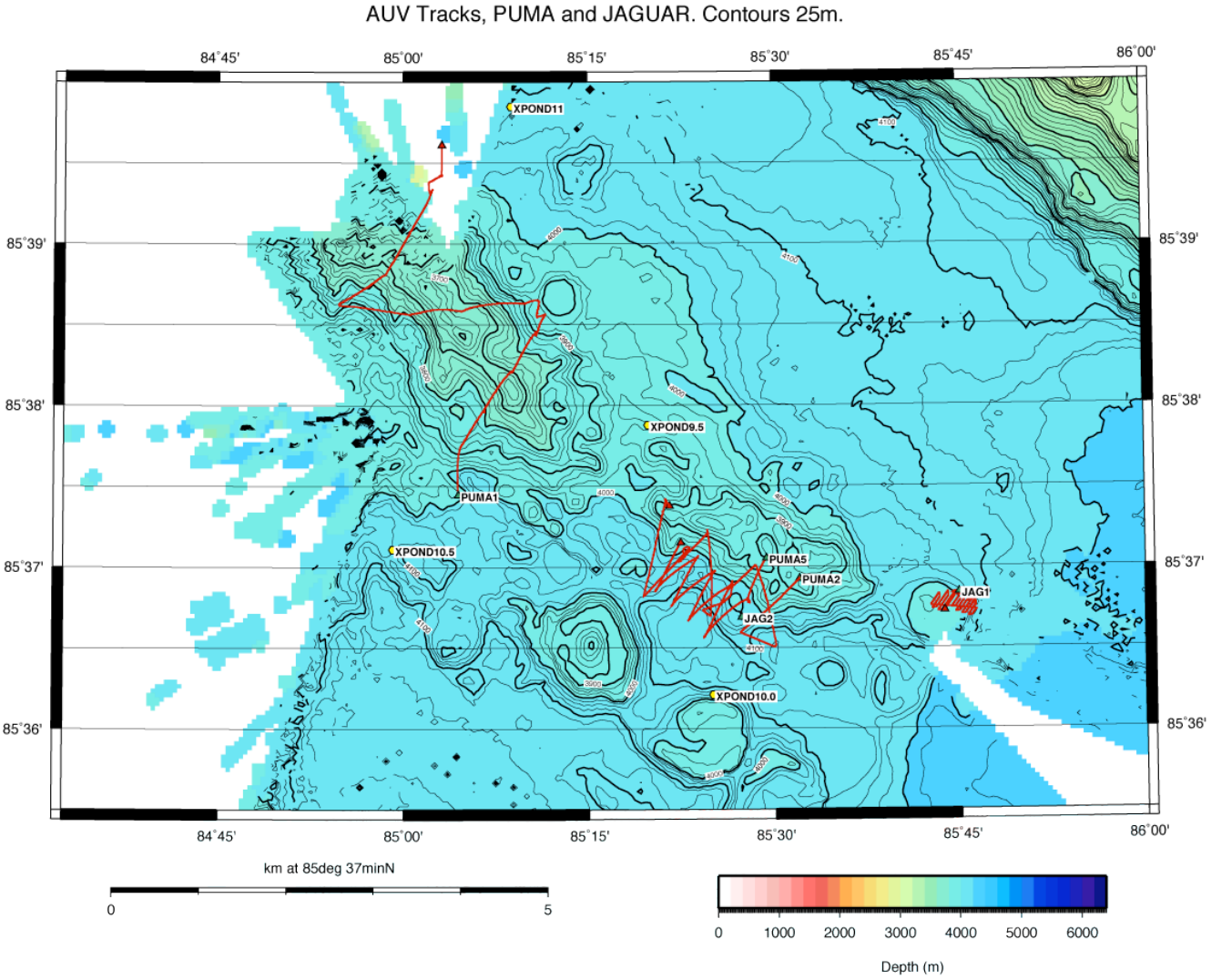

Figure 19. AUV tracklines from the 85°E site. Transponder locations shown as yellow stars.

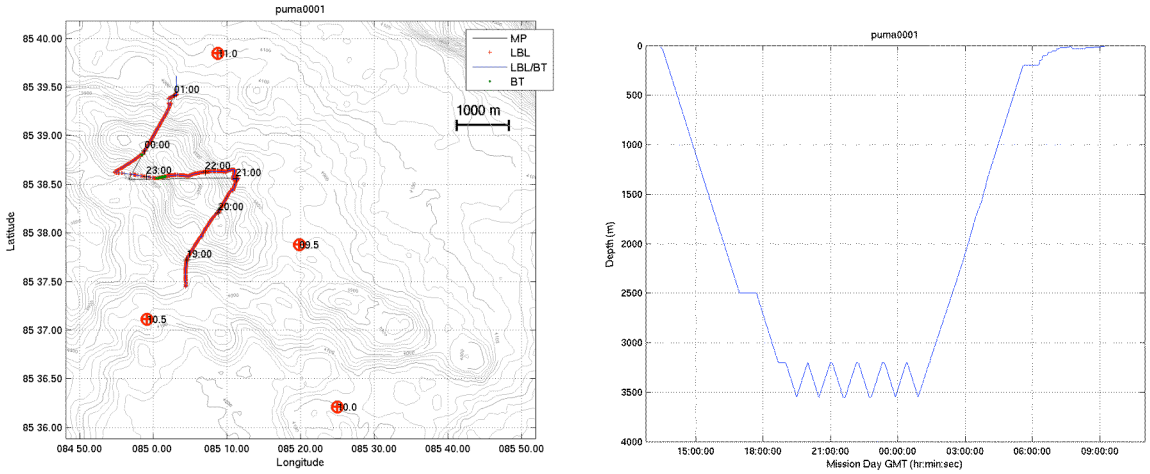

a.

Figure 20. Track and depth plot for Puma Dive #0001.

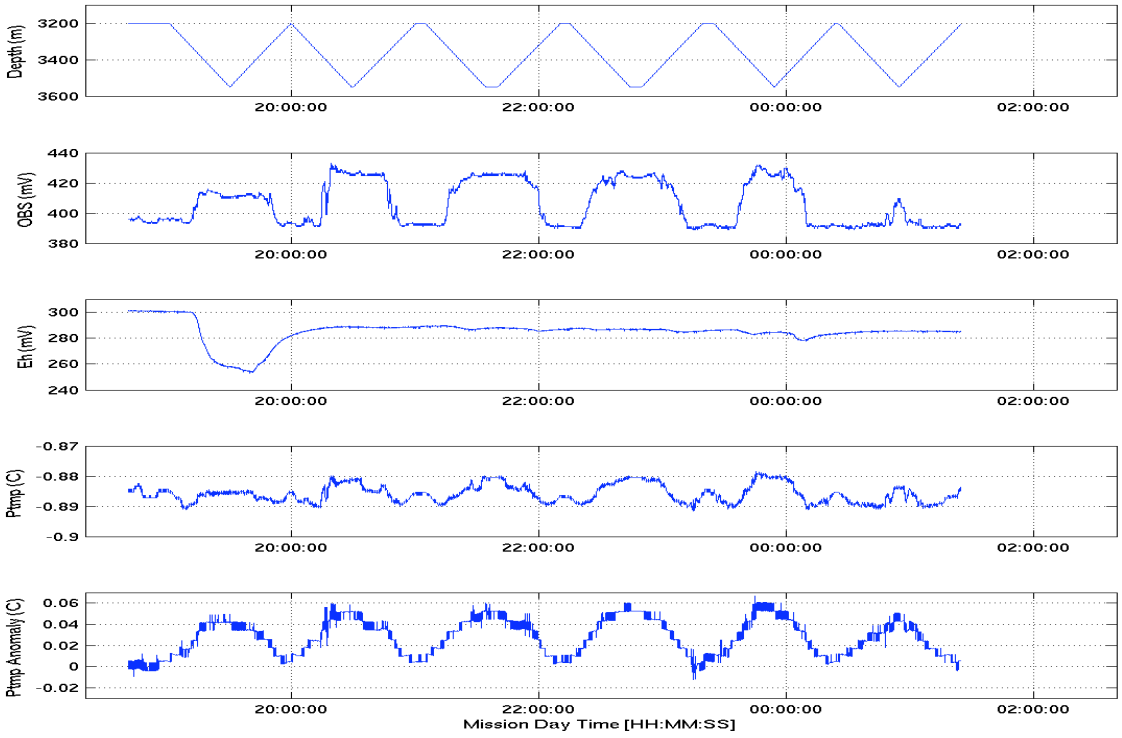

Figure 21. Sensor data profiles for Puma Dive #0001.

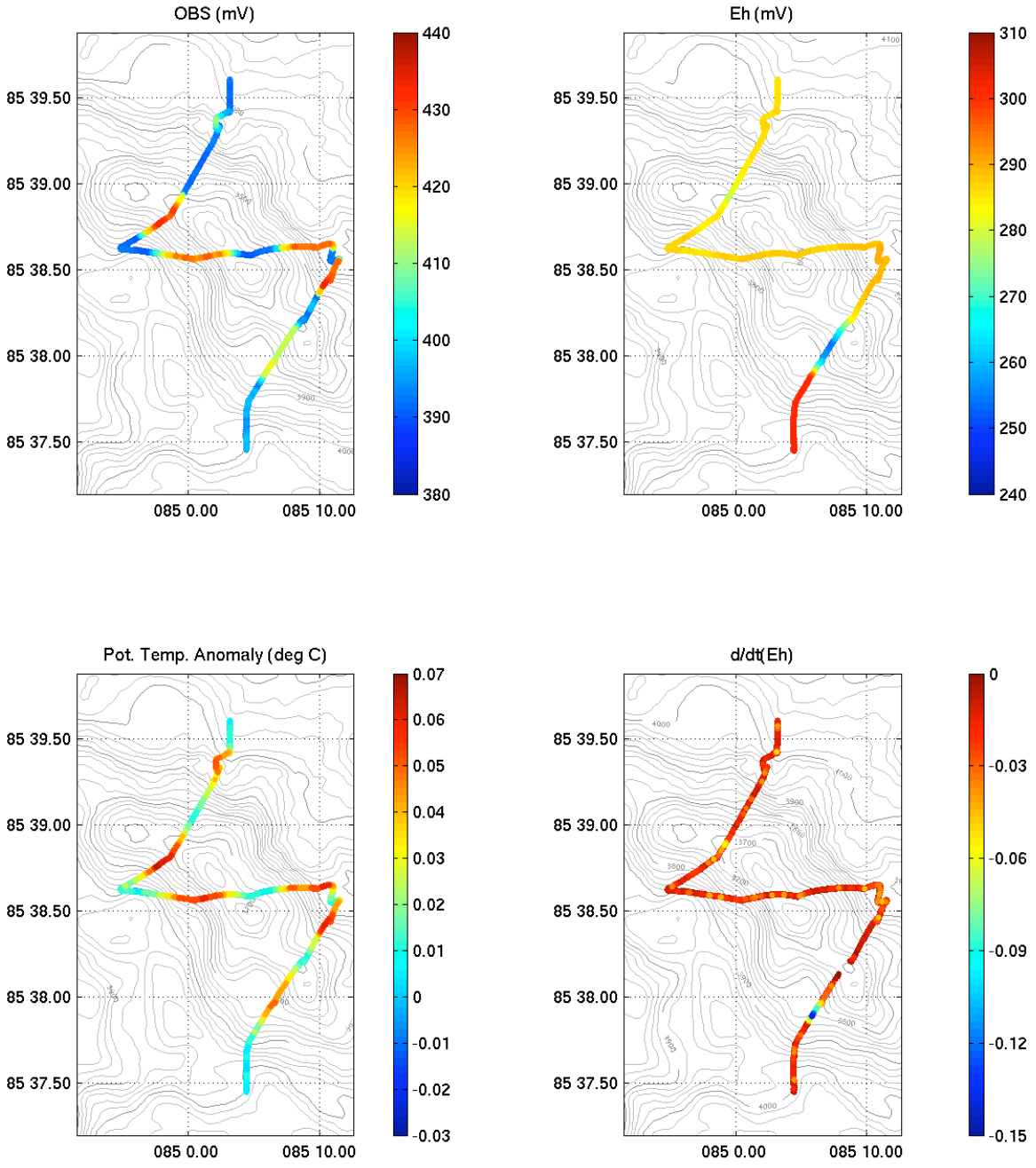

Figure 22. Sensor data profiles plotted as a function of x-y position for Puma Dive #0001.

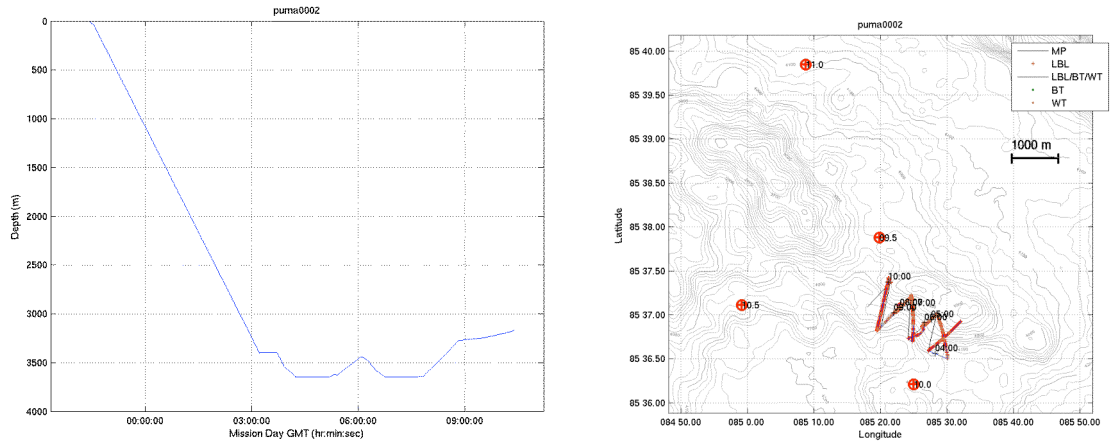

Figure 23. Depth and x-y tracks for Puma Dive #0002.

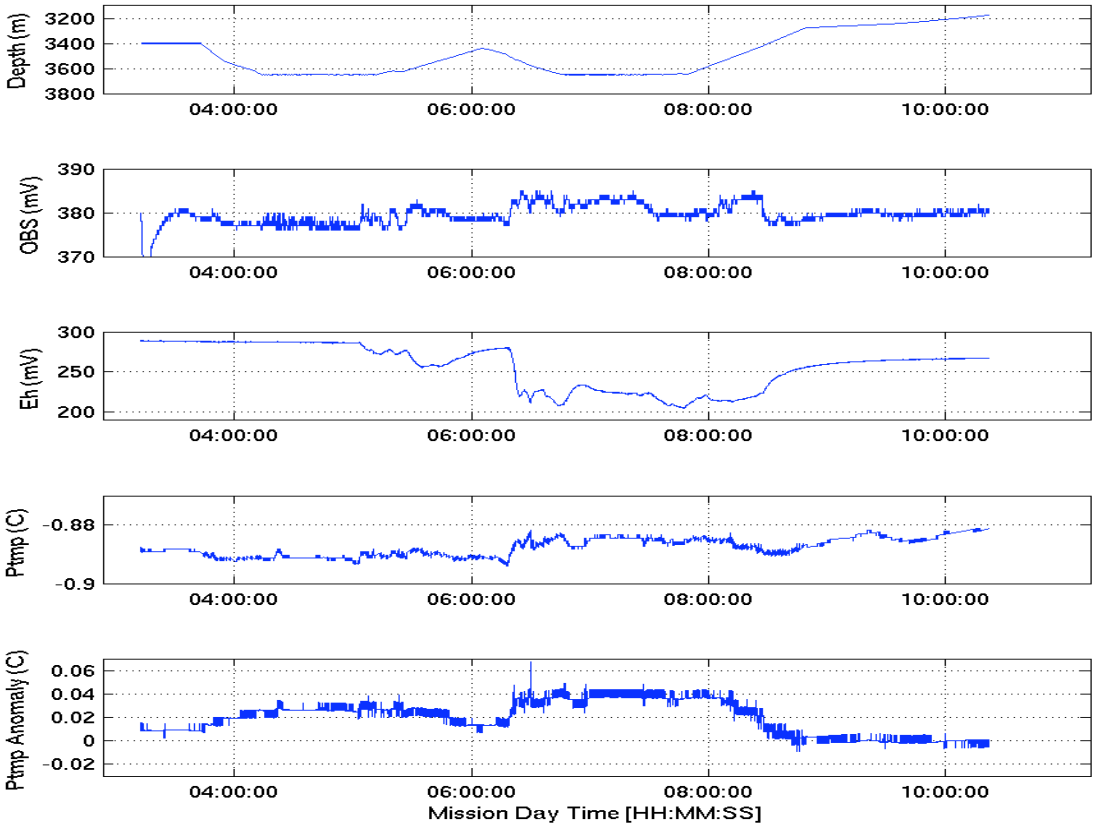

Figure 24. Sensor data profiles for Puma Dive #0002.

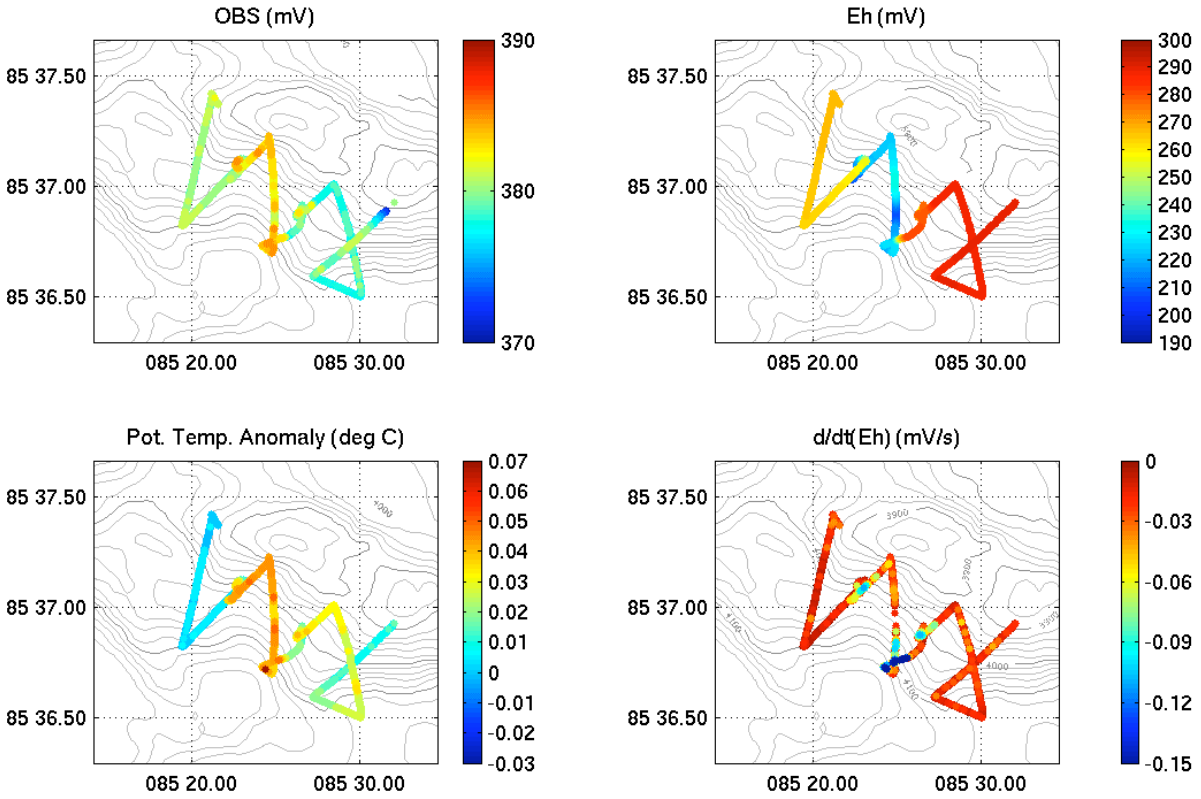

Figure 25. Sensor data profiles plotted as a function of x-y position for Puma Dive #0002.

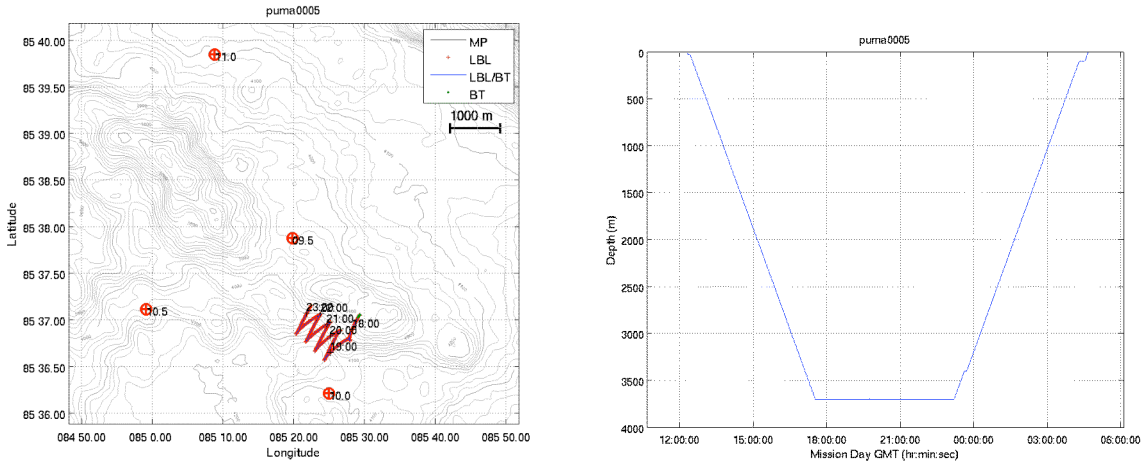

Figure 26. Depth and x-y tracks for Puma Dive #0005.

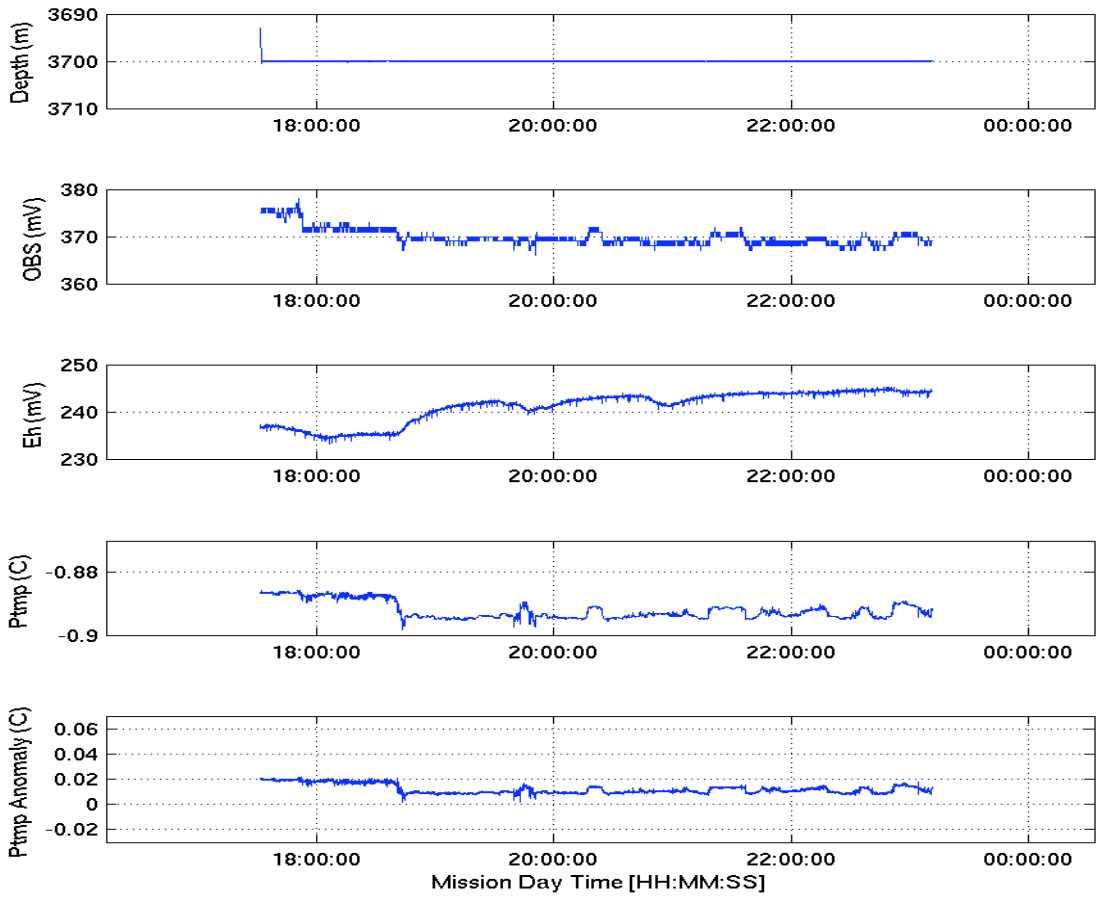

Figure 27. Sensor data profiles for Puma Dive #0005.

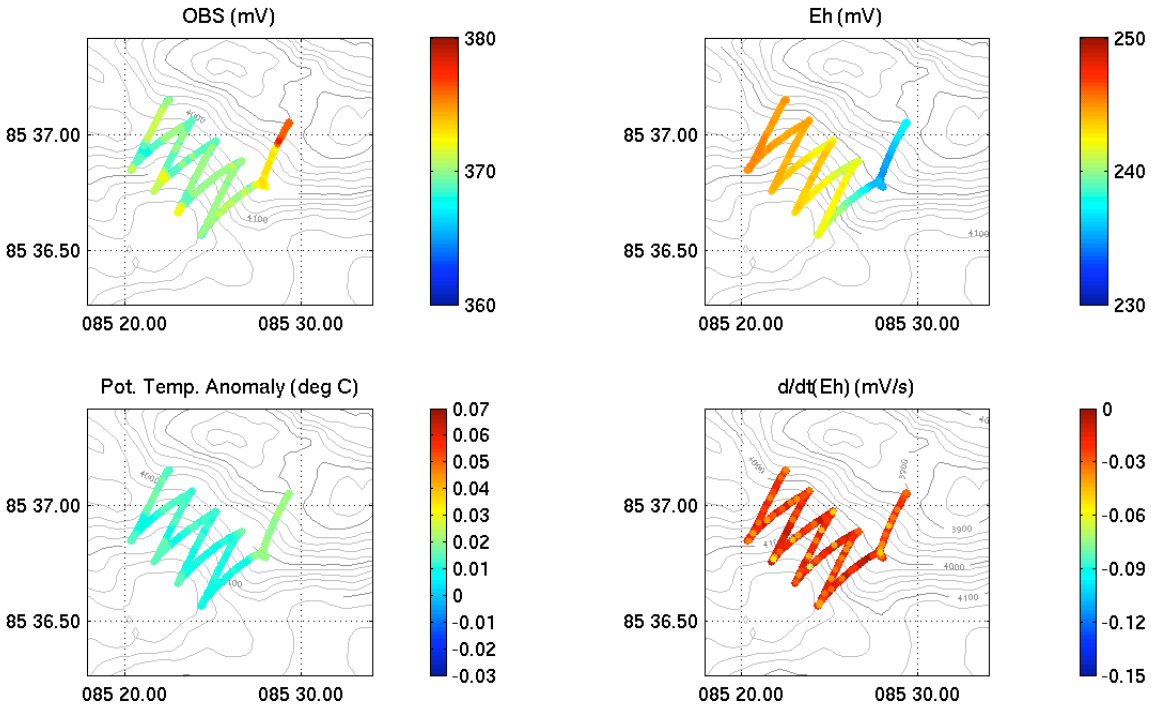

Figure 28. Sensor data profiles plotted as a function of x-y position for Puma Dive #0005.

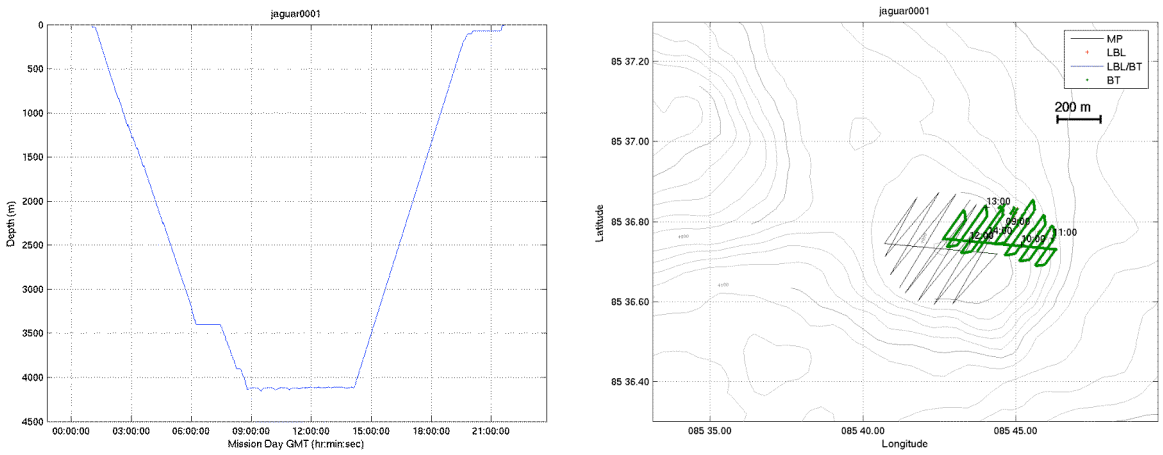

Figure 29. Depth and x and y data for Jaguar Dive #0001. Note that in trackline plot the programmed tracklines are shown as a thin black line while the realized trackline is the solid green line.

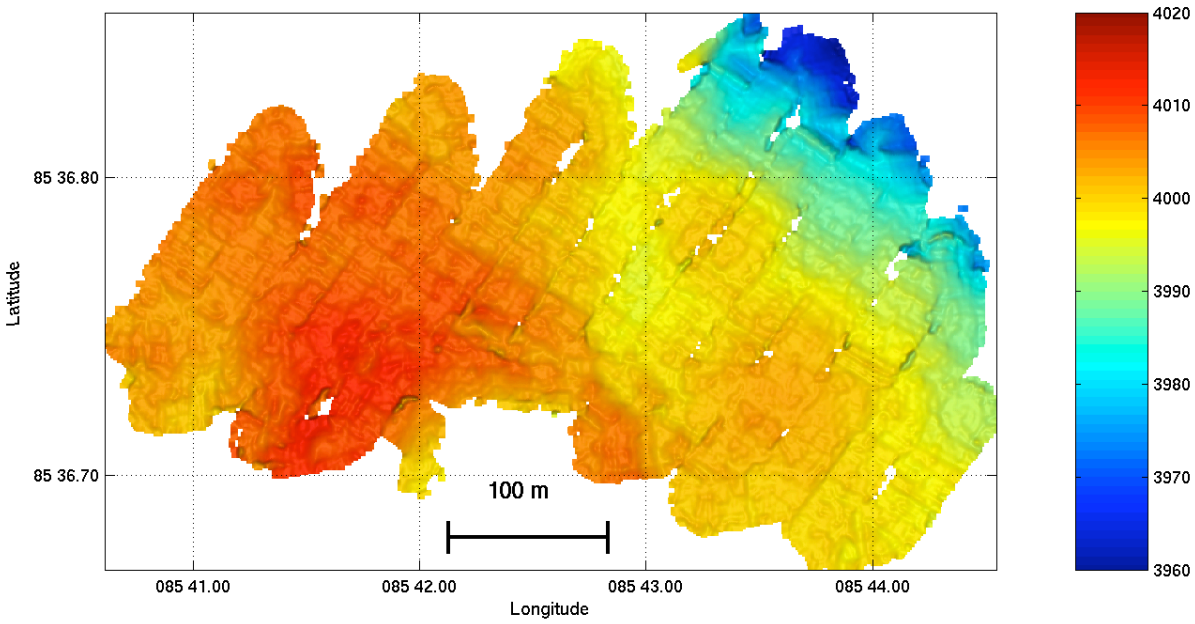

Figure 30. First pass microbathymetric map for JAGUAR Dive #0001.

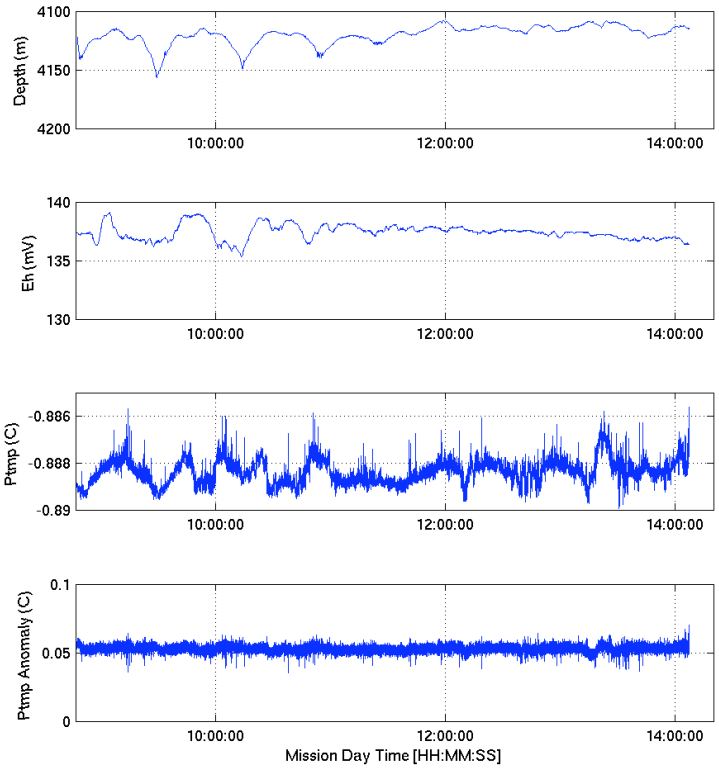

Figure 31. Sensor data time-series data for JAGUAR Dive #0001.

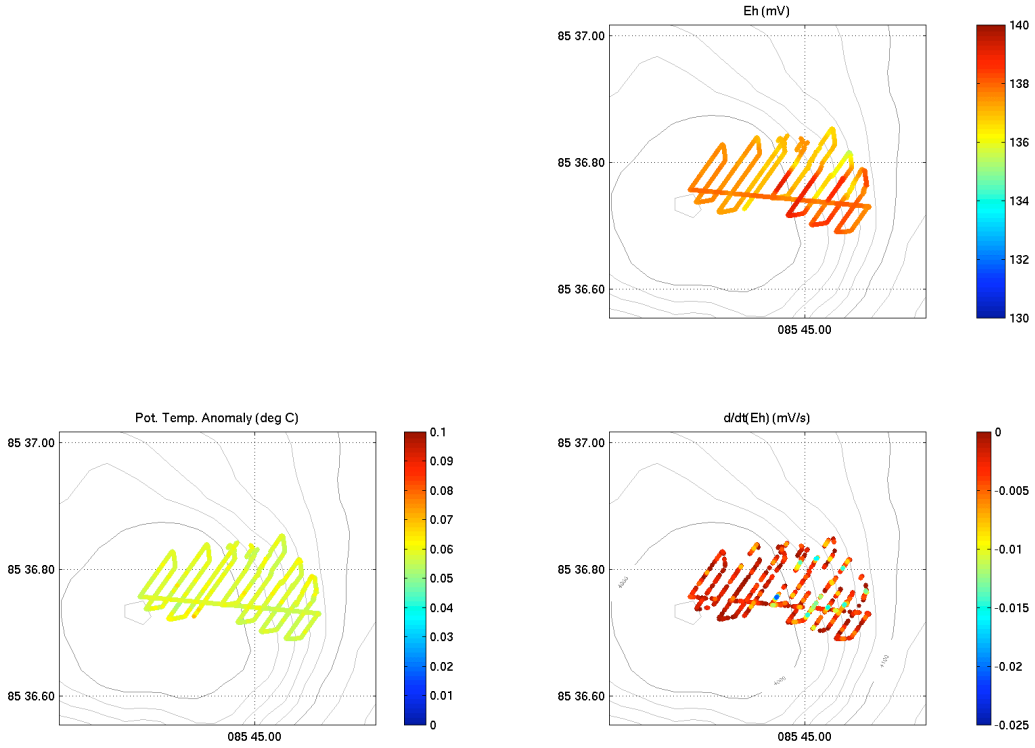

Figure 32. Sensor data profiles plotted as a function of x-y position for JAGUAR Dive #0001.

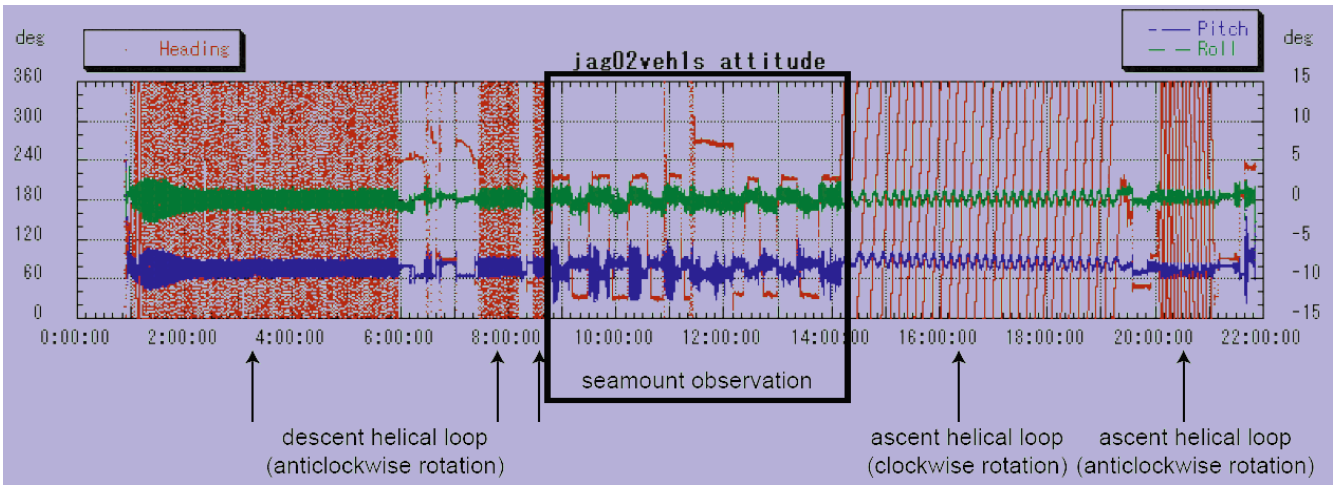

Figure 33. JAGUAR vehicle attitude data as a function of time for Dive #0001. The high fidelity of the true north seeking three axis fiber optic gyroscope on the vehicle should help resolve the magnetic data quite well.

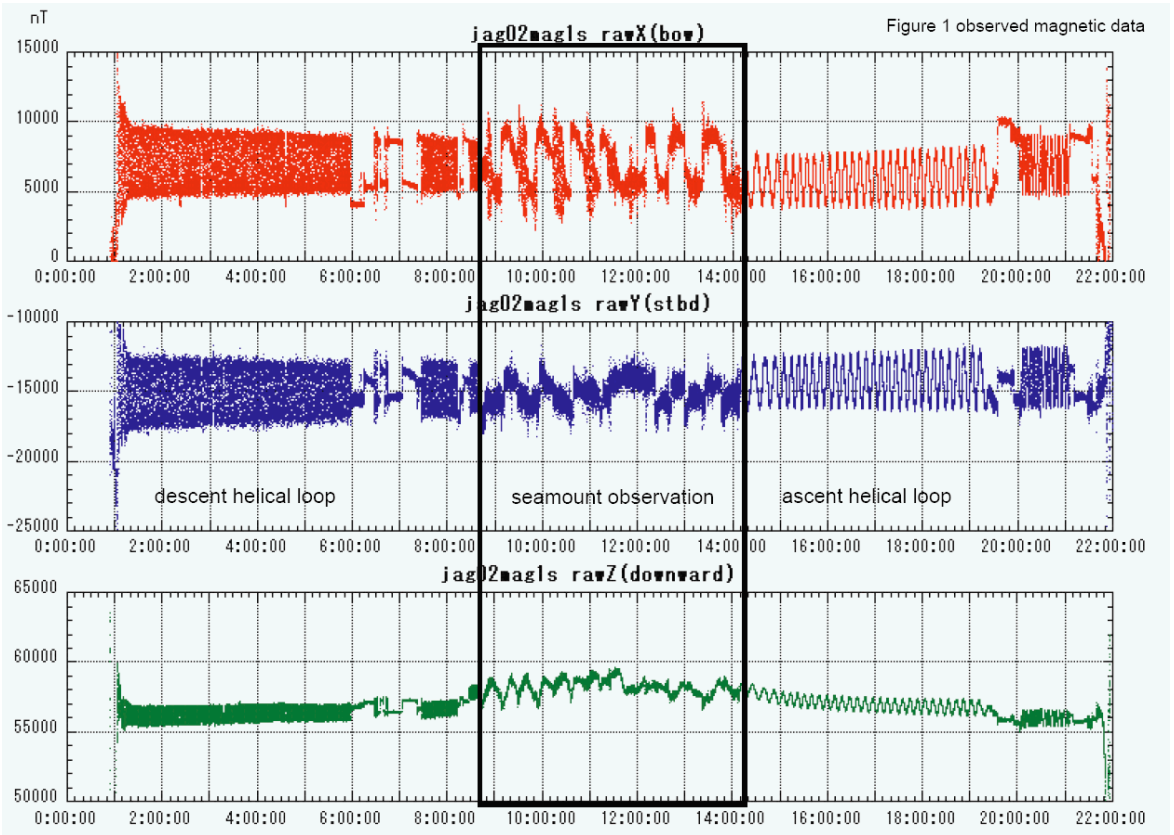

Figure 34. Three-axis magnetometer data as a function of time for JAGUAR Dive #0001.

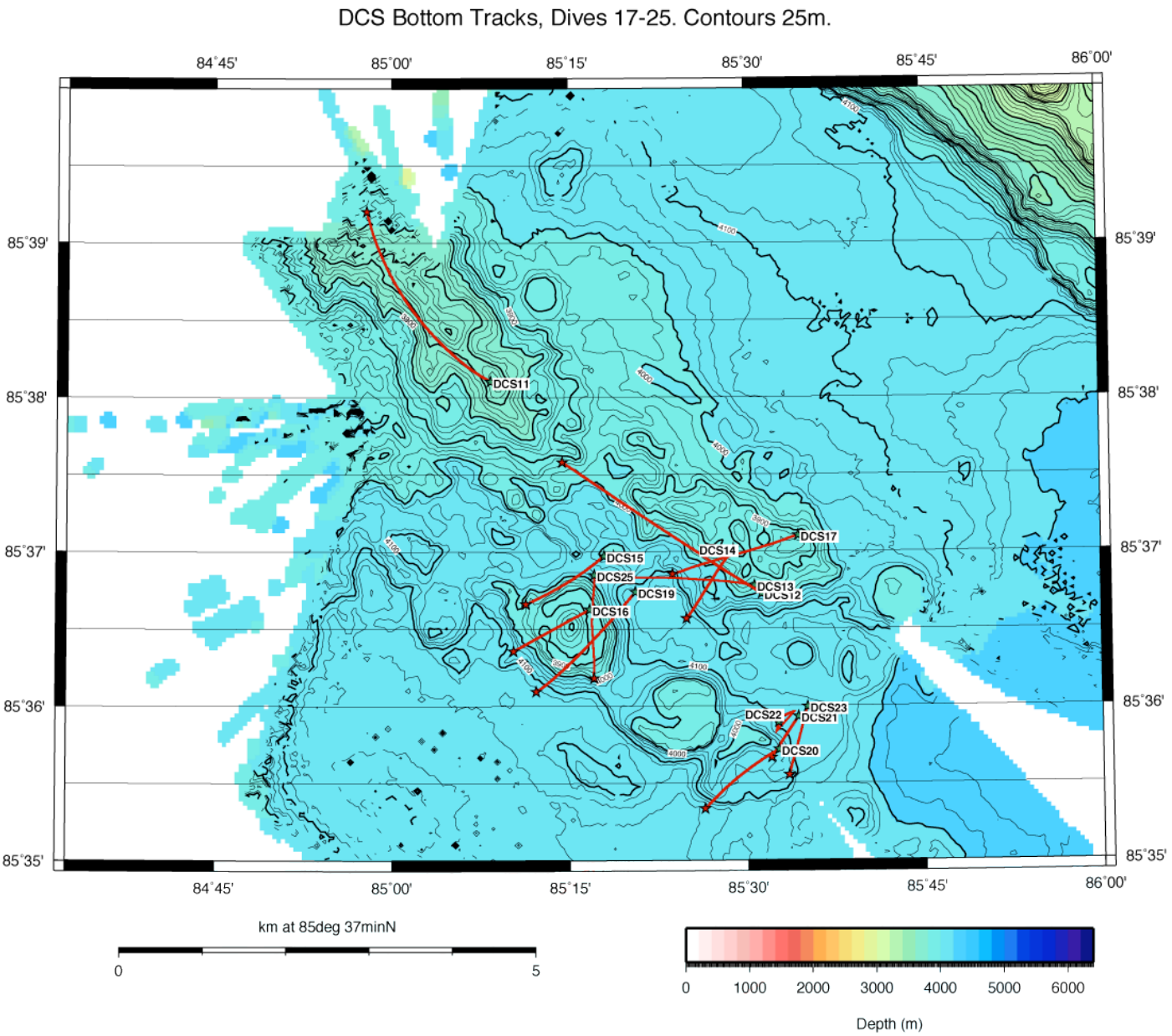

Figure 35. CAMPER dive tracks from the 85°E site.

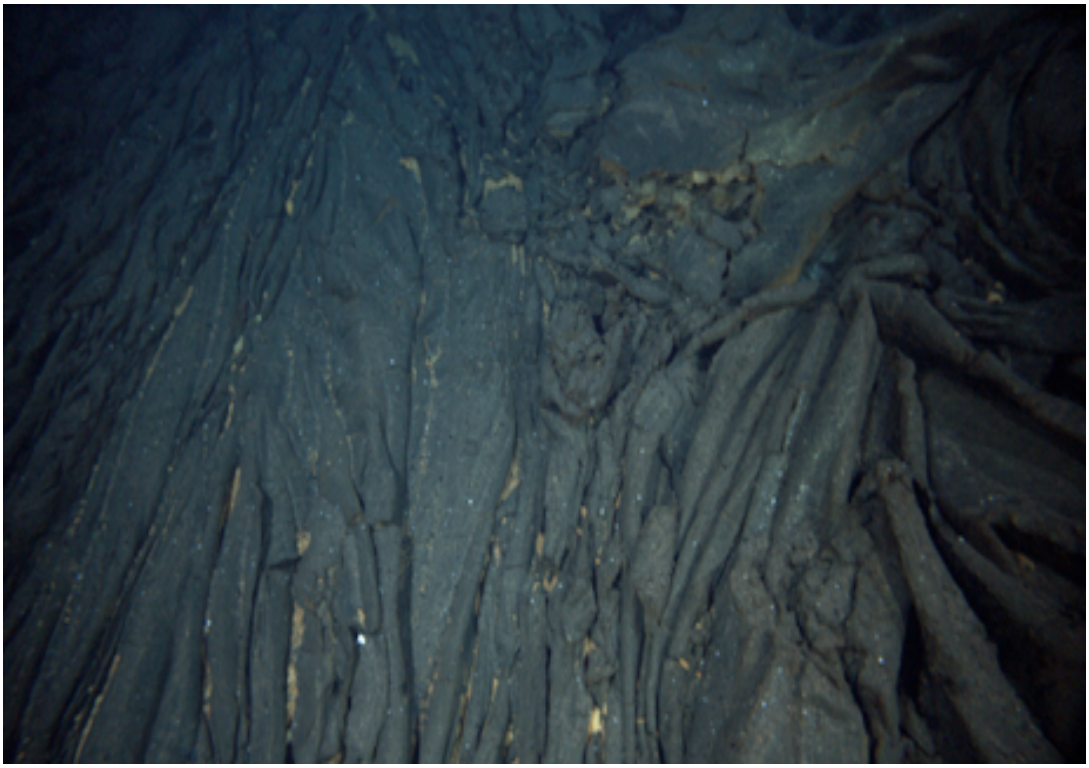

Figure 36. CAMPER frame grab of a fresh sheet flow on the Oden volcano.

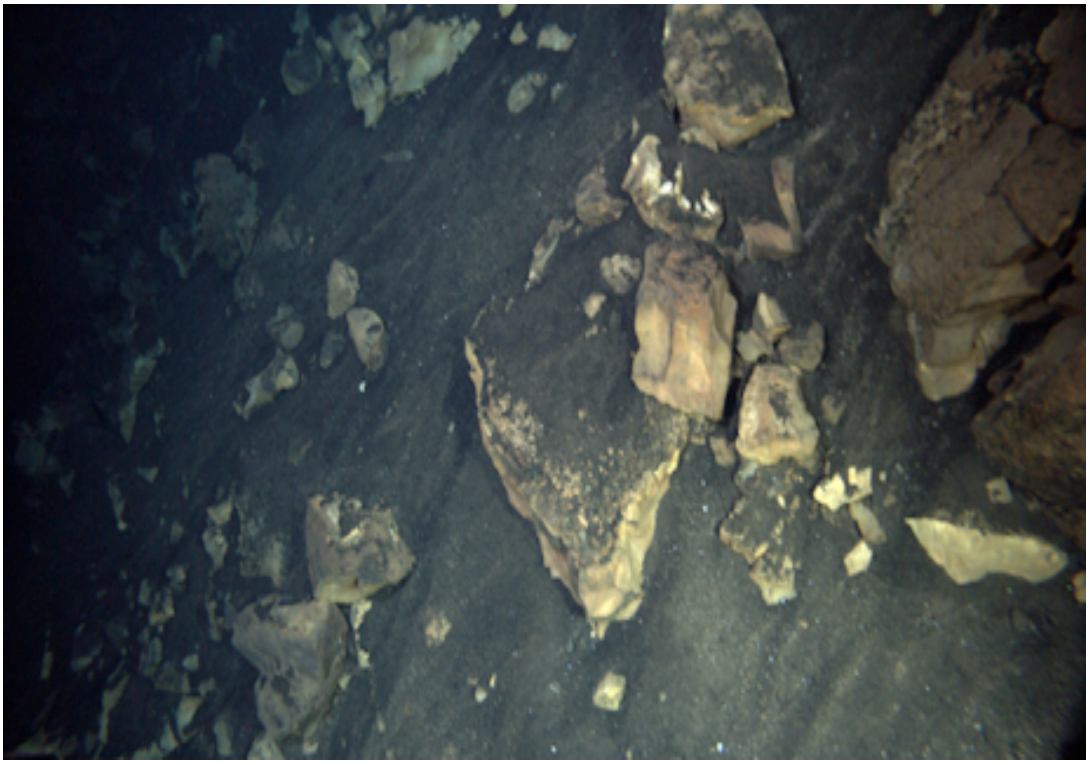

Figure 37. CAMPER frame grab of volcanic ‘sediment’ on top of broken pillow fragments.

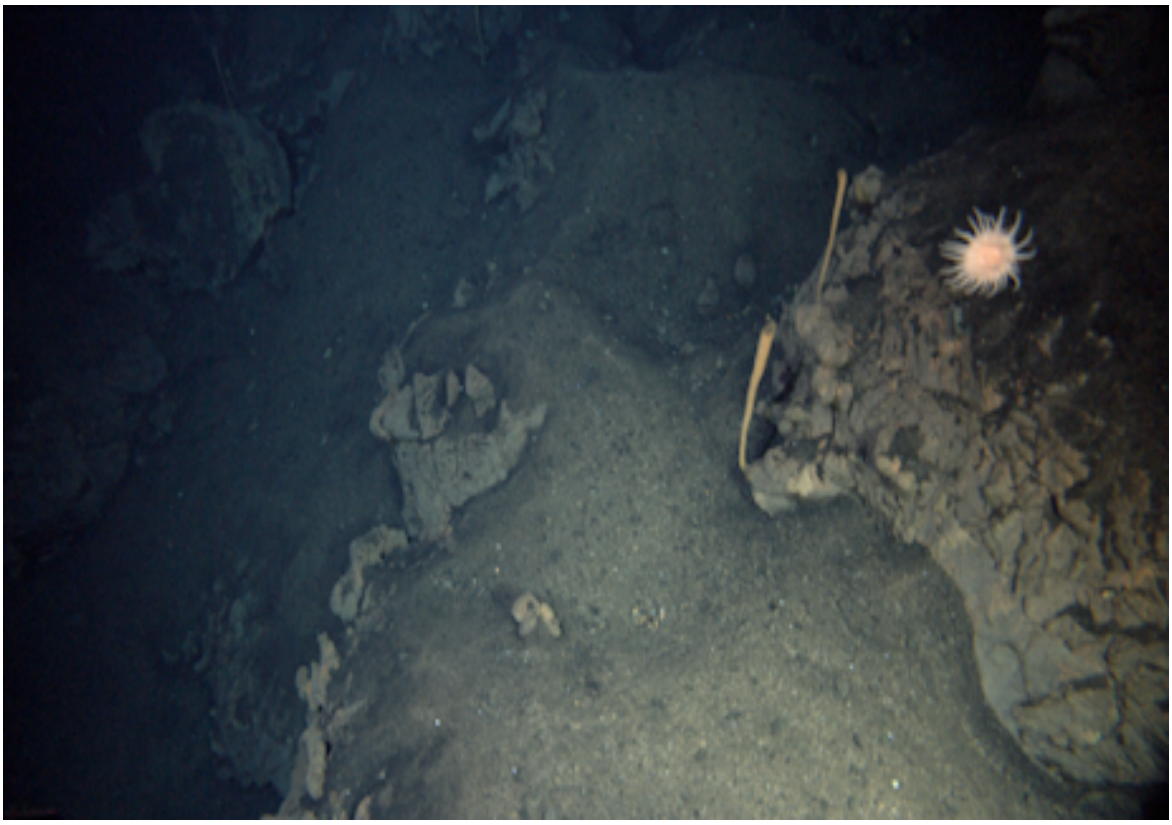

Figure 38. Hexactinellid sponges and an anemone on broken pillow lava.

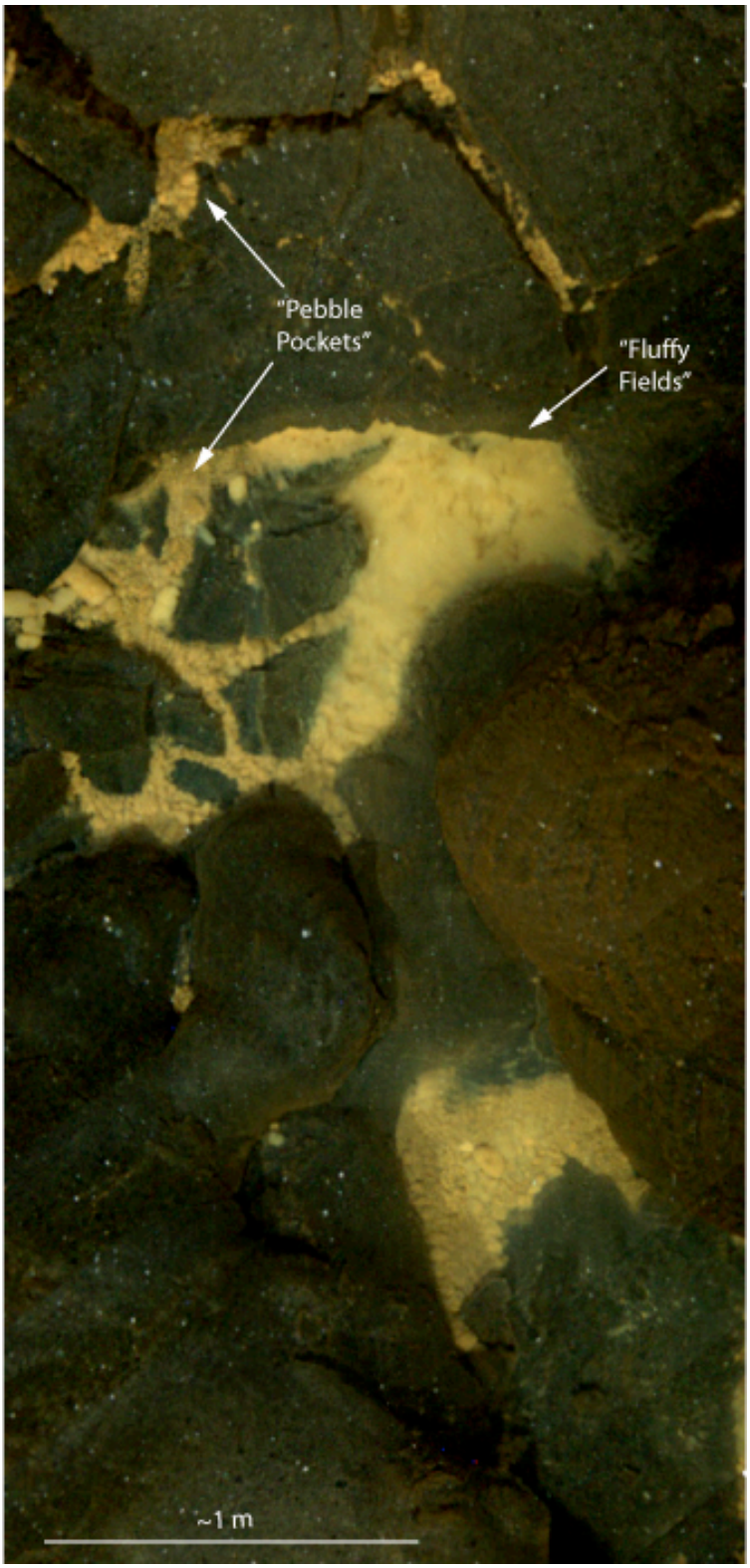

Figure 39. Mosaic Image of the “Fuffy Fields” and “Pebble Pockets” on Oden volcano (11 high-definition images).

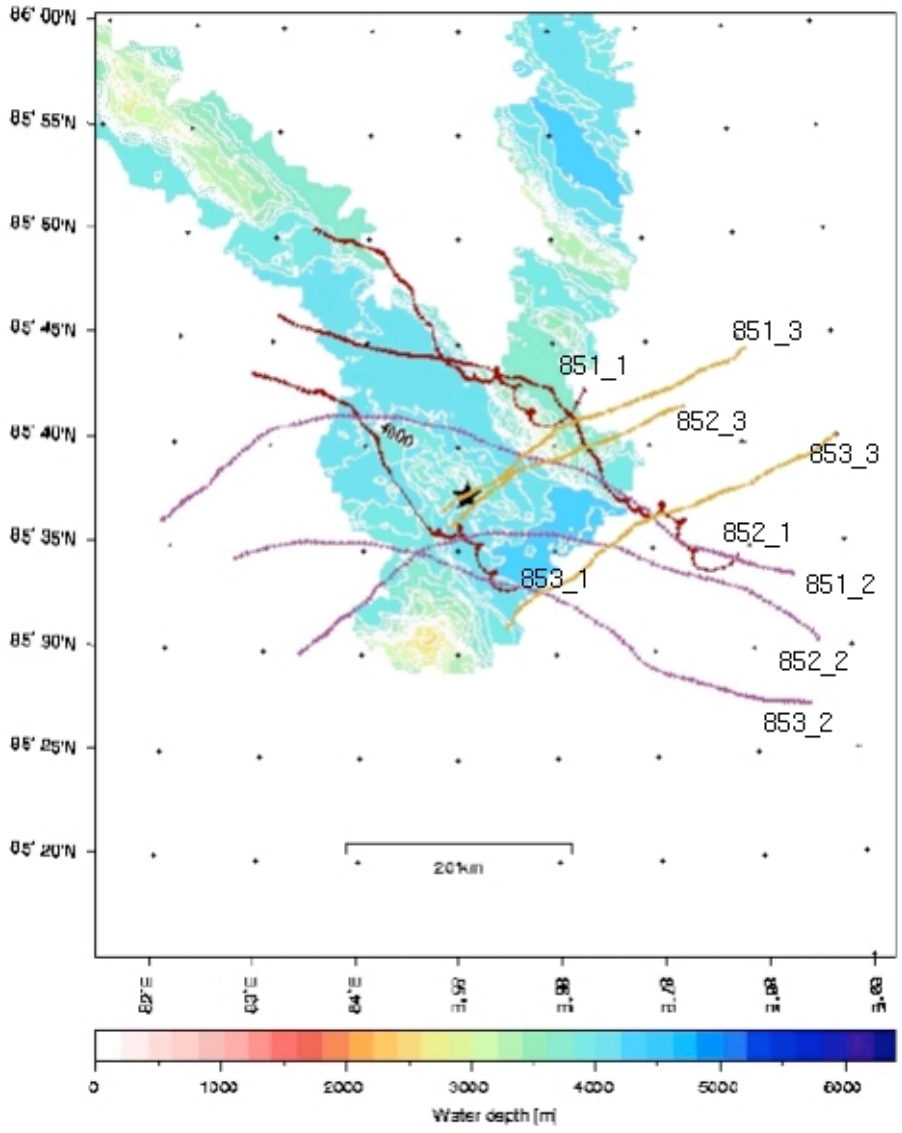

Figure 40. Drift paths of the central stations of the seismological arrays. The deployment points of the arrays are labelled with the array number. The dots represent hourly GPS positions.

Appendix

Appendix A. Multi-beam program

GENERAL

The Swedish icebreaker Oden is equipped with the following hydroacoustic systems.
- Kongsberg EM 120 1°x1° multibeam echo sounder with raw data logger.
- Kongsberg SBP120 3° sub-bottom profiler.

SYSTEM DESCRIPTION, HYDROACOUSTIC SYSTEMS.

b. EM 120 1°x1° multibeam echo sounder.

The EM 120 can perform seabed mapping to full ocean depth. The nominal sonar frequency is 12 kHz with an angular coverage sector of up to 150 degrees and 191 beams per ping as narrow as 1 degree. The transmit fan is split in several individual sectors with independent active steering according to vessel roll, pitch and yaw. This place all soundings on a "best fit" to a line perpendicular to the survey line, thus ensuring a uniform sampling of the bottom and 100% coverage. The EM 120 transducers are linear arrays in a Mills cross configuration with separate units for transmit and receive.
The Raw Data Logger is an application for recording and displaying raw data from the multibeam echo sounder system. The main purpose is to log the samples throughout the water column for all the 128 receiver staves. Sample data is sent from the Transceiver Unit at up to 12,000 samples per second. The data rate is up to 6.1 Mbytes per second.

c. SBP120 3° sub-bottom profiler.

The **SBP120** Sub-Bottom Profiler is an extension to the EM 120 Multibeam Echo Sounder. The primary application of the SBP120 is to do imaging of sediment layers and buried objects.
The normal transmit waveform is a linear chirp (which is an FM pulse where the frequency is swept linearly). The outer limits for the start and stop frequencies of the chirp are 2.5 kHz and 7 kHz, providing a maximum vertical resolution of approximately 0.3 milliseconds. In addition to linear chirps, the system offers CW pulses, hyperbolic chirps and Ricker pulses.

DATA DESCRIPTION.

During the AGAVE expedition, data were continually recorded on both hydroacoustic systems around the clock. This includes transits from Longyearbyen to site one, between sites, and from site two to Tromsö. The systems have only been in standby when so required by other onboard operations such as AUV dives. There were no scheduled time for collection of multi-beam or sub-bottom data but data collection was done during the day-to-day operation of the ship. Data was stored locally on each system and then once a day, normally around 24:00 UTC, copied to a central storage array. Each dataset in it's own folder named as yyyy-mm-dd. Post processing of the data will take place after the end of the AGAVE cruise.

d. EM 120 1°x1° multi-beam echo sounder.

EM120 data collected when drifting turned out to be of high quality. Data quality during icebreaking varied with ice conditions, velocity of the ship and if the thrusters and/or lubrication system where used. Data is stored in catalog named “EM120”, and from there on in subcatalogs “raw” and “grid”. The “grid” catalogs contain the screen representation of the raw files and are not necessary as they can be generated again from the grid files using SIS software. They are only supplied as a matter of convenience.

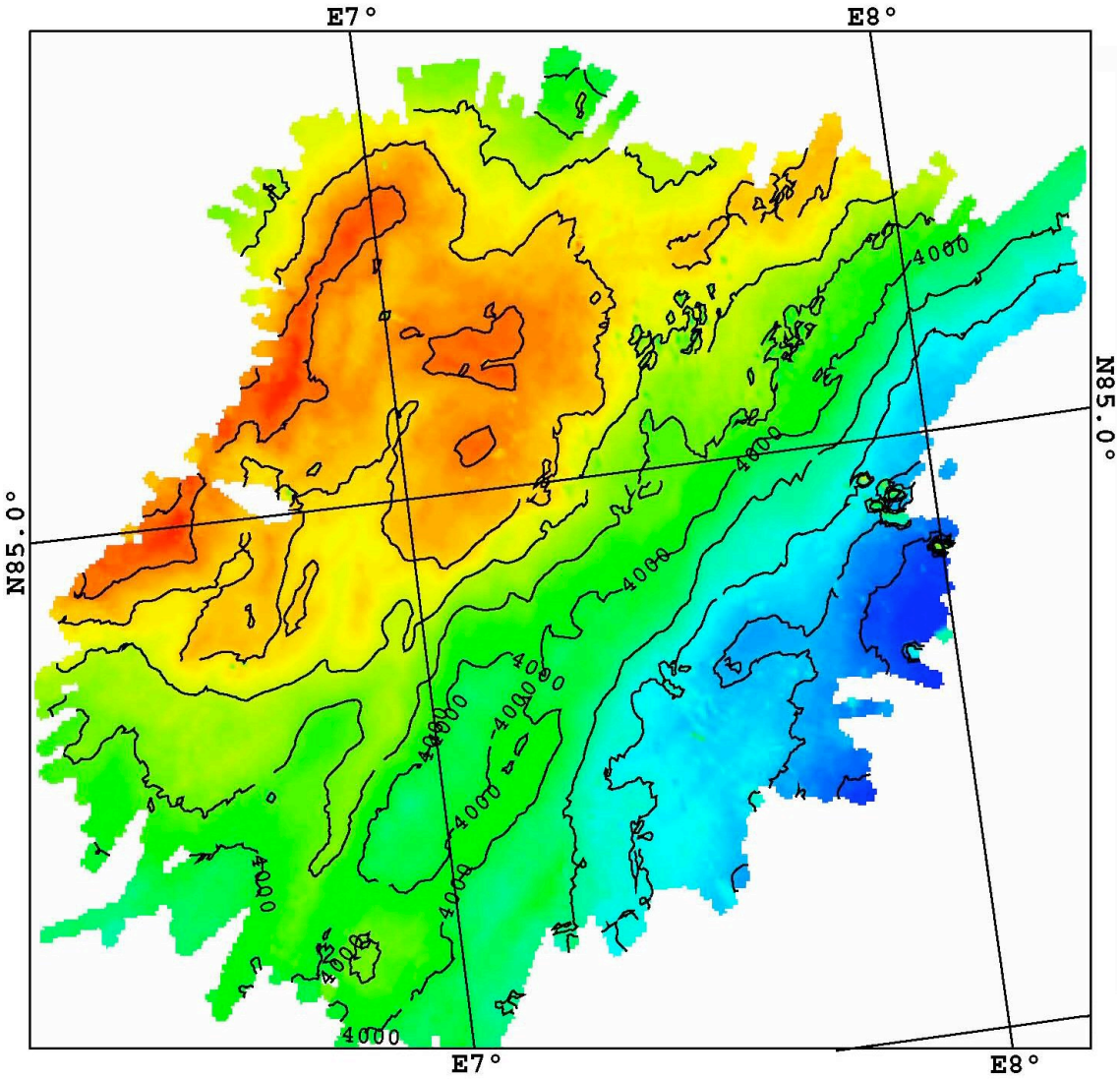

Site 1 Multi-beam coverage.

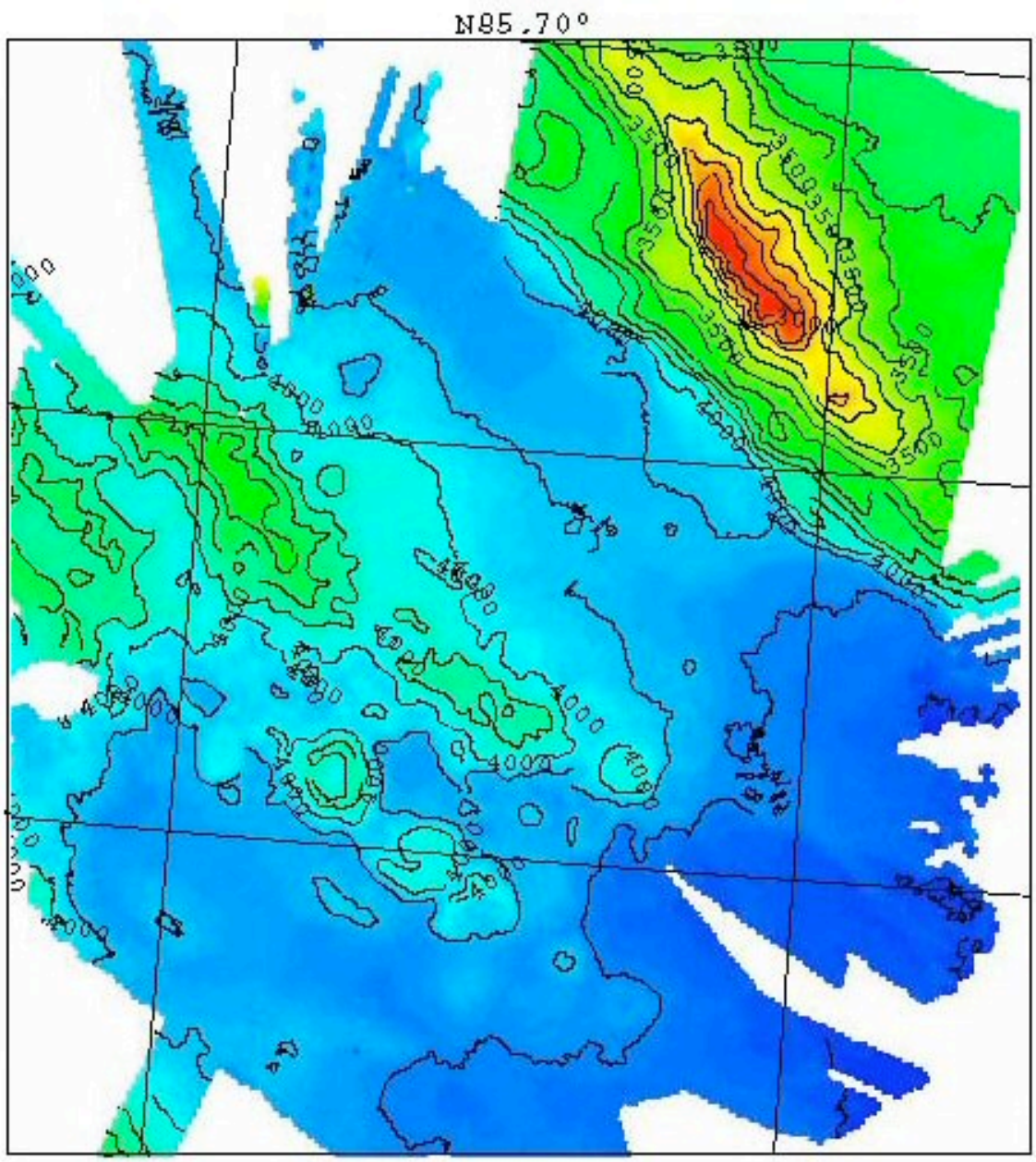

Site 2 Multi-beam coverage.

e. SBP120 3° sub-bottom profiler.

SBP120 data obtained at the Gakkel ridge is poor to non-existent due to hard rocky bottom with little to no sediments. Data is stored in a catalog named “SBP120” and from there on in subfolders, one for each 24h period. The SBP120 also collects RAW data that is stored in a catalog named RDL.

Appendix B. CTD Program and System Description

B1. CTD Rosette configuration and operation

The CTD rosette system used during AGAVE SWEDARCTIC 2007 was built around a 1.8-m diameter aluminum frame. The rosette bottle sampler was a Seabird 24-bottle carousel. We used 22 10-liter bottles as two bottle positions were used for additional instruments. The main CTD package was a Seabird SBE 9+ pumped system, equipped with dual conductivity and temperature sensors. We had a number of auxiliary sensors connected to the main Seabird system to obtain data in real time including a Seabird oxygen sensor, Seapoint OBS sensor, a SeaTech Transmissometer, and an Eh sensor. The rosette was also equipped with an internally recording Lowered Acoustic Doppler Current Profiling (LADCP) system consisting of dual RDI Workhorse ADCPs, along with a stand-alone battery package and a Laser In-Situ Scattering and Transmissiometry (LISST) instrument. Details of these sensors are given below.

Conductivity, temperature and pressure sensors

We used a standard Seabird SBE 9+ system sampling at 24 Hz, consisting of a pumped TC duct with dual conductivity (SBE 4Cs) and dual temperature (SBE 3+) sensors. The duct is pumped using a SBE 5T pump. The temperature and conductivity difference between the two sensors were displayed during data acquisition and was typically less than 0.0002 and 0.003, respectively. Accuracy of the temperature and conductivity sensors are nominally 0.001 °C and 0.003 S/m. During cold conditions we had the sensors continuously flushed with warm water using tubing connected to a water bottle that was pulled off right before deployment. The behavior of the package was very stable throughout the cruise. Data acquisition was in real time using the SBE 11+ V2 deck unit with integrated NMEA for position data that was read from the ships main DGPS system.

Eh sensor

Eh was measured through SBE 9+ auxiliary channel. The Eh sensor was composed of a set of electrodes and a transformer. Electrodes were Pt electrode, which were coiled 0.7 mm thick pure Pt wire, and a reference electrode, which is Ag-AgCl electrode sealed in saturated KCl solution. The electronic junction between Ag-AgCl electrode and seawater was performed through porosity controlled zirconia plug. The transformer had two functions. One was to make electric isolation between electrodes side and SBE side by an isolation amplifier. The other was to make the electric input from the electrodes receivable voltage range by SBE 9+. Input voltages between +500 mV and -500 mV were linearly converted to the range between +5 V and 0 V. An inverse function to calculate electrodes voltage was embedded in the Seasave acquisition system. Note that any Eh data at any each depth does not mean equilibrated Eh value because of slow response of electrodes. Pt electrode surface situation change in time, which resulted Eh range difference through casts.

*OBS sensor*s

Seapoint turbidity meters: S/N 10978 (with custom 5x normal gain) and S/N 1941. The turbidity

sensors acquired data through the Seasave system. Calibration is somewhat vague for these sensors so we displayed the raw output voltage during CTD casts.

S/N 10978 was broken and replaced after CTD02. S/N 1941 was replaced for CTD16 with a Sea Tech Light Scattering Sensor: S/N 211. We used this sensor as a replacement for the second Seapoint sensor, displaying raw voltage from the auxiliary channel. Beginning with CTD17, Seapoint S/N 1941 was used for the duration of the cruise, on its own channel rather than jointly with the Eh sensor. See Table B1.1 for a summary of sensor change outs

Transmissometers
Two 25 cm Wetlabs transmissometers were used during the cruise as detailed in Table B1.1. Both exhibited substantial drift.

LISST sensor
Laser In-Situ Scattering and Transmissometry instrument for deep water (LISST-Deep manufactured by Sequoia Scientific, INC.) was attached on the CTD cage together with its data logging and battery pack (manufactured by Kaiyodenshi Co. Ltd.). LISST-Deep has thin source of laser beam and 32 ring detectors for scattering measurement as well as center detector for transmission measurement. The optical path length was 20 cm. The volume scattering function angle range of 32 ring detectors was 1.7 to 340 mrad. The averaged 6 samples were stored in the logger in every 2 seconds.

LADCP system
We used a Lowered Acoustic Doppler Current Profiling (LADCP) system from the Woods Hole Oceanographic Institution consisting of dual RDI Workhorse ADCPs and a stand-alone battery package. The system was originally configured with a downward-looking 150 kHz RDI Workhorse and a 300 kHz upward-looking RDI Workhorse. After completion of Site 1 we decided to replace the 150 kHz ADCP for a 300 kHz one instead. The main reason being that the newer firmware and larger memory of the 300 kHz Workhorse enabled us to download data faster between casts and allowed us to do yo-yo's without running out of memory.

Data was downloaded and the battery pack charged between each cast. Each 300 k Hz ADCP was configured to use ten 10-m bins vertically with a ping rate of 2 pings per second.

Niskin bottles
We encountered problems with bottle leaks on several casts, as detailed in the sample tables (B3.1-29). Leaks were noted and addressed whenever they were encountered, with the following replacements made when leaks could not be fixed after multiple attempts:

After CTD04 - replaced No. 22
After CTD17 - replaced No. 7
After CTD24 - replaced No. 15
After CTD26 - replaced No. 12

Operational Strategy for CTD operations

The CTD was operated from the bow of icebreaker Oden lowered from a telescopic A-frame using standard conducting CTD cable. Data acquisition, water sampling and winch controls were located in a heated double container. The CTD was brought out on a pallet onto a wagon that was pushed out to the A-frame for each deployment. Recovery was similar and the CTD was brought into the heated container for water sampling. To clear ice we often used Oden's flushing system and sometimes thrusters to blow ice away from the bow to enable ice-free deployment and recovery.

Each CTD cast started by lowering the CTD to 5-8 m depth to wait for the Seabird pump to start and for the sensors to equilibrate after which we brought the CTD up the surface to start our down cast. We used a constant 60 m/min (1 m/s) lowering speed.

To try to detect plumes from hydrothermal vents we often used a yo-yo strategy. When finding evidence of a plume (any combination of warm anomaly in temperature, Eh signal, and/or transmissometer signal) we yo-yo'd the CTD through his layer while drifting, typically from the bottom and 1000 m up, to obtain higher spatial resolution. Typical ice drift speeds during the cruise were 0.1-0.3 knots, giving an approximate horizontal resolution of 100-300 m for each yo-yo. Water samples were taken whenever an interesting signal was found, at non-standard depths.

CTD data was processed using Seabird software and standard techniques. Our standard output consisted of one-second time-averaged data to enable easy plotting of individual yo-yos along with bottle summary files for all water samples. Each main PI was supplied with a CD containing all raw data, time-averaged processed data, plots for each cast and documentation before disembarking the ship.

B2. CTD Cast Summary

CTD casts are summarized (dates, times, locations) in Table B2.1 (Site 1) and Table B2.2 (Site 2).

B3. Water sampling and analysis

Water samples were collected from the rosette for analysis of hydrothermal tracers (helium, methane, hydrogen, manganese & iron - Edmonds), plume particle geochemistry (Edmonds), microbiology (Elisabeth Helmke), and identification of protists (Tim Shank/Mark Dennett). A summary of bottles fired and samples collected for each cast is available in electronic format as an Excel spreadsheet, with file name AppendixB3Tables.xls. No samples were collected on casts 5, 9, 10, 11, 21, 25, and 31.

Samples for microbiology, protists, and particle geochemistry were all collected from dedicated bottles. Tracer samples were collected from separate bottles in the order: helium, methane/hydrogen, Mn/Fe.

Geochemistry

Helium samples were collected in 5/8" o.d. copper tubing and sealed using a hydraulic crimper at approximately 4000 psi for shipment to the NOAA/PMEL laboratory in Newport, Oregon. Samples will be analyzed by mass spectrometry pending funding.

Samples (100 mL) for shipboard analysis of methane and hydrogen were collected in gas-tight 140 cc syringes. Helium (40 cc) was added to each syringe, and the syringes were shaken to extract dissolved gases into the headspace. After the samples attained room temperature, the headspace gas mixture was injected into an SRI 8610D gas chromatograph and analyzed for CH_4 and H_2. Analyses were completed within four hours of the CTD being brought on deck. Detection limits varied between casts but were on the order of 2 nM (seawater concentration). Background seawater has concentrations of approximately 1 nM, and plume concentrations were readily detectable.

Samples (250 mL) for shore-based analysis of dissolved Mn and Fe by flow injection analysis were collected in acid-cleaned HDPE bottles.

Particulate material was collected for geochemical analysis from dedicated bottles. Sample containers were rinsed 3x with sample, then the water was filtered through acid-cleaned 0.45 um filters in Teflon filter holders, overpressured using filtered ship's air at a pressure of 8-10 psi. All filter handling was done in a laminar flow bench. Filtrate volume was recorded for each sample. Samples will be analyzed pending funding.

Microbiology

For qualitative taxonomic analysis of the microbial communities by means of the 16S rRNA gene, microbes of 8 l or 16 l water samples respectively were collected on polycarbonate-filters with 0.2 um pore size. The filters were stored at -80°C for further processing in the home laboratory.

The taxonomical structure will be analysed by fluorescence in situ hybridization (FISH). Different volumes of samples were preserved with 4% formalin. After 2 hours the preserved microbes were collected on polycarbonate-filters (0.2 um pore size). The filters were rinsed with particle free PBS-buffer and distilled water. Air-dried filters were stored at -80° C until analysis with FISH in the home laboratory.

Total bacterial count preservations were fixed with formalin (final concentration, 2% [vol/vol]) and stored at 2°C before staining and enumeration in the home laboratory.

Viable bacterial counts were determined by means of the most-probable-number-method (MPN). For MPN calculations, two replicates of successive 10-fold dilutions were prepared using a nutrient-poor medium. Duplicate sets were prepared for each dilution. Four sets were prepared and incubated at 1°, 22°C, and 60°C at atmospheric pressure as well as at 1°C and 45MPa. MPN-growth will be evaluated by means of turbidity or cell count examination in the home laboratory.

Secondary production was estimated by means of labelled leucine. Fifty millilitres of the samples were supplied with leucine (final concentration, 50nM) and incubated at 1° and 22°C at atmospheric pressure as well as at 1°C and 45MPa. The experiments were stopped after 36 hours and will be analysed for leucine incorporation in the home laboratory.

Microbiology samples are summarized in Table B3.1.

Protists/Protozoans

Water samples for shore-based detection and analysis of protists and protozoans were collected via two in-line filter systems. A 0.22um Sterivex filter with a 202 um Nytex-prefilter were used in conjunction with a small pump to filter the contents (10L) for each sample. Filters were then removed from the in-line system, placed in a lysis buffer and frozen at -80°C. Phylogenetic analyses will be conducted by Mark Dennett at the WHOI via a project funded by the Ocean Life Institute at WHOI to identify the potential presence of protists and protozoans at different depths in the water column. Samples are summarized in Table B3.2.

AGAVE CTD Configuration Summary 8-Aug-11 G.Tuppe

Station No.	Transmissometer	EH/OBS Cable	OBS Sensor	Remarks/Comments
1	WHOI	Shared	Hedy-Seapoint	
2	WHOI	Shared	Hedy-Seapoint	Turbidity (OBS) Sensor broken-replaced
3	WHOI	Shared	Ko-ichi-Seapoint	
4	WHOI	Shared	Ko-ichi-Seapoint	
5	WHOI	Shared	Ko-ichi-Seapoint	
6	WHOI	Shared	Ko-ichi-Seapoint	
7	WHOI	Shared	Ko-ichi-Seapoint	
8	WHOI	Shared	Ko-ichi-Seapoint	
9	WHOI	Shared	Ko-ichi-Seapoint	
10	WHOI	Shared	Ko-ichi-Seapoint	
11	U Texas	Shared	Ko-ichi-Seapoint	
12	U Texas	Shared	Ko-ichi-Seapoint	
13	U Texas	Shared	Ko-ichi-Seapoint	
14	U Texas	Shared	Ko-ichi-Seapoint	
15	U Texas	Shared	Hedy-Seapoint	Tried Hedy's sensor once more - OK in air - NG in water
16	U Texas	* Shared	Ko-ichi-Seatech	* Ko-ichi had a different Y cable for the Seatech OBS

During transit from 7E to 85E, replaced lower LADCP (150Khz) with 300Khz Workhorse-faster data offload and more modern software. Also removed Y cable for OBS & EH. Removed flourometer and Ko-ichi (Seatech)-installed Ko-ichi OBS (Seapoint) to former flourometer channel Installed Separate cable for EH - same channel

17	U Texas	Separate	Ko-ichi-Seapoint
18	U Texas	Separate	Ko-ichi-Seapoint
19	U Texas	Separate	Ko-ichi-Seapoint
20	U Texas	Separate	Ko-ichi-Seapoint
21	U Texas	Separate	Ko-ichi-Seapoint
22	U Texas	Separate	Ko-ichi-Seapoint
23	U Texas	Separate	Ko-ichi-Seapoint
24	U Texas	Separate	Ko-ichi-Seapoint
25	U Texas	Separate	Ko-ichi-Seapoint
26	U Texas	Separate	Ko-ichi-Seapoint
27	U Texas	Separate	Ko-ichi-Seapoint
28	U Texas	Separate	Ko-ichi-Seapoint
29	U Texas	Separate	Ko-ichi-Seapoint
30	U Texas	Separate	Ko-ichi-Seapoint
31	U Texas	Separate	Ko-ichi-Seapoint
32	U Texas	Separate	Ko-ichi-Seapoint

Table B2.1. CTD cast times and positions from Site 1, 7 E.

CTD station#	Date	Start Latitude N	Start Longitude E	Finish Latitude N	Finish Longitude E	Start time (UTC)	Time at bottom (UTC)	End time (UTC)
1	2007 07 04	84 57.271	6 57.276	84 57.042	7 00.244	19:26	20:43	22:04
2	2007 07 05	85 00.972	7 24.660	85 00.955	7 25.496	8:00	9:05	10:19
3	2007 07 05	85 01.703	7 16.424	85 01.580	7 16.440	11:56	12:53	13:44
4	2007 07 05	85 00.258	7 31.378`	85 00.140	7 31.916	15:20	16:30	17:52
5	2007 07 05	85 00.186	7 42.578	85 00.082	7 43.532	18:40	19:53	20:56
6	2007 07 06	84 59.250	7 13.687	84 59.023	7 14.700	22:47	23:53	1:36
7	2007 07 06	84 58.554	7 17.467	84 58.547	7 19.106	3:15	4:10	5:03
8	2007 07 06	84 59.355	7 19.841	84 59.071	7 28.764	6:56	8:06	10:45
9	2007 07 06	84 59.284	7 07.608	84 59.080	7 08.626	12:48	13:49	16:00
10	2007 07 07	84 59.364	7 15.733	84 59.290	7 16.270	4:50		6:05
11	2007 07 07	84 59.090	7 18.969	84 58.934	7 21.022	8:17	9:23	10:33
12	2007 07 07	84 59.126	7 17.017	84 59.126	7 19.705	11:32	12:39	15:54
13	2007 07 07	84 58.884	7 04.638	84 58.812	7 10.368	20:05	20:55	22:31
14	2007 07 08	84 59.384	7 12.548	84 58.415	7 16.391	8:07	not recorded	12:41
15	2007 07 10	84 59.150	7 10.650	84 58.340	7 05.830	12:41	13:51	14:52
16	2007 07 10	84 55.270	7 39.120	84 54.763	7 34.238	21:10	not recorded	0:44

Table B2.2. CTD cast times and positions from Site 2, 85 E.

CTD station#	Date	Start Latitude N	Start Longitude E	Finish Latitude N	Finish Longitude E	Start time (UTC)	Time at bottom (UTC)	End time (UTC)
17	2007 07 15	85 38.723	85 00.390	85 37.748	84 53.878	10:56	12:09	15:08
18	2007 07 15	85 38.520	85 14.970	85 38.852	85 04.176	19:50	21:00	22:44
19	2007 07 16	85 37.627	85 13.637	85 37.834	85 16.508	0:06	1:23	3:03
20	2007 07 17	85 39.404	84 52.217	85 39.542	84 50.820	9:20	not recorded	11:56
21	2007 07 17	85 37.728	85 04.710	85 37.598	85 02.146	12:51	14:01	15:10
22	2007 07 17	85 38.434	85 04.846	85 38.668	84 59.500	17:18	18:19	21:12
23	2007 07 18	85 37.807	85 06.428	85 38.329	85 01.091	13:15	14:22	18:20
24	2007 07 18	85 35.710	84 49.410	85 36.600	84 46.644	20:47	22:04	23:19
25	2007 07 19	85 36.887	85 37.609	85 37.337	85 33.738	11:13	12:20	14:10
26	2007 07 19	85 36.984	85 24.401	85 37.165	85 17.443	16:50	18:14	20:12
27	2007 07 21	85 36.744	85 30.154	85 36.799	85 19.810	0:25	1:46	5:12
28	2007 07 21	85 36.953	85 36.041	85 37.122	85 23.261	7:03	8:11	12:59
29	2007 07 24	85 38.890	86 12.187	85 40.309	85 22.232	0:45	1:49	14:18
30	2007 07 25	85 36.744	85 47.392	85 36.816	85 34.164	6:56	8:05	11:07
31	2007 07 25	85 37.375	85 33.235	85 36.563	85 19.023	20:22	21:33	1:38
32	2007 07 27	85 36.883	85 44.458	85 36.677	85 38.174	14:33	16:19	17:30
33	2007 07 28	85 36.726	85.18.654	85 36.392	85 07.560	7:49	8:58	13:09
34	2007 07 29	85 37.117	85 27.817	85 36.969	85 19.013	9:20	not recorded	12:37
35	2007 07 29	85 36.712	85 20.743	85 35.746	85 05.198	20:28	21:39	7:43
36	2007 07 30	85 35.990	85 34.826	85 35.449	85 19.291	23:34	0:46	6:36

Table B3.1. Water samples processed for microbiology studies (E. Helmke)

	CTD #	sample depth (m)	DNA	FISH	preparations done for total counts	viable counts	sec. production
	1	4060	y	y	y	y	n
	2	30	y	y	y	y	n
		300					
		2900					
		3400					
	3	2900	y	n	n	n	n
	4	3150	y	y	n	n	n
	6	2800	y	y	y	n	n
		2835	y	y	y	n	n
		2850	y	y	y	n	n
	7	2800	y	y	y	n	n
	12	2850	y	n	n	n	n
		3200	y	n	n	n	n
	13	30	y	n	n	n	n
	14	30	y	y	y	y	n
		300	y	y	y	y	n
		2700	y	y	y	y	n
		2850	y	y	y	y	n
		2900	y	y	y	y	n
		3694	y	y	y	y	n
	15	3684	y	n	n	n	n
	16	5244	y	y	y	y	y
		4000	y	y	y	y	y
		3000	y	y	y	y	y
		2000	y	y	y	y	y
		300	y	y	y	y	y
		30	y	y	y	y	y
site	85° N, 85°E						
	17	30	y	y	y	y	n
		300	y	y	y	y	n
		2500	y	y	y	y	n
		3400	y	y	y	y	n
		3450	y	y	y	n	n
		3500	y	y	y	n	n
		3827	y	y	y	y	n
	18	30	y	y	y	n	y
		300	y	y	y	n	n
		3350	y	y	y	y	y
		3852	y	y	y	y	y
	19	3000	y	y	y	n	y
		3400	y	y	y	n	y
		3891	y	y	y	n	y
	23	3884	y	y	y	n	n
		3598	y	y	y	n	n
	24	bottom	y	y	y	n	n
	27	30	n	y	y	n	n
		bottom	n	y	y	n	n
	28	bottom	y	y	y	n	n
	29	bottom	y	y	y	n	n
		3800	y	y	y	n	
	30	4071	y	y	y	y	n
		4054	y	y	y	y	n
	33	3650	y	y	y	n	n
		3974	y	y	y	n	n
		3990	y	y	y	n	n
		3993	y	y	y	n	n
	35	bottom	y	y	y	n	n

DNA: for qualitative analysis of the microbial communities
FISH (fluorescence in situ hybridisation) for quantitative analysis of the microbial communities
total counts: quantitative estimation of the total bacterial biomass
viable counts:quantification of cultivatable bacteria
sec. prod: secondary production, to estimate bacterial production by means of leucine

Table B3.2.

AGAVE Gakkel Ridge Cruise
July-August, 2007
IB Oden
Shank/Dennett Water Samples taken for Protist Identification

Sample #	Cast #	Bottle #	Date	Temp (C°)	Salinity	Start Lat (°N)	Start Lon (°E)	End Lat (°N)	End Lon (°E)	Depth (dbar)ϕ	Filtered Vol. (L)*
1	1	2	7/4/07	-0.918	34.938	84 57.271	6 57.276	84 57.042	7 0.244	4063	9.5
2	1	3	7/4/07	-0.918	34.937	84 57.271	6 57.276	84 57.042	7 0.244	3200	9.5
3	1	6	7/4/07	1.307	34.870	84 57.271	6 57.276	84 57.042	7 0.244	300	9.5
4	26	10	7/19/07	1.370	34.864	Sampled at cast end		85 37.165	85 17.443	250	9.5
5	26	11	7/19/07	1.370	34.864	Sampled at cast end		85 37.165	85 17.443	250	9.5
6	26	12	7/19/07	-1.139	34.249	Sampled at cast end		85 37.165	85 17.443	100	9.5
7	26	13	7/19/07	-1.139	34.249	Sampled at cast end		85 37.165	85 17.443	100	9.5
8	26	14	7/19/07	-1.822	33.874	Sampled at cast end		85 37.165	85 17.443	50	9.5
9	26	15	7/19/07	-1.822	33.874	Sampled at cast end		85 37.165	85 17.443	50	9.5
10	29	10	7/24/07	-0.926	34.940	85 38.890	86 12.187	85 40.309	85 22.232	3484	9.5
11	29	11	7/24/07	-0.926	34.940	85 38.890	86 12.187	85 40.309	85 22.232	3484	9.5
12	29	14	7/24/07	1.263	34.837	85 38.890	86 12.187	85 40.309	85 22.232	250	9.5
13	29	15	7/24/07	1.263	34.837	85 38.890	86 12.187	85 40.309	85 22.232	250	9.5
14	29	16	7/24/07	1.203	34.241	85 38.890	86 12.187	85 40.309	85 22.232	100	9.5
15	29	17	7/24/07	1.203	34.241	85 38.890	86 12.187	85 40.309	85 22.232	100	9.5
16	29	18	7/24/07	-1.828	33.879	85 38.890	86 12.187	85 40.309	85 22.232	50	9.5
17	29	19	7/24/07	-1.828	33.879	85 38.890	86 12.187	85 40.309	85 22.232	50	9.5
18	32	6	7/27/07	1.258	34.836	Sampled at cast end		85 36.677	85 38.174	251	9.5
19	32	7	7/27/07	-1.120	34.258	Sampled at cast end		85 36.677	85 38.174	101	9.5
20	32	8	7/27/07	-1.812	33.872	Sampled at cast end		85 36.677	85 38.174	51	9.5

ϕ any samples taken at > 1°C or 200 to 500 dbar are considered to be Atlantic inflow water
* a small amount of drip leakage at the 22 um filter occurred

Appendix C. AUV Operations and Vehicle Descriptions

The AUV efforts on AGAVE were centered around two identical AUVs, Jaguar and Puma, that are based on deeper (5000m rated) versions of the Seabed Autonomous Underwater Vehicle. These vehicles were specially outfitted for working under-ice. The vehicles conducted 9 missions over the course of the expedition. These missions demonstrated robust under-ice behavior and yielded significant scientific data in the form of CTD measurements, Eh measurements, three axis magnetic data, optical backscatter data and microbathymetric mapping capabilities. Several missions lasted 20 hours or more and were conducted at depths up to 4100m, which we believe are the deepest dives, by any scientific AUV.

C.1 VEHICLE DESIGN

The vehicle design is a hover-capable concept that utilizes two hulls where the top hull contains most of the vehicle buoyancy while the bottom hull contains a large fraction of the vehicle weight. The large metacentric height implies a vehicle that is stable in pitch and roll. The basic electronic, propulsion and battery systems are identical for both vehicles although they differ in the sensor suite that is on each vehicle.

Figure C1. The Jaguar and Puma Autonomous Underwater Vehicles. These vehicles are based on the highly successful Seabed AUV design but are rated to work at depths up to 5000m and are outfitted with a sensor suite for hydrothermal vent studies.

Table C1 summarizes the characteristics that are shared by the vehicles. Tables C2 and C3 list the sensors that were mounted on each vehicle during the AGAVE cruise.

Depth Rating	5000m
Size	2.0m(L) x 1.5m(H)
Speed	0.0-0.6m/s (typical 0.35m/s)
Batteries	6kWhr rechargeable Li-ion (24 hr endurance)
Propulsion	3 DC thrusters – Fore 100N, Vertical 50N
Navigation / Attitude	Depth – Paroscientific pressure sensor Attitude – Ixsea Octans north seeking FOG
Position	Seafloor and Ship-based Long baseline acoustic transponders, RDI Navigator ADCP
Telemetry	WHOI Micromodem
Surface Communication	RF radio modem with minimum range of 2 km
Electronics	PC104 based with isolated 5V, 12V, 24V and 48V power distribution
Software	Proprietary code running on the Linux Operating System
Emergency Recovery Equipment	Novatech strobe / radio beacon. Avalanche beacon. Relay LBL transponder.

Table C1. Vehicle characteristics for Jaguar and Puma

Multi-beam	Delta-T Imagenex
Camera	1,4,11 Mbit 12 bit cameras with 50 W-second strobe
Chemical Sensors	Eh sensor
CTD	Seabird SBE-49 Fastcat pumped CTD
Magnetometer	3-axis flux gate sensor

Table C2. Jaguar Sensor Listing

Chemical Sensors	Eh sensor
Optical	Optical Backscatter System
CTD	Seabird SBE-49 Fastcat pumped CTD
Laser Ranging and Optical Backscatter (LROBS)	Custom designed laser ranging device for hydrothermal plume detection at a distance

Table C3. Puma Sensor Listing

C.2 SENSORS

While most of the sensors on both platforms were commercial off the shelf technology, a few are custom designs and are discussed below.

The Eh Sensor

Eh was measured on PUMA via a RS-232C auxiliary channel. The Eh sensor was composed of a set of electrodes and a transformer. Electrodes were Pt electrode, which were coiled 0.7 mm thick pure Pt wire, and a reference electrode, which consists of an Ag-AgCl electrode sealed in saturated KCl solution. The electronic junction between Ag-AgCl electrode and seawater achieved through a porosity controlled zirconia plug. The transformer served dual functions to electrically isolate the electrodes from the AUV via an isolation amplifier as well as to digitize the electrode voltage in mV twice at two hertz and to transmit the value to the vehicle via RS232C.

Note that any Eh data at any depth is not equilibrated Eh value because of the slow response of the electrodes. Also the Pt electrode surface situation changes with time, resulting in Eh range differences through dives. On Jaguar Eh was measured by a stand-alone data logger. The time stamp of the logger was set by hand-held GPS receiver before the dive and checked by the same device after the dive.

3-Axis Fluxgate Magnetometer

The three-component magnetometer was a fluxgate magnetometer sampled at 10 Hz. Three component magnetic data allows us to infer the direction of magnetization, magnetic reversal boundary and the strike of the fault. It is expected that data obtained near the seafloor reflect the magnetic characteristics of shallow rock types and their distributions.

C.3 AUV FEATURES SPECIFIC TO ARCTIC OPERATIONS

The Operating Paradigm

The fundamental difference between open ocean operations and working under-ice is the need to surface in open (ice-free) water after concluding a mission. Given that holes in the ice can close in short order and that typical drift rates (0.2 knots) vary spatially and with time the ability to have vehicle control at all times was an important design parameter. Our operating paradigm called for us to drive to the surface and park the vehicle at 100meters below the surface and then drive it to an open pool near the ship where the vehicle was commanded to a shallow enough depth to allow it to be visually picked up before it was commanded to surface to be picked up and craned aboard.

Acoustic Communications

In order to accomplish this goal we significantly modified the vehicle software and hardware to implement a methodology that allowed an operator to use 32 byte telemetry packets to and from the vehicle to drive it in depth and x and y from the surface ship.

We used the WHOI micromodem working with error-correcting QPSK codes to telemeter data back and forth from the vehicle. The fields that were telemetered included vehicle x, y, depth, altitude, goal x, goal y, goal depth and a goal ID that was a proxy for progress along the

mission as well as vehicle health status.

Acoustic Navigation

Long-baseline (LBL) acoustic navigation is a standard navigation technology for deep-sea survey and was employed to provide globally referenced position estimates for both the Jaguar and Puma AUVs in the form of deterministic two-beacon position fixes. Both AUVs were equipped with WHOI micromodems for acoustic communication with the support vessel and for interrogating a net of up to four Benthos series 6000 transponders that were operated in the 7kHz-13kHz frequency range. Under-ice operations, particular ice-induced ship drift, necessitated atypical adaptations of this technology both during routine recoveries and in support of impaired-vehicle recovery.

Two beacons deployed fore and aft off the ship provided moving-baseline spherical navigation during routine recoveries thus enabling the vehicle to be driven prior to surfacing into whatever open water was available near the drifting ship. This ship-LBL system relied on the availability of acoustic communications with the vehicle to telemeter raw travel-times to the ship.

For routine recoveries, vehicle position was determined acoustically through some combination of the vehicle's acoustic modem, fixed deep transponders, and ship-deployed transponders. However in case of vehicle malfunction a backup relay transponder on the vehicle could be activated. In addition, in the absence of acoustic telemetry one could also listen in to the vehicle as it pinged the bottom transponders and derive an independent navigation estimate without disturbing its ping cycles. Finally, in the case of a completely dead vehicle rising to the surface and being stuck under ice, we could also activate the backup relay transponder and by ranging to it from different directions using a helicopter triangulate the position of the vehicle. The avalanche beacon on the vehicle combined with a receiving device on the helicopter could further narrow down the vehicle position down to a meter.

The techniques employed for these tasks included standard spherical navigation with a moving baseline, ranging adapted for a moving origin, and hyperbolic navigation. Illustrative examples utilizing these techniques are included in the appendix.

Acoustic Transponder Deployment, Calibration, Use and Recovery

Acoustic transponders on the seafloor are crucial for precise underwater navigation. There were significant deviations from typical deployments of transponders in ice as compared to open water. We originally started deploying the transponders by driving the ship to the drop point and casting them off the stern. We later utilized the helicopter to fly to a convenient open lead and deployed them by landing on the ice.

The problem of calibrating the transponders was far more serious. Open water typically requires us drive a circle around the transponders at a radius equal to the water depth to calibrate its position. This was clearly untenable given the time and effort this would require given an icebreaker. Instead we again utilized the helicopter to fly to five points of opportunity around each transponder and dipped a transducer from the helicopter while it hovered in the air. We were somewhat wary of our calibration with such few points but such a methodology seemed to work quite well as was evidenced by vehicle tracking and eventual transponder recovery.

The bottom transponders worked well. This was a function of both the quiet Arctic environment as well as low vehicle noise on both the Jaguar and Puma vehicles.

We originally assumed that our transponders would not be recoverable. However on releasing the first transponders we realized that they tended to surface very close to their calibrated position. Further they either showed up in a pool around the icebreaker or very close and were easily recoverable. We believe this process was facilitated by weak currents, significant buoyancy of the beacons themselves, and their robustness.

C.4 VEHICLE ENGINEERING PERFORMANCE AND SCIENTIFIC DATA INVENTORY

Over the course of the AGAVE cruise the Jaguar and Puma AUVs were deployed (to depths greater than 150 on 9 occasions. This statistic includes the first deep test dive for each vehicle. Vehicle scientific data and vehicle performance for each dive is summarized below. Five of the nine dives yielded significant scientific data. The depth profile, x-y tracks, and scientific data for these dives are included in the appendix.

The highlights of this work include

- The first deep dives with an AUV under ice-covered conditions in the Arctic Ocean. These dives number among the deepest dives conducted by an AUV anywhere in the world's oceans.
- These dives were accomplished on scientific AUVs that cost significantly less than other such assets.
- The use of sophisticated low-bandwidth telemetry and control algorithms for dealing with Arctic conditions.
- The use of unique navigation schemes to allow routine use in an ice-covered environment with significant ice drifts.

-

Dive ID	Start Time (GMT)	CTD	EH	OBS	MAG	BATHY	Latitude, Longitude	Max. Depth	Descent Time	Bottom Time	Ascent Time	Recovery Time
Puma 0000	10 July 2007, 04:12	●	●	●			84°59'N, 07°00'E	1025m	1h42m	0h00m	1h24m	3h08m
Puma 0001	16 July 2007, 13:26	●	●	●			85°39'N, 85°02'E	3417m	5h32m	6h43m	4h09m	3h48m
Puma 0002	19 July 2007, 22:26	●	●	●			85°37'N, 85°27'E	3512m	4h51m	7h10m	8h01m	1h21m
Jaguar 0000	21 July 2007, 20:55	●	●		●		85°38'N, 85°07'E	2234m	3h58m	0h00m	8h00m	~6h
Puma 0003	22 July 2007, 21:58	●	●	●			85°38'N, 85°05'E	192m	0h23m	0h00m	0h17m	1h30m
Puma 0004	23 July 2007, 18:39	●	●	●			85°38'N, 84°55'E	293m	0h28m	0h00m	0h31m	1h34m
Puma 0005	25 July 2007, 12:17	●	●	●			85°37'N, 85°26'E	3560m	5h28m	5h40m	5h07m	0h38m
Jaguar 0001	27 July 2007, 01:02	●	●		●	●	85°37'N, 85°45'E	3995m	7h54m	5h20m	5h44m	2h00m
Jaguar 0002	29 July 2007 01:05	●	●		◗	●	85°37'N, 85°23'E	4062m	7h18m	19h31m	<5h	~2h30m

Table C4. Vehicle dive summary.

Table C4 lists all the dives that were conducted and summarizes scientific data and vehicle data for each dive. Several interesting issues associated with Arctic operations are illustrated in this table. The sum of the descent and ascent time was close to a constant, as ballasting the vehicle light or heavy tended to equalize the time between the ascent and descent.

In general, this cruise demonstrated that AUV work under-ice in the Arctic ocean is possible and AUVs hold out the general promise of unrestricted access to the seafloor in the deepest parts of ice-covered ocean. However, further work needs to be pursued to perfect these technologies. In particular, there is a need to continue to focus on certain critical components including

- optimum ballasting operations for vehicle performance and safety.
- a full complement of acoustic navigation schemes for safe vehicle deployment and recovery

Further experience in such environments to allow vehicle operators to fine-tune vehicle performance and gain the necessary experience to improve vehicle bottom time.

Appendix D. CAMPER Operations and Vehicle Description

The "Camper" vehicle is a fiber-optic video-guided sampling system that is towed nominally at an altitude between ~1.5 and 3 meters above the seafloor. The imaging, sampling, and sensing capabilities were designed to obtain high-resolution seafloor imagery and identify and collect benthic samples using either a clamshell "grab" sampler or a suction "slurp" sampler (Figure D1). Both samplers were hydraulically lowered to the seafloor and then actuated to sample a target on the seafloor. The "grab" sampler and "eyeball" camera allowed a collected sample to be inspected to determine if the seafloor target was obtained. If not, the sampler could release the sample and be lowered again to obtain another sample. Two 5-horsepower thruster motors were used to orient the vehicle and maintain position during sampling. This multi-purpose vehicle was outfitted with five video cameras, including an obliquely-mounted HD Sony HDWF900R color camera, a downlooking Prosilica 1920 HD camera, and an Insight tilt and rotate "eyeball" camera (see Table x). During this cruise, the Camper was towed at drift speeds between 0.15 and 0.3 knots, and all sensor data were logged at the surface.

Figure D1. The CAMPER during recovery, with John Kemp on deck.

Table D1. Features of the Drop-Camera System or "Camper" Vehicle during AGAVE

Video	Prosilica 1920 HD camera HD Still camera recorded to a RAID hard drive (downlooking) Insight tilt and rotate zoom "eyeball" video camera (downlooking) HD 3-chip video camera (mounted obliquely at a ~45° angle) DSPL SeaCam looking upward
Lighting	2 400W HMI lights 1 HID 250W light 4 Deep-Sea Systems 200W HID Max Sea lights
Sensors	Seabird Cat 49 CTD (depth was inoperable during the cruise) Paroscientific 8000 series pressure sensor RDI ADCP 4 beam Doppler, altitude and speed over ground Octans laser-ring gyro Eh probe recording a measurement every 0.5 seconds* Parker hydraulic pump LROBS (laser optical backscatter system) Imagenex sonar
Benthic sampling gear	Clamshell grabber Slurp suction sampler 2 Niskins that actuated when either sampler was lowered

*Eh was measured through Camper's RS-232C auxiliary channel. The Eh measurement device was composed of a set of electrodes and a transformer. Electrodes were Pt electrodes, which were coiled 0.7 mm thick pure Pt wire, and a reference electrode, which is an Ag-AgCl electrode sealed in saturated KCl solution. The electrode voltage in mV was recorded twice per second and transmitted through RS232C. Note that Eh data at each depth during Camper dives may not be equilibrated Eh values because of the slow response of the electrodes. Pt electrode surface characteristics change over time, resulting in Eh rangedifferences through different dives.

CAMPER SAMPLE LOG

Date	Dive #	Time (Z)	Position °N	Position °E	Depth (m)	Sampler/Samples
7/09/07	9	2005	85°01.02'	7°12.39'	3173	Corer – Sediment core & water
7/18/07	11	0453	85°38.13'	85°07.77'	3703	Grab – rock
7/23/07	12	0800	85°37.58'	85°14.39'	4000	Slurp – sediment & water; Grab – volcanic glass sediment
7/24/07	13	2351	85°36.83'	85°21.28'	4116	Slurp – microbial mat, glassy sediment & wa
		0019	85°36.83'	85°19.45'	4090	Grab – pillow basalt
7/26/07	14	1122	85°36.59'	85°25.15'	4140	Grab – pillow basalt with muddy sediment
7/26/07	15	1750	85°36.72'	85°12.91'	3984	Slurp – microbial mat, sediment & water
		1817	85°36.68'	85°11.94'	3942	Grab – glass from pillow basalt
7/28/07	16	0327	85°36.45'	85°12.37'	3903	Niskin bottle (triggered by slurp) – water; Slurp – microbial mat, sediment & water
		0359	85°36.40'	85°11.39'	3969	Niskin bottle (triggered by grab) – water
		0420	85°36.38'	85°10.73'	4003	Grab – glass from pillow basalt
7/28/07	17	2004	85°36.89'	85°35.36'	4037	Grab – sponge and pillow basalt
		2024	85°36.88	85°24.66'	4072	Slurp – volcanic glass sediment & water
7/30/07	19	1707	85°36.51'	85°17.94'	3915	Niskin bottle (triggered by slurp) – water
		1733	85°36.45'	85°17.22'	3894	Slurp – microbial mat, water & sediment
		1851	85°36.28'	85°15.10'	3910	Grab – sheet flow
7/31/07	20	1008	85°35.67'	85°31.65'	4023	Grab – pillow bud
7/31/07	21	1748	85°35.79'	85°33.11'	4121	Grab – pillow basalt with clay(?) sediment

Table D2. CAMPER sample log

Dive	Date	Target	On Bottom (Z)	Location °N; °E	Off Bottom (Z)	Location °N; °E	Bottom Time (hrs)	Eh Start	Depth Covered (m)	Reason for ending dive	Observation highlights	Sampled
6	Jul 6	End of CTD#6	N/A	N/A	N/A	N/A	N/A	N/A	N/A	LROBS GF	N/A	N/A
7	Jul 6	End of CTD#6	22:38	8 4 84°59.19 7° 24.10	23:36	84° 58.74 7° 25.36	0:58	20:47	4005– 4018	passed target	jellies, benthic shrimp, various animal tracks, brittle stars on pelagic sediment	Grab: None Slurp: None
8	Jul 9	End of CTD#6	12:10	84° 59.32 7° 14.57	13:30	84° 59.03 7° 16.44	1:20	10:27	3600– 3880	desire for another dive at northern target-top of Knoll	peridotite outcrops; South-facing scarp at 3800m, fault, shrimp, holothurian tracks, brittle stars on sedimented bottom; passed east of target by 250m	Grab: sediments Slurp: None
9	Jul 9	Top of Knoll and deeper sediment for sampling	18:56	85° 1.185 7° 7.882	20:16	85° 01.02 7° 12.39	1:20	18:14	3158– 3173	passing the top of the Knoll and mini-core sampling completed	Pelagic mud, anemone, shrimp, tracks, large brittle stars	Grab: sediments Slurp: None Mini-core samples at 3166m.
10	Jul 17	Margin of the northern Rift high	N/A	N/A	N/A	N/A	N/A		N/A	passing target via ice drift; decided to reposition	water column features; Eh low at 3360m 250mV down to 222mV	Grab: None Slurp: None
11	Jul 18	Top of the northern valley high following CTD hit	04:33	85°38.109 85°08.235	10:13	85°39.207 85°57.854	5:20	03:20	3671– 3815	passing of the Donut target on the W-NW side	Talus, coarse-sediment, sponge,anemone, shrimp octopus, fish	Grab: Pillow basalt Slurp: None
12	Jul 23	Southern margin of the southern valley high following CTD hit	03:15	85°36.729 85°31.222	08:42	85°37.581 85°14.396	5:27	02:00	3917– 4026	passing target via ice drift;	Sponges and anemones on pillow basalts, sediment slope, talus, lobates	Grab: Basaltic glass Slurp: sediments and water
13	Jul 24	Across the southern rift below the PUMA box	21:06	85°36.0 85°33.5	00:32	85°36.831 85°18.681	3:26	19:35 :40	3940– 4155	passing target via ice drift;	Pillows, volcanic sediment, sponges, anemones, shrimp, amphipods, swimming polychaete	Grab: basaltic glass (3 pieces); pillow basalt (7 pieces) Slurp: "orange pebbly" sediments with ~some fluff,
14	Jul 26	Downslope on the southern knoll	09:01	85°37.028 85°17.905	11:31	85°36.568 85°24.930	3:05	07:52 :00	3985– 4003	Reached rippled pelagic sediment at 4140m	talus with fresh volcanic sediments, shrimp, sponges	Grab: Pillow basalt and muddy sediment Slurp: None
15	Jul 26	The "Donut"	15:32	85°36.97 85°17.905	18:37	85°36.66 85°11.326	3:05	14:22 :00	3985– 4003	complete passing of the Donut target on the W-NW side.	talus with fresh volcanic sediments and "orange pebble field"	Grab: glass from pillow basalt Slurp: "orange pebble field" material
16	Jul 28	Across the "Donut" crater	01:11	85°36.624 85°76.690	04:35	85°36.357 85°10.282	3:24	00:16 :00	3902– 4017	complete passing of the Donut crater on the W- SW side.	talus with fresh volcanic sediments, sponges, shrimp, amphipods, "orange pebble fields", and yellow "Fluff Fields"	Grab: glass from pillow basalt Slurp: "Fluff Field" material, Niskins: sample above Fluff Field and basalt
17	Jul 28	SE PUMA box crossing near Plume 4 CTD hit starting from top of the SE hill	15:16	85°36.624 85°76.690	20:52	85°36.854 85°23.712	5:36	14:19 :00	3866– 4132	complete passing of the Target and potentially "active" area.	Sponges, anemones, glass sediment, shrimp, 1-2m wide fissure, pillows, talus, polychaete	Grab: sponge and pillow basalt Slurp: volcanic glass sediment Niskin: above basalt
18	Jul 30	NE of Donut to communicate with Jaguar and run SW	N/A	N/A	N/A	N/A	N/A	10:00 :00	0-1800	Jaguar ascending	N/A	None
19	Jul 30	Eh high hydrogen plume on the eastern-northeastern side of the Donut	15:23	85°36.734 85°20.568	20:37	85°36.093 85°22.177	5:14		3885– 4150	complete passing of the target	Fluff mat, pillows, amphipods, hazy water in pillow, sheet flow	Grab: sheet flow Slurp: fluff microbial mat Niskin: above basalt
20	Jul 31	Across the	09:37	85°35.716	13:08	85°35.335	3:29	8:39:	4083– 4027	Sufficient	Smokey water 50	Grab: pillow bud

Table D3. CAMPER dive table.

AGAVE Drop-Camera System Video Inventory

	DVD	DVD	DVCam	DVCam	HDCam	HDCam
	Eyeball Camera	**Lange Camera**	**Eyeball Camera**	**Lange Camera**	**Lange Camera**	**Prosilica Camera**
Dive 7	1 of 1		1 of 1			
Dive 8	1 of 2	1 of 2	1 of 1	1 of 1	1 of 2	8:37:00
	2 of 2	2 of 2			2 of 2	
Dive 9	1 of 1		1 of 1	1 of 1	1 of 1	1:01:00
Dive 10	1 of 1		1 of 1			0:13:00
Dive 11	1 of 3	1 of 3	1 of 2	1 of 2	1 of 3	0:00:00
	2 of 3	2 of 3	2 of 2	2 of 2	2 of 3	
	3 of 3	3 of 3			3 of 3	
Dive 12	1 of 3	1 of 3	1 of 2	1 of 2	1 of 3	5:31:00
	2 of 3	2 of 3	2 of 2	2 of 2	2 of 3	
	3 of 3	3 of 3			3 of 3	
Dive 13	1 of 2	1 of 2	1 of 2	1 of 2	1 of 2	0:23:29
	2 of 2	2 of 2	2 of 2	2 of 2	2 of 2	
Dive 14	1 of 1	1 of 1	1 of 1	1 of 1	1 of 2	2:03:49
					2 of 2	
Dive 15	1 of 2	1 of 2	1 of 3	1 of 2	1 of 2	3:03:30
	2 of 2	2 of 2	2 of 3	2 of 2	2 of 2	
			3 of 3			
Dive 16	1 of 2	1 of 2	1 of 2	1 of 2	1 of 2	3:22:42
	2 of 2	2 of 2	2 of 2	2 of 2	2 of 2	
Dive 17	1 of 3	1 of 3	1 of 2	1 of 2	1 of 3	5:29:10
	2 of 3	2 of 3	2 of 2	2 of 2	2 of 3	
	3 of 3	3 of 3			3 of 3	
Dive 18	0	0	0	0	1 of 1	0:00:00
Dive 19	1 of 3	1 of 3	1 of 2	1 of 2	1 of 3	4:26:48
	2 of 3	2 of 3	2 of 2	2 of 2	2 of 3	
	3 of 3	3 of 3			3 of 3	
Dive 20	1 of 2	1 of 2	1 of 2	1 of 2	1 of 2	3:27:56
	2 of 2	2 of 2	2 of 2	2 of 2	2 of 2	
Dive 21	1 of 1	1 of 1	1 of 1	1 of 1	1 of 1	1:38:39
Dive 22	1 of 1	1 of 1	1 of 1	1 of 1	1 of 1	0:48:14
Dive 23	1 of 1	1 of 1	1 of 1	1 of 1	1 of 1	1:29:13
Dive 24	0	0	0	0	0	0:00:00
Dive 25	1 of 2	1 of 2	1 of 1	1 of 1	1 of 2	3:01:47
	2 of 2	2 of 2			2 of 2	

Table D4. CAMPER tape inventory

The Long-Range Optical Backscatter Sensor (LROBS)

Sensor Description:

The Long-Range Optical Backscatter Sensor (LROBS) is a plume-finding instrument devised by Al Bradley. The instrument was designed and built by Clifford Pontbriand in collaboration with Al Bradley and Rob Reves-Sohn. A laser beam illuminates the water column to both sides of the instrument, and the light detector, a narrow-beam telescope, is scanned along the illuminating laser beam by a moving mirror. The light sensor itself is a photomultiplier tube, which remains the most sensitive light sensor technology available. The range resolution of the system depends in part on the baseline available (the separation of transmitter and receiver), but since range is computed as the product of the baseline and the tangent of the mirror angle it is nonlinear: the tangent function has an asymptote at 90 degrees. It is important to note that the *effective* range of the sensor is not so constrained: the light signal is present whatever the range resolution. In fact, there is a tradeoff between signal strength and range resolution, since a more proximal source and detector yields more backscatter returned to the detector (the same reason video systems separate the lights from the cameras). The effective range is the most important aspect of the system, since it enables an exciting in-situ operating mode mentioned below.

The LROBS sensor is designed to be used on an AUV platform. The system design was intended to be able to coincide with a bathymetric survey or at least "mow the lawn" beneath a neutral plume in a level 2 survey in hopes of intersecting the buoyant stem of a hydrothermal vent plume. The "whiskers" of the laser beams would give close to full coverage of the survey area, which is an improvement over the current point-measurement OBS sensors. The real improvement would be the ability to detect the edge of the plume stem in-situ, and further down the road, to use one laser beam "whisker" to follow the stem down to its source on the seafloor using a "boxing" algorithm.

Test Plan:

The original plan for implementing the LROBS sensor was to use it on the PUMA AUV to search for hydrothermal vents. The AUV was to survey the neutral plume found during CTD casts, yo-yoing beneath the plume periodically in hopes of intercepting the stem. Due to technical issues, the sensor was not fully operational on any of the PUMA dives.

With the end of PUMA AUV operations, we decided to conduct LROBS engineering trials on the CAMPER towed vehicle. CAMPER does not have the same survey capabilities as an AUV, but it offers the ability to monitor ground faults and switch power to the instrument, along with a live serial port to the instrument for real-time monitoring and control. The first CAMPER experiment was to determine the feasibility of operating the sensor near the bottom with vehicle lights on. The second experiment was to profile the water column on ascent with the vehicle lights off, thereby determining appropriate sensor settings and making backscatter measurements through the water column.

Results:

The instrument was too sensitive to operate with vehicle lights on, but the experiment with the lights off was a success. Two qualitative observations are immediately apparent: The light signal varies with angle in an interesting yet predictable way, originally increasing as the volume of intersection between the laser beam and the telescope receive beam increases. The signal then falls off as the telescope receive beam sweeps further out along the laser beam, eventually losing sight of the beam entirely. The return scan is symmetrical, as seen in Figure D2. Note that there are two signal peaks, indicating one complete scan out and back to one side. The vehicle obscures the other laser beam, so there is no signal on the other half of the scan. Figure D2 shows all of the light level data from 2700 meters to 400 meters plotted against mirror angle count in blue, with data from two scans plotted in red. This serves to show the symmetry and consistency of the data, since the peaks of the individual scans coincide approximately with the "cluster" peaks. The second observation is that for the most part a change in backscatter signal strength is seen over all ranges in a complete scan, indicating a large area, uniform change in particle density. The presence of scattering particles in the water column is consistent with observations made on several CAMPER descents. The OBS data from CTD casts near the test site do not show this variation, however (Figure D3, LROBS vs. OBS data). This may speak to the sensitivity of the LROBS sensor, but it may also indicate real differences in volume backscatter in the two regions. A better experiment would be to have the OBS and the LROBS on the same vehicle, as was the intent for the PUMA dive plan.

Conclusions:

Work remains to be done regarding data interpretation and visualization, both post-processed and real-time. Although the instrument needs to see more use in structured engineering dives on an AUV in a hydrothermal environment, the data obtained from a vertical profile through the water column aboard CAMPER did provide useful engineering data supporting our hopes of improving the spatial coverage of AUV-based optical backscatter measurements.

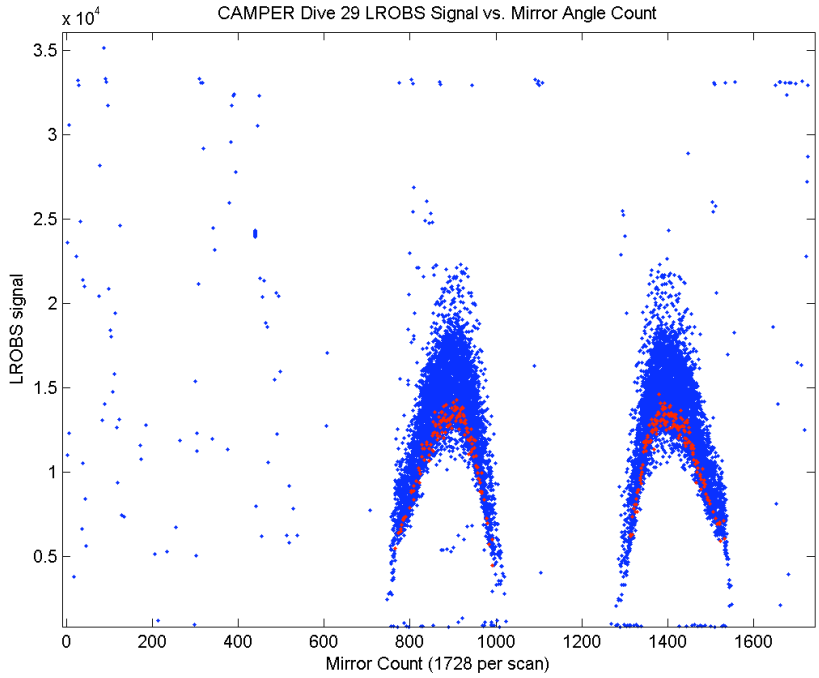

Figure D2. LROBS signal vs. mirror angle.

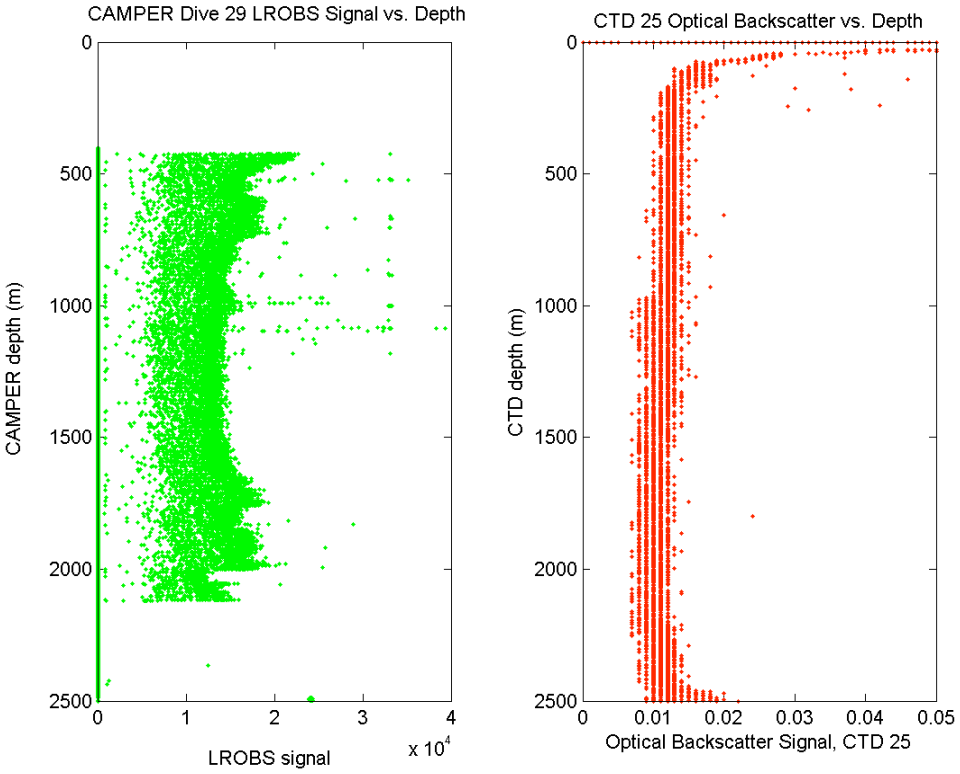

Figure D3. Comparison of LROBS signal vs. OBS signal from CTD25.

Appendix E. Seismic Program Details

E1. Station instrumentation

Each seismological array consisted of four individual seismic stations (Figure E1). The stations are equipped with a Mark 4L3C short period three component seismometers. We used Reftek RT130 data logger with GPS receivers locking every 20 minutes GPS coordinates and time. The data loggers were programmed to record continuously at a sampling rate of 100 Hz with a pre-amplification of 32. An absorbed-glass-mat rechargeable battery with a capacity of 80 Ah served as power source. The central array stations were additionally equipped with a Xeos technology ARGOS transmitter which transmits the state-of-health of the data logger and which can be tracked allowing to monitor the position of the seismometer ice floes. The Argos transmitter had an independent power source (AGM battery) to ensure its functionality for save retrieval of the instruments.

The seismometers stem from the geophysical instrument pool of the Geoforschungszentrum Potsdam. 4 datalogger and the ARGOS transmitter were borrowed from the IRIS/PASSCAL instrument pool. The remaining equipment is from the Alfred Wegener Institute.

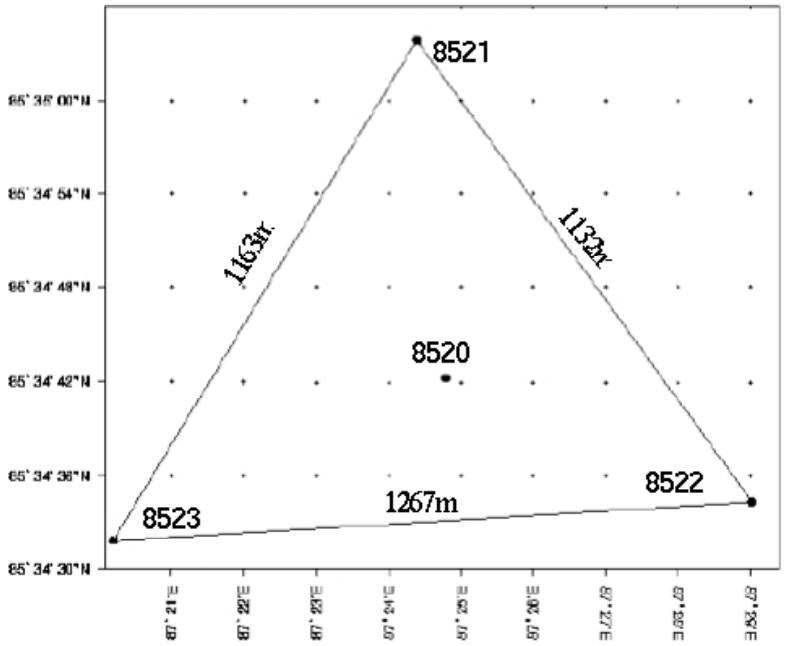

Figure E1. Example of an array configuration. Black dots are seismometer locations. Stations are numbered longitude (85), array number (2) and station number (0-3), with 0 being the central station, and 1,2,3 in direction 0°, 120° and 240°, respectively.

E2. Station setup

We selected multi-year ice floes of at least 1 km size. Slightly elevated places with good snow cover away from major pressure ridges were suitable seismometer sites. Soft snow was removed from the ice floe and the icy ground was leveled. A wooden plate served as seismometer platform. The seismometer was then leveled, a bucket put over it and covered with an about 1 m high snow heap. Less snow would melt and leave the seismometer unsheltered. The datalogger, battery and ARGOS transmitter were housed in an insulated red box with the GPS

antenna strapped to its lid. A flag was mounted at a distance of at least 10 m to mark the seismic station but to avoid coupling of wind induced motion into the ice. The data loggers were pre-programmed on board the ship such that station deployment took about 15-20 minutes per station. Recovery of a station took less than 10 minutes.

E3. Data inspection

After recovery of the seismic stations, the raw data were converted into *segy* format and a quality check was performed. The data show a great variety of seismic signals ranging from local over regional to teleseismic earthquakes and from icequakes to helicopter and ship-generated noise. The latter signals are clearly identified by high signal amplitudes and uniform signal frequencies. Earthquakes can be distinguished from icequakes by quasi-simultaneous signal onset on all array seismometers and by larger signal amplitudes on the vertical than on the horizontal component of the seismometers (Figure E2). Figure E3 shows the vertical component records of two consecutive local earthquakes of a small earthquake swarm consisting of about 15 events. Compared to the single array technique used for the pilot study in 2001, records from a network of three seismological arrays will allow locating epicenters of earthquakes occurring within the network with high accuracy. Figure E4 shows the record of a teleseismic earthquake. Records of regional and global earthquakes with well-defined magnitudes can be used to calibrate the signal amplitudes of the ice floe recordings and assess the differences in ground coupling of the individual seismometer sites.

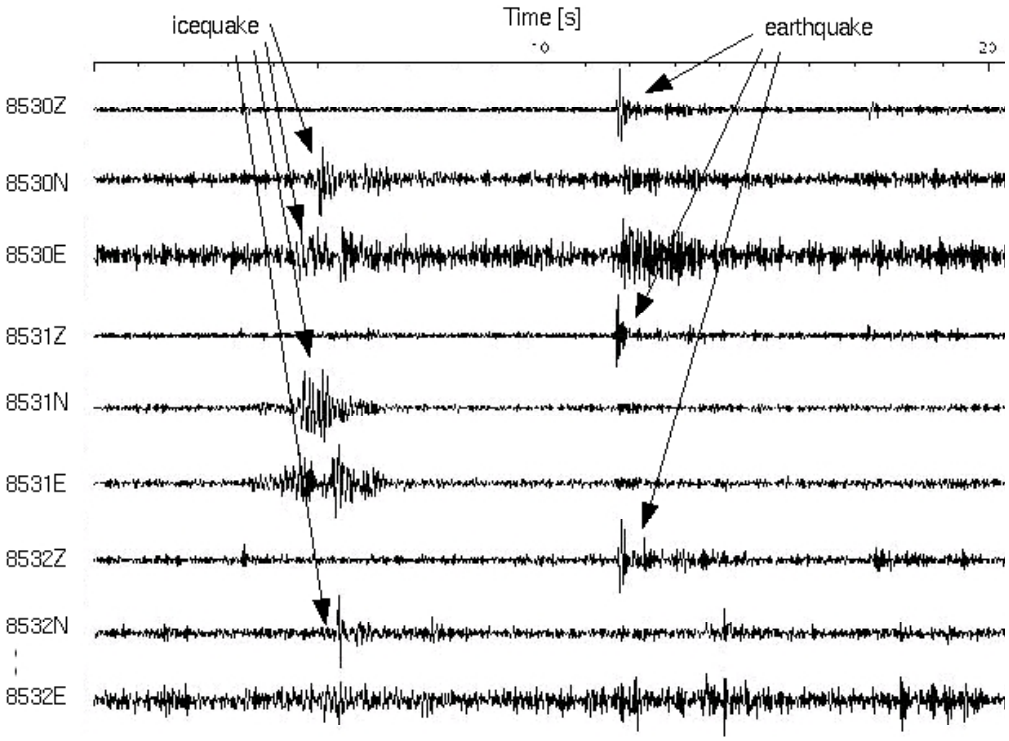

Figure E2. Earthquakes show large simultaneous onsets on the vertical component seismograms (e.g. 8530Z) and little energy on the horizontal components. Icequakes produce diffuse onsets on the horizontal component records (e.g. 8530N, 8530E). The amplitudes of the horizontal components are blown up by a factor of 3-6 relative to the vertical component records. Band-pass filtered data 8-26 Hz.

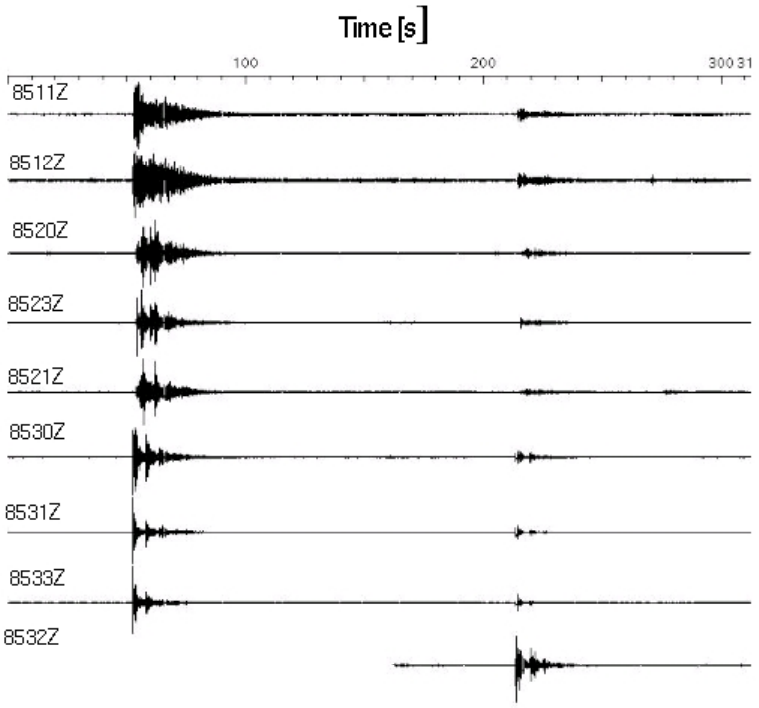

Figure E3. Vertical component records of two local events. Note the different signal shape on the three arrays. The records of array 853 show multiple signal reflections in the water column. Band-pass filtered data 8-26 Hz.

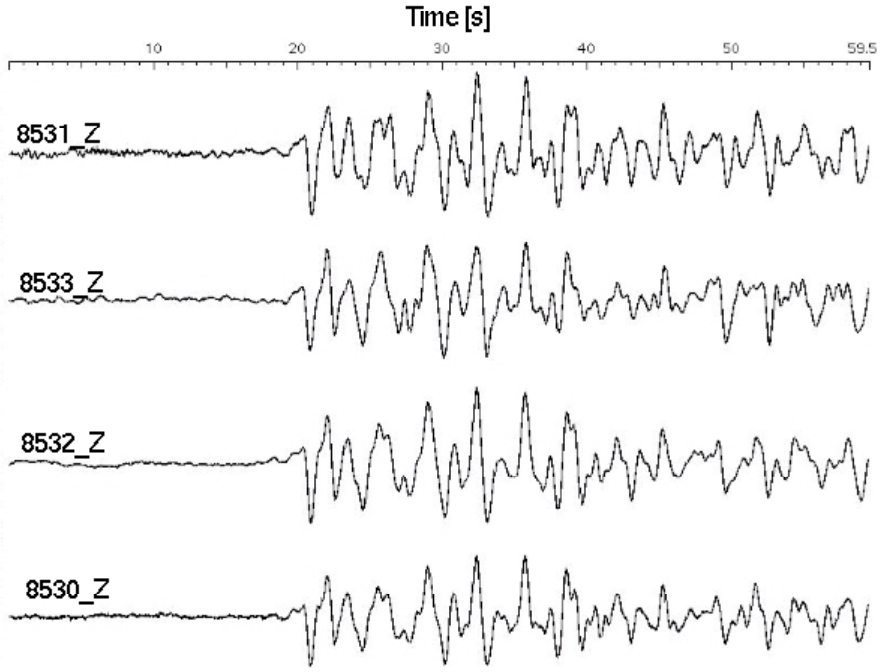

Figure E4. P-phase of a magnitude 6.6 teleseismic earthquake on July 16, 2007, 01:13 UTC, in Japan which can be used for magnitude calibration. The waveforms are unfiltered and show high coherency over the array.

E4. Station operating times

Reftek	Station		Date	Time	GPS Lat	GPS Long
991C (Passcal)	0810	Deployment	05.07.2007	13:15	84° 54.23'	4° 46.79'
		Recovery	09.07.2007	13:55	84° 44.07'	6° 23.77'
	8510_1	Deployment	15.07.2007	11:40	85° 43.03'	86° 22.81'
		Recovery	20.07.2007	12:54	85° 50.42'	83°.23.12'
	8510_2	Deployment	21.07.2007	09:45	85° 33.49'	88° 26.86'
		Recovery	27.07.2007	08:50	85° 36.11'	81° 53.06'
	8510_3	Deployment	27.07.2007	09:50	85° 44.51'	88° 04.55'
		Recovery	31.07.2007	14:50	85° 36.85'	84° 49.34'
9869 (Passcal)	0811	Deployment	05.07.2007	13:52	84° 54.40'	4° 46.46'
		Recovery	09.07.2007	14:15	84° 44.19'	6°24.41'
	8511_1	Deployment	15.07.2007	12:14	85° 43.13'	86° 20.24'
		Recovery	20.07.2007	12:40	85° 50.62'	83° 22.03'
	8511_2	Deployment	21.07.2007	10:00	85° 33.91'	88° 26.00'
		Recovery	27.07.2007	09:00	85° 36.51'	81° 52.09'
	8511_3	Deployment	27.07.2007	10:35	85° 44.67'	88° 03.35'
		Recovery	31.07.2007	15:00	85° 37.07'	84° 49.05'
9179 (AWI)	0812	Deployment	05.07.2007	14:15	84° 53.97'	4° 49.47'
		Recovery	09.07.2007	14:30	84° 43.69'	6° 27.97'
	8512_1	Deployment	15.07.2007	12:43	85° 42.58'	86°22.71'
		Recovery	20.07.2007	12:20	85° 50.17'	83° 26.60'
	8512_2	Deployment	21.07.2007	10:30	85° 33.49'	88° 27.59'
		Recovery	27.07.2007	08:20	85° 36.15'	81° 55.90'
	8512_3	Deployment	27.07.2007	10:50	85° 44.27'	88° 05.15'
		Recovery	31.07.2007	14:30	85° 36.80'	84° 52.22'
9170 (AWI)	0813	Deployment	05.07.2007	14:55	84° 53.91'	4° 45.29'
		Recovery	09.05.2005	13:35	84° 43.96'	6° 21.43'
	8513_1	Deployment	15.07.2007	13:26	85° 42.49'	86° 15.96'
		Recovery	20.07.2007	13:10	85° 50.27'	83° 18.40'
	8513_2	Deployment	21.07.2007	10:40	85° 33.38'	88° 23.15'
		Recovery	27.07.2007	08:30	85° 35.98'	81° 51.98'
	8513_3	Deployment	27.07.2007	11:15	85° 44.18'	88° 00.43'
		Recovery	31.07.2007	14:40	85° 36.72'	84° 47.87'
988E (Passcal)	0820	Deployment	06.07.2007	10:10	85° 00.82'	5° 32.84'
		Recovery	10.07.2007	18:50	84° 44.55'	7° 45.27'
	8520_1	Deployment	15.07.2007	15:04	85° 34.90'	87° 56.55'
		Recovery	22.07.2007	20:00	85° 46.41'	83° 00.94'
	8520_2	Deployment	22.07.2007	21:00	85° 30.24'	88°40.34'
		Recovery	27.07.2007	15:00	85° 29.92'	83° 21.27'
	8520_3	Deployment	27.07.2007	15:55	85° 41.79'	87° 23.39'
		Recovery	30.07.2007	23:00	85° 36.17'	84° 52.82'
9171 (AWI)	0821	Deployment	06.07.2007	11:50	85° 00.99'	5° 34.39'
		Recovery	10.07.2007	19:00	84° 44.77'	7° 44.74'
	8521_1	Deployment	15.07.2007	16:30	85° 35.11'	87° 55.36'
		Recovery	22.07.2007	19:45	85° 46.71'	83° 01.22'
	8521_2	Deployment	22.07.2007	21:50	85° 30.61'	88° 38.32'
		Recovery	27.07.2007	14:30	85° 30.14'	83° 21.27'

	8521_3	Deployment	27.07.2007	17:05	85° 41.93'	87° 21.10'
		Recovery	30.07.2007	22:40	85° 36.41'	84° 54.14'
9173 (AWI)	0822	Deployment	06.07.2007	11:30	85° 00.65'	5° 37.81'
		Recovery	10.07.2007	19:20	84° 44.46'	7° 46.44'
	8522_1	Deployment	15.07.2007	15:45	85° 34.47'	87° 58.45'
		Recovery	22.07.2007	19:25	85° 46.19'	83° 06.97'
	8522_2	Deployment	22.07.2007	22:35	85° 30.54'	88° 38.68'
		Recovery	27.07.2007	14:25	85° 29.94'	83° 24.14'
	8522_3	Deployment	27.07.2007	17:15	85° 41.57'	87° 20.29'
		Recovery	30.07.2007	23:00	85° 36.04'	84° 53.45'
9172 (AWI)	0823	Deployment	06.07.2007	12:00	85° 00.53'	5° 35.59'
		Recovery	10.07.2007	19:30	84° 44.45'	7° 42.28'
	8523_1	Deployment	15.07.2007	16:10	85° 34.34'	87° 48.29'
		Recovery	22.07.2007	20:15	85° 46.27'	82° 55.65'
	8523_2	Deployment	22.07.2007	21:30	85° 30.23'	88° 35.73'
		Recovery	27.07.2007	15:10	85° 29.75'	83° 17.16'
	8523_3	Deployment	27.07.2007	16:10	85° 41.66'	87° 20.10'
		Recovery	30.07.2007	23:20	85° 36.05'	84° 49.99'
9483 (Passcal)	0830	Deployment	06.07.2007	14:45	84° 53.65'	6° 26.31'
		Recovery	10.07.2007	13:35	84° 39.63'	8° 33.77'
	8530_1	Deployment	15.07.2007	19:09	85° 33.19'	85° 35.99'
		Recovery	20.07.2007	20:30	85° 43.39'	82° 46.65'
	8530_2	Deployment	20.07.2007	21:30	85° 27.26'	88° 32.09'
		Recovery	25.07.2007	21:20	85° 34.46'	82.40.49'
	8530_3	Deployment	27.07.2007	06:30	85° 40.06'	88° 57.94'
		Recovery	31.07.2007	20:55	85° 31.20'	85° 28.60'
9174 (AWI)	0831	Deployment	06.07.2007	14:58	84° 53.81'	6° 26.88'
		Recovery	10.07.2007	14:45	84° 39.24'	8° 35.02'
	8531_1	Deployment	15.07.2007	19:29	85° 33.48'	85° 34.63'
		Recovery	20.07.2007	20:06	85° 43.71'	82° 48.69'
	8531_2	Deployment	20.07.2007	22:00	85° 27.60'	88° 31.42'
		Recovery	26.07.2007	21:40	85° 34.76'	82° 39.68'
	8531_3	Deployment	27.07.2007	06:50	85° 40.25'	88° 57.50'
		Recovery	31.07.2007	21:15	85° 31.37'	85° 28.38'
9175 (AWI)	0832	Deployment	06.07.2007	15:20	84° 53.29'	6° 30.24'
		Recovery	10.07.2007	14:20	84° 38.99'	8° 38.23'
	8532_1	Deployment	15.07.2007	19:45	85° 32.96'	85° 34.74'
		Recovery	20.07.2007	20:14	85° 43.26'	82° 50.54'
	8532_2	Deployment	20.07.2007	22:40	85° 26.99'	88° 32.81'
		Recovery	26.07.2007	21:00	85° 43.24'	82° 45.22'
	8532_3	Deployment	27.07.2007	07:10	85° 39.90'	88° 58.73'
		Recovery	31.07.2007	20:30	85° 31.17'	85° 30.82'
9169 (AWI)	0833	Deployment	06.07.2007	15:58	84° 53.24'	6° 23.09'
		Recovery	10.07.2007	13:50	84° 39.18'	8° 31.11'
	8533_1	Deployment	15.07.2007	20:30	85° 32.88'	85° 23.25'
		Recovery	20.07.2007	20:47	85° 43.14'	82° 40.67'
	8533_2	Deployment	20.07.2007	22:25	85° 27.03'	88° 25.46'
		Recovery	26.07.2007	21:10	85° 34.20'	82° 36.14'
	8533_3	Deployment	27.07.2007	07:30	85° 39.89'	88° 54.56'
		Recovery	31.07.2007	20:40	85° 31.15'	85° 26.99'

Appendix F. Ice Drift Estimation and Forecasting

The one single factor, which influenced the operation the most and made the difference between failure and success, was the ice condition. Thus, maximal efforts were devoted to understanding, foreseeing and possibly controlling the ice conditions faced by the expedition. During the expedition several critical decisions had to be made which are directly or indirectly related to assessment of ice conditions.

The observations from earlier cruises as well as other data from submarine cruises, satellite data etc. show that ice coverage can vary from almost open water to 10/10 of pack ice. However, in general this is an area where severe ice conditions are encountered and the operation must be planned taking worst-case scenarios into account. The operating window July to mid August is in the early part of the Arctic summer and the ice situation eased up during the expedition

Since ice and weather must be dealt with in real time on a continuous basis based on the actual situation and forecasts a system for ice and weather management was prepared. For the weather part Dr. Bertil Larsson organized a set of background weather data to be sent up each day. Dr. Larsson is a meteorologist with considerable experience of Arctic weather observation and forecasting and he has visited the Arctic Ocean area at four occasions.

The background weather and especially the 1-hour resolution wind prediction were used in the forecast. The ice forecast was “adjusted” to the actual ice movement measured through a system of drifting buoys.

F1. Background

The ice drift buoys technique was developed for the IODP ACEX expedition in 2004. Swedish Polar Research Secretariat (SPRS) was contracted by the European IODP contractor BGS for the Ice management for the expedition, covering chartering of icebreakers, personnel ice background studies, and developing methods. The SPRS project leader, Ulf Hedman, organized the preparations into categories; vessels charter, (Oden and Sovietsky Sojus), Fleet management, Ice/weather management and science logistics.

F2. Ice & weather management

As a background study a 10-year historical data set was assembled by INTAARI St. Petersburg consisting of extensive data such as, ice concentration, thickness, distribution age, movement and so forth.

Ulf Hedman introduced the idea of a real time drift buoy system to real time monitor the ice drift and to get fast information in change of speed and direction. The system was planned to consist of 4 buoys to be placed on four fairly large floes to be able to detect also any rotation. Earlier methods to study ice detailed ice movement had been done trough observations from the bridge or relative measurements on the ships radar. These methods are not exact enough and the drift buoy system provided accurate data. During ACEX we learned that a system of 4 buoys is not required. There is practically no rotation within an area so one buoy is sufficient.

For ACEX the task was to predict the ice drift angle so the drill ship always was facing the ice drift. For AGAVE the task has been much more difficult and beyond what we can predict with a high degree of certainty. Here we needed to position the ship so it would drift over a box of less than 20x20 meters on the seafloor 3 hrs after we parked in the ice. No chance to adjust for errors compared to ACEX where we could adjust the heading of the drill ship to stay over the drilling site.

F3. Drift buoys

During AGAVE two types were used. AIS buoys with full AIS capability meaning that they appear on the ships navigational systems, radars etc where you can read the real time. AIS is an international system for vessels where a GPS is combined with a FM transceiver where your vessel sends out ID and position and you can receive info on other vessels within VHF range. These buoys are expensive and therefore we developed our own SPRS version for ACEX. These were not brought into play again. This type simulates an AIS but with simpler hardware. They operate over a FM radio link and is received through its own system onboard and recorded in our science server. The drawback with the simpler receivers is that you cannot se them in the navigational systems.

The buoys were deployed by helicopter and had to be moved every second day in order not to drift out of reach. We typically placed them 2 nm up drift and had them passing us with up to 4 nm. The range for the AIS buoy is up to 10 nm and the SPRS type reaches about 5nm. A map with buoy drifts from site 2 is shown in Figure F1, below.

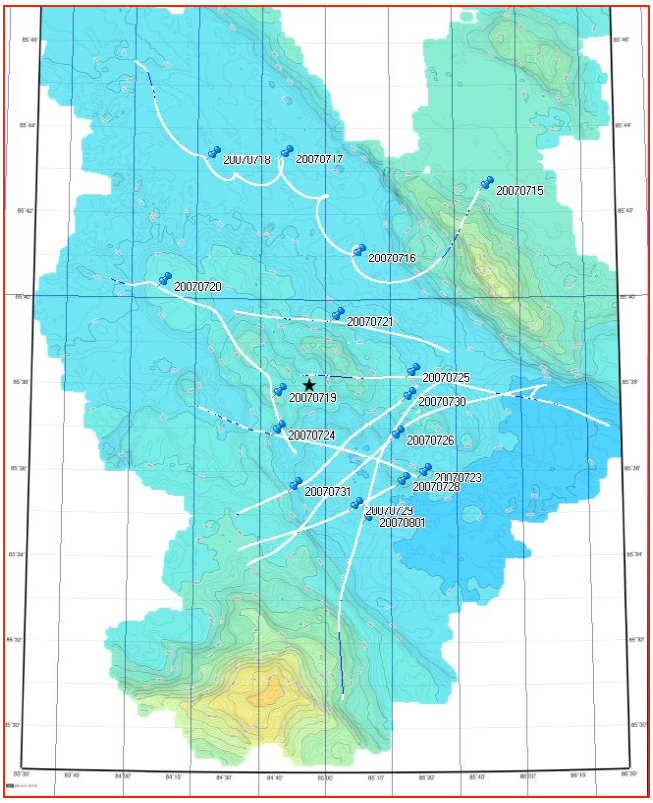

F4. General considerations for ice drift forecasting

Arctic Ocean is covered by one giant ice floe. Due to the movement of the ice it is more or less broken, especially during summer. The separate ice floes have all sizes from very big (hundreds of square kilometers) and down to very small pieces. The ice we have met during the AGAVE expedition is formed outside the east Siberian cost (Laptev Sea and East Siberian Se). It is slowly moving, first to northwest (almost up to the North Pole) and then to the southwest (east of Greenland). It is melting on the way out into the Atlantic Ocean. That large-scale journey takes about three years.

F5. Large-scale movement

The resulting movement is not along a straight line. Many factors will cause the local ice to drift in all directions and at different speeds. Speeds up to 0,5 knots are common in the open ocean. Very seldom the speed will reach 1 knot. The distribution of weather systems has big influence on the ice drift. Other factors involved are the moon (tides), Coriolis and latitude. The separate floe will act like a sailing ship and is reacting very fast on changes in wind speed and directions, especially when the speed is increasing.

The over all drift direction is downwind and 45-60 degrees to the right and the drift speed is between 1 and 2,5 % of the wind speed. That means that if the wind is northerly the drift direction will be to SW or WSW. That causes also that there will be a large-scale divergence (dilution) in a low-pressure system area, and a convergence (press) in a high-pressure system. As the wind speed in reality is changing from one area to another the resulting press and dilution are more complicated.

F6. Small-scale movement

Sometimes there will be a so-called 'inertial oscillation'. Why and when it is starting is not easy to predict. Factors involved are: quick change in wind speed or direction, tidal current (especially when the moon has a very high or low declination), Coriolis and many others. The oscillation is almost like a circle with a diameter between 0 and 1 nautical mile. The circulation is always clockwise. All floes in an area are moving with the same speed and direction and without own rotation. A full cycle is made in exact 12 hours at the North Pole. On other latitudes the 12 hours should be divided with sine for the latitude. On 85 deg north that gives 12 hrs and 3 minutes. When the diameter is known it is easy to calculate the speed along the periphery of the circle; bigger diameter gives higher speed. If that speed is the same as the overlaid speed caused by the wind, the resulting speed will be between 0 and twice the speed. In the point where the speed is 0 the direction will suddenly change 180 degrees. If the overlaid speed is lower than the oscillation in speed, the movement will sometimes be upwind. If the overlaid speed is higher, the resulting movement will be along a downwind line but with variable directions and speeds. (See attached images).

F7. Forecasts during AGAVE

The ice drift forecasts during AGAVE were made twice a day. The wind forecast was coming from the European weather centre (ECMWF) via the Swedish meteorological institute (SMHI). To check that we were using correct parameters, and to find out if there was an oscillation or not, we put transponders (AIS) on large ice floes. The different parameters were changed to get the forecast fit the pattern from the AIS buoys (real drift). That was more or less complicated, especially when there was an oscillation. The resulting data file with positions every hour up to 48 hours was then presented via Fugawi software. If the AIS buoys during an operation showed other direction and/or speed the forecast was recalculated. All together we made and used about 125 forecasts. Another product distributed was the expected drift with 3 hours resolution and the accumulated drift up to 48 hours (see table below).

Site 2 - Forecast 07-30 12 UTC					**Total overlayed drift**		
Time (local)	Drift_Dir	Speed kn	Dist 3hrs	'Up_Ice'	Drift_Dir	Naut. Miles	'Up_Ice'
2007073014	222	0.12	0.35	42			
2007073017	225	0.14	0.43	45	225	0.43	45
2007073020	222	0.14	0.43	42	224	0.86	44
2007073023	214	0.16	0.47	34	220	1.32	40
2007073102	217	0.16	0.47	37	219	1.79	39
2007073105	207	0.14	0.43	27	217	2.21	37
2007073108	202	0.16	0.47	22	214	2.66	34
2007073111	204	0.16	0.47	24	213	3.13	33
2007073114	201	0.16	0.47	21	211	3.59	31
2007073117	195	0.16	0.47	15	209	4.04	29
2007073120	185	0.16	0.47	5	207	4.47	27
2007073123	180	0.18	0.55	0	204	4.96	24
2007080102	172	0.18	0.55	352	201	5.43	21
2007080105	169	0.20	0.59	349	198	5.93	18
2007080108	168	0.20	0.59	348	195	6.45	15
2007080111	169	0.18	0.55	349	193	6.94	13
2007080114	161	0.16	0.47	341	191	7.34	11

Forecasts are made 00 and 12 UTC. We will receive the result about 8 hours later (10 am and 10 pm local time).

Yellow columns containes the expected drift that specific hour.
Blue 'Up_Ice' means the heading the ship should use to meet the ice.

Total drift' means accumulated drift from start to a specific time.
Up_Ice' and 'Naut. Miles' can be used in a sat image to find the area that has moved into the site at the specific time

Appendix G. Ship handling considerations for vehicle operations

G1. General

The utilization of Oden for deploying and recovering equipment is dependent on mainly two factors, the ice conditions, and what kind of equipment will be used. The equipment in question also determines where on the vessel the deployment or recovery will take place. Oden has a main A-frame on the stern and a smaller one on the bow. Also Oden is equipped with two cranes, one on the aft deck and one on the bow. Both are situated on the port side and can be set up with a man basket. The main A-frame has during this expedition been used for deploying the camper, the forward A-frame for deploying CTD and the cranes for deploying and retrieving AUVs and transponders. The maneuvering and positioning of the ship therefore varies a lot depending on the equipment.

G2. Ice conditions

It should be noted that the ice conditions during this expedition have been very favorable compared to a normal summer. It is our opinion that all operations that have taken place during the expedition would have been possible with normal ice conditions as well but would have taken longer time. Under severe ice conditions AUV operations would probably have to be timed to days with god conditions.

G3. CTD

From a maneuvering point of view the CTD is the easiest piece of equipment. In the beginning we would look for open pools to deploy it in. This required a reasonably solid ice edge at the leeward side of pool for the icebreaker to rest against. Towards the end the preferred method was instead to do it in solid ice. As opposed to most ships Oden has a square shaped bow. This means that once in position the ship can back up ½-1 ships length and leave an area of open water in front of the vessel. The ship also has a flush/thrusters system in the bow that will help keep the area where the CTD is deployed free of ice even during difficult ice conditions. A few times the flush has had to be switched off for operational reasons (it interferes with the acoustic modems used to communicate with the AUVs) and in those cases the icebreaker has had to go astern a couple of meters to create open water to get the CTD up.

G4. AUV

Deploying and recovering the AUVs ideally requires a reasonably sized pool of open water. If the AUV is under command it can be driven to an existing pool. If it isn't however the icebreaker will have to make a pool. This is done by first crushing the ice in a defined area and then pushing it to one side, either by flushing it away with the propellers or by moving the ship sideways and thus pushing the ice to one side. This is a time consuming operation and can only be done effectively if there isn't any pressure in the ice. If there's pressure in the ice the timing has to be very precise as the ice will start moving in as soon as the engines and thrusters are stopped. If the AUV resurfaces under the ice, the ice will have to be broken very carefully. The hull shape of Oden and the large rudders makes it extremely course stable and maneuverable, which means that this operation can be performed with high precession even when ice ridges are present. Experience during the expedition shows that this can be done without any significant damages to the vehicles. The most difficult situation is if the AUV resurfaces in an area of broken ice. Again, due to its hull shape Oden has a tendency to push broken ice in front of her. Under those circumstances there is a risk of damaging the AUV by crushing it between ice floes. The icebreaker should then just be used to relieve pressure from a distance and the AUV retrieved with helicopter.

G5. Camper

The camper operations have looked very much like the CTD operations. At first open pools were used, but after a while fast ice turned out to be a better alternative. As the camper is deployed from the stern

the icebreaker would just be stopped in the track and either there'd be enough open water behind to deploy the camper without doing anything, or one engine would be left running to keep the track free of ice. The engine kept running would just be disconnected while the camper was being lowered through the top 10-15 meters.

G6. Transponders

The transponders have proved to rise very straight from their positions on the bottom. This gives the icebreaker a possibility to create a small opening in the ice to retrieve them. The fact that the position will be quite accurate means that the opening doesn't have to be very big. The transponders have also proven to be very sturdy, so even if they resurface under the ice, the ice can be broken beside or even on top of them to let them float up through the crushed ice. The icebreaker can then easily be maneuvered to let a person hook them up from a man basket from one of the cranes.

G7. Positioning

The biggest challenge was the positioning of the icebreaker so that the various instruments would hit close enough to their targets. In this aspect the light ice conditions presented more difficulties than severe ice conditions would. Even in thick, difficult ice the icebreaker can, in time, get to almost any position and stay there. This is not the case in loose ice. If the position happens to be in an open pool or an area with very loose ice the icebreaker will always, sooner or later, end up at the leeward side of the pool, which can be a considerable distance off the target. The solution to this is to go further upstream to a better area, but this also means longer drift time and lowered accuracy in drift predictions.

G8. Operational restrictions

The machinery of Oden is built for high power output and does not take idling very well, so whenever the screws are disconnected, for any reasons, time is of essence. If the screws have been disconnected for more than five minutes they have to be connected again or the engines have to be stopped. Once the engines are stopped they can't be restarted again for half an hour. This has to be taken into consideration when planning any operation.

Appendix H. Participant List

Name	Institution	Position
Principal Investigators		
Reves-Sohn, Robert	WHOI	Chief scientist, lead geophysicist
Singh, Hanumant	WHOI	Co-chief, lead engineer
Shank, Timothy	WHOI	Co-chief, lead biologist
Humphris, Susan	WHOI	Co-chief, lead geologist
Edmonds, Henrietta	U. Texas, Austin	Co-chief, lead chemist
Collaborators		
Winsor, Peter	WHOI	physical oceanographer
Schlindwein, Vera	AWI	seismologist
Helmke, Elisabeth	AWI	sediment microbiologist
Liljebladh, Bengt	Goteburg University	physical oceanographer
Nakamura, Ko-ichi	AIST	water chemistry
Engineering and Instrumentation		
Kemp, John	WHOI	deck operations
Forte, Phil	WHOI	engineering
Bailey, John	WHOI	engineering
Jakuba, Mike	WHOI	engineering
Tupper, George	WHOI	engineering
Pontbriand, Clifford	WHOI	engineering
Weyer, Frank	freelance	engineering
Graduate Students		
Upchurch, Lucia	U. Texas, Austin	science
Kunz, Clayton	WHOI	engineering
Murphy, Chris	WHOI	engineering
Willis, Claire	WHOI	science
Stranne, Christian	Sweden	science
Sato, Taichi	ORI, U. Tokyo	engineering
Linder, Julia	AWI	science
Tausenfreund, Maria	AWI	science
Media and Outreach		
Linder, Chris	WHOI	photographer
Lippsett, Lonny	WHOI	journalist
Ruddick, Devin	WHOI	videographer
Lloyd, Erica	freelance	journalist